

AN ANALYTICAL STUDY OF THE
DIFFUSION KINETICS OF A RADIATION-INDUCED
CHEMICAL REACTION SYSTEM

by *S. J. Coolbaugh*

MORRIS JACKSON COOLBAUGH

B. S., Kansas State University, 1964

A MASTER'S THESIS

submitted in partial fulfillment of the
requirements for the degree

MASTER OF SCIENCE

Department of Nuclear Engineering

KANSAS STATE UNIVERSITY
Manhattan, Kansas

1968

Approved by:

Richard E. Faw
Major Professor

TABLE OF CONTENTS

1.0 INTRODUCTION	1
2.0 DEVELOPMENT OF THE THEORY	3
2.1 General Theory of Diffusion-Kinetics in Radiation Chemistry	3
2.2 Development of the Finite Difference Form of the Diffusion Kinetics Equations	7
2.3 Development of the Finite Difference Form of the Reaction Integrals	21
2.4 Stability of the Finite Difference Form of the Diffusion-Kinetics Equation	25
2.5 The Reaction Scheme Considered and Development of the Equations Describing the Rate of Product Formation as a Function of Dose Rate	33
3.0 DISCUSSION AND RESULTS	42
4.0 ACCURACY OF THE FINITE DIFFERENCE SOLUTION AND ANALYSIS OF ERRORS FOR THE RUNS	73
5.0 CONCLUSIONS	82
6.0 SUGGESTIONS FOR FURTHER STUDY	83
7.0 ACKNOWLEDGMENT	84
8.0 LITERATURE CITED	85
9.0 SELECTED REFERENCES	86
A.0 APPENDIX	88
A.1 Justification for the Variable Transformation	88

A.2 Explanation of the Computer Program Used in this Work	91
A.2.1 Sample Input Data for Program DIFFUSE	114
A.3 Selected Data for Figures 1-12	115

LIST OF TABLES

I.	List of runs and the values of the parameters	43
II.	Spur size as a function of time	66
III.	Radical concentrations at half-maximum positions as a function of half-maximum position	68
V.	Comparison of the two-radical model results	74
VI.	Effect of the time mesh size on the numerical results . . .	77

LIST OF FIGURES

1. Variation of $2N_{R_2}^T(t)$, $\sum_R N_{RS}^T(t)$, $N_P^T(t)$, and $N_R^T(t)$ with time for the parameters given for Run 1	45
2. Variation of $2N_{R_2}^T(t)$, $\sum_R N_{RS}^T(t)$, $N_P^T(t)$, and $N_R^T(t)$ with time for the parameters given for Run 2	46
3. Variation of $2N_{R_2}^T(t)$, $\sum_R N_{RS}^T(t)$, $N_P^T(t)$, and $N_R^T(t)$ with time for the parameters given for Run 3	47
4. Variation of $2N_{R_2}^T(t)$, $\sum_R N_{RS}^T(t)$, $N_P^T(t)$, and $N_R^T(t)$ with time for the parameters given for Run 4	48
5. Variation of $2N_{R_2}^T(t)$, $\sum_R N_{RS}^T(t)$, $N_P^T(t)$, and $N_R^T(t)$ with time for the parameters given for Run 5	49
6. Variation of $2N_{R_2}^T(t)$, $\sum_R N_{RS}^T(t)$, $N_P^T(t)$, and $N_R^T(t)$ with time for the parameters given for Run 6	50
7. Variation of $2N_{R_2}^T(t)$, $\sum_R N_{RS}^T(t)$, $N_P^T(t)$, and $N_R^T(t)$ with time for the parameters given for Run 7	51
8. Variation of $2N_{R_2}^T(t)$, $\sum_R N_{RS}^T(t)$, $N_P^T(t)$, and $N_R^T(t)$ with time for the parameters given for Run 8	52
9. Variation of $\sum_R N_{RS}^T(t)$, $N_P^T(t)$, and $N_R^T(t)$ with time for the parameters given for Run 9	53
10. Variation of $2N_{R_2}^T(t)$, $\sum_R N_{RS}^T(t)$, $N_P^T(t)$, and $N_R^T(t)$ with time for the parameters given for Run 10	54
11. Variation of $2N_{R_2}^T(t)$, $\sum_R N_{RS}^T(t)$, $N_P^T(t)$, and $N_R^T(t)$ with time for the parameters given for Run 11	55
12. Variation of $2N_{R_2}^T(t)$, $\sum_R N_{RS}^T(t)$, $N_P^T(t)$, and $N_R^T(t)$ with time for the parameters given for Run 12	56

13. Variation of the radical concentration, [R], with distance from the center of the spur with time as a parameter. Data for Run 1 . .	57
14. Variation of the intermediate product concentration, [RS], with distance from the center of the spur with time as a parameter. Data for Run 1 .	58
15. Variation of R_2 concentration with distance from the center of the spur with time as a parameter. Data for Run 1 .	59
16. Variation of the solute concentration, [S], with distance from the center of the spur with time as a parameter, Data for Run 1 . .	60
17. Plot of radical concentrations at the half-maximum position vs. the half-maximum position .	70
18. Variation of N_{RR}^* , $\sum_R N_R(t)$, and $2N_{R_2}$ with time for the data given in Section 3.0 .	76
19. Variation of $N_R(t)$ and \sum_R with time. Data for Run 2	79
20. Variation of $N_{RS}^T(t)$ and $N_P^T(t)$ with time. Data for Run 1	80

NOMENCLATURE

$\overset{\bullet}{A}$	Angstroms
\bar{B}_i	a matrix of elements defined in the section on stability
$(b_{jk})_i$	the elements of the matrix \bar{B}_i
c_o^i	spatially-constant solute concentration of i^{th} species
$c_i(j,k)$	concentration of species i at the location $\rho = j\Delta\rho$ and $x = k\Delta x$
$\bar{c}_i(k)$	a matrix of concentrations defined in the section on stability
D_i	diffusion coefficient for the i^{th} species
F_i	a quantity defined as $4\pi\{D_i[t_o^i + t_o^l(e^{m\Delta x} - 1)]\}^{3/2}$ for spurs
$G_i(j,k)$	a quantity defined as the reaction terms present in the finite difference solution for species i divided by $c_i(j,k)$
I	dose rate
K	defined as $10^3 \frac{\mu I}{e N_A}$
k_{jk}^i	rate constant for the second order reaction of species j with species k to produce species i
\bar{k}_{ij}	rate constant for the second order disappearance reaction of species i by reaction with species j
L	length of cylindrical track of radicals produced by rad- iation
$L_{ij}(t)$	the number of i^{th} radicals created or destroyed by reaction of species i with j up to time t

M	an integer, equal to $\chi/\Delta\chi$
N	number of reacting species
N_A	Avagadro's number
$N_i(R)$	the number of radicals present in the volume bounded by $r = R$
$N_i(t)$	the number of radicals of species i present at time t
N_o^i	number of free radicals in a spur or track
\bar{N}_P^T	defined as $N_P^T(\bar{t})$ where \bar{t} is the time at which $N_R(t)$ levels off
\bar{N}_R	defined as $N_R(\bar{t})$ where \bar{t} is the time at which $N_R(t)$ levels off
\bar{N}_{RS}^T	defined as $N_{RS}^T(\bar{t})$ where \bar{t} is the time at which $N_R(t)$ levels off
$N_P^T(t)$	the total number of P molecules that have been formed by reaction up to time t
$N_R(t)$	the total number of radicals present at time t
$2N_{R_2}^T(t)$	twice the total number of R_2 molecules that have been formed by radical recombination up to time t
$N_{RS}^T(t)$	the total number of RS molecules that have been formed by reaction up to time t
P	a final product
r	radial coordinate
$r_{1/2}(t)$	value of the half-maximum position at time t
R_o^i	empirical constant, related to the initial size of the spur for the i^{th} species

R	a free radical
R_2	a solute
RS	an intermediate product
$[R]_{1/2}$	concentration of the radicals at half-maximum at time t
$[R]_0$	initial concentration of the radicals in the center of the spur
S	a solute
t	time coordinate
t_o^i	scaling factor, corresponding to time, for the i^{th} species
V	volume considered in the calculations
w	twice this value is the energy required to create a radical pair
WNR(ℓ)	a weighting function used in numerical integration

α	a constant; 1 for cylindrical tracks, 2 for spurs
β_{jk}	a constant, close to 1, used in the section on stability
$\delta(r)$	Dirac delta function as a function of r
$\Delta\rho$	finite increment along the ρ axis
Δx	finite increment along the x axis
ϵ	energy deposited in a spur by the radiation
λ	eigenvalue of the matrix \bar{B}_i
μ	density of system considered
π	a constant equal to 3.1415926
ρ_i	dimensionless, independent variable, corresponding to radial position for the i^{th} species

$\sum_R(t)$ the sum of the reaction loss terms and the number of
radicals present at time t

x dimensionless, independent variable, corresponding to
time

∇^2 Laplacian operator

1.0 INTRODUCTION

One of the growing fields of interest in the last few years has been that of initiation of chemical chain reactions by the application of radiation, with perhaps the greatest application in polymerization studies. To date, the work that has been done in this field has been experimental, with attempts to explain the results in terms of the effects of overlapping of the clusters of radicals formed by the radiation process. Three situations have been postulated as 1) formation of clusters of free radicals with a separation distance large compared to their effective diameter so that most of the radical reaction is complete before their concentrations become uniform; 2) formation of clusters of free radicals with separation distances small compared to their effective diameters so that the initial distribution of radicals can be considered as uniform; 3) formation of clusters with a separation distance comparable in size to their effective diameters so that there is some reaction between neighboring clusters in an overlapping region before the complete randomization of the radicals. For these cases the rates of production of the chain reaction product should be a linear function of the dose rate for the first situation, and range to a function of the square root of the dose rate for the third situation.

The major purpose of this work is to develop a general computational scheme applicable to the solution of the equation representing the diffusional and kinetic behavior of reacting species in a single cluster, and to apply this method to the investigation of the spatial-

time behavior of a particular type of chain reaction. The data obtained from the history of a single cluster cannot give actual numerical knowledge on the effects of the dose rate on overlap reactions but it is possible to obtain estimates of the effects for extreme cases of dose rates and to indicate to some extent the dose rates at which overlap effects become important. Also of importance in this work is the proof that overlap effects to some extent are more important for chain reaction systems than for non-chain reaction systems, and the indication that the use of a modified form of the prescribed-diffusion hypothesis should give useful results even with the complex reaction scheme considered. The results of this work will also form the basis for future computations where the effects of spur overlap are calculated.

2.0 DEVELOPMENT OF THE THEORY

2.1 General Theory of Diffusion-Kinetics in Radiation Chemistry

In order to explain the observed effects of radiation on media in which chemical reactions are initiated by the radiation it has been found necessary to develop what is commonly known as the diffusion-kinetics model. This model assumes that the result of absorption of radiation energy by a system is the cause of production of a variety of reactive species from the material initially present with an inhomogeneous spatial distribution, these species then undergoing diffusion and chemical reaction. The over-all process is divided into three stages. The first stage is termed the physical stage and consists of the dissipation of the energy in the system during the time interval of 10^{-15} seconds or so. The second stage is the physiochemical stage during which processes take place that lead to the establishment of thermal equilibrium. This stage has a duration of approximately 10^{-11} seconds for aqueous solutions. The third stage is the chemical stage during which the reactive species diffuse and react chemically until chemical equilibrium is reached. This stage usually has a duration of 10^{-8} seconds or greater.

The assumptions of the diffusion-kinetics model are as follows. The reactive species formed by the absorption of the radiation are in thermal equilibrium by the time the chemical stage starts and have a specific spatial distribution which depends on the type and energy of radiation used. These species then diffuse according to macroscopic diffusion laws and react chemically according to the same

rate-laws that would be obeyed if the species were distributed homogeneously. Ultimately chemically stable products are formed which can be determined by chemical analysis.

In general the deposition of the radiation energy in the medium is a highly-localized process of a statistical and complex nature. The primary effect of this energy deposition is to cause the loss or gain of electrons by species initially present, or dissociation, or both. In aqueous solutions this leads to the formation of the free radicals H and OH by dissociation of the water. The term "free radicals" is restricted to molecular species in which there is at least one unpaired electron associated with an atom of a non-metallic element whose valency shell normally comprises an even number of electrons, all paired. The presence of these highly-reactive free radicals leads to a system of chemical reactions different from that expected assuming only ordinary ionization processes occur.

In order to determine the initial spatial distribution of the reactive species, it is necessary to know the linear energy transfer in the medium and to also assume a value for the amount of energy deposited in each discrete interaction of the radiation with the medium. Once a value for the energy deposited is assumed, then the uncertainty principle limits the extent to which we can localize the wave packet associated with the excitation produced by a primary particle. The extent of the uncertainty is usually several times larger than the size of any one species so that the excitation cannot in any reasonable approximation be considered localized in a single molecule. This region is commonly termed a "spur". It then becomes necessary to assume a form for the spatial

distribution of primary species formed within this spur. The two distributions most commonly used are Gaussian and square, and it has been found that either give essentially the same results for any diffusion-kinetics calculation.

The next consideration is the separation of one spur from another. Due to the statistical nature of the interaction of the radiation with the medium the size of each spur and the separation distance are statistical quantities. In order to bring the complexity of the problem to a manageable level it is necessary to perform the calculations assuming each spur is of average size. It is also necessary to perform the calculations for two limiting cases only. Thus it is necessary to assume that the spur separation distances are large enough on the average that reaction between species in different spurs is negligible compared to the reactions within a spur, or to assume that the separation distances are small enough that overlap between spurs occurs to such a great extent that a homogeneous cylindrical track is formed before intraspur reactions are appreciable. The complexity of the computational problem is reduced in either case since only the radial spatial variable is necessary to adequately describe the diffusion of the species with time, as opposed to the set of three coordinate variables necessary otherwise. It should be noted that for the case of the cylindrical tracks, it is also necessary to assume that the average distance between tracks is sufficiently large so that track overlap effects are negligible and to assume that the tracks are sufficiently long so that track end effects are negligible.

One other method that has been used with some success is to assume

a form for the intraspur spatial concentrations as a function of time. This reduces the complexity of the problem such that it is then possible to take into account the statistical nature of the variations of spur size and separation distance. This method obtains its best results when the reaction rates are low enough that negligible distortion of the initial spatial form of the concentrations occurs with time.

The most serious criticism of the model is that there are so many adjustable parameters in the solution that it should be possible to find a set of parameters to fit any result desired. This criticism, however, would not be justified if adequate knowledge of the values of the parameters were available from experiment. If all the rate constants and diffusion coefficients were known the model could be rigidly tested even without accurate knowledge of the initial distribution parameters. This follows because for a given medium and physical conditions, the distribution parameters depend only on the type and energy of the radiation used so that the number of experimental results to be explained could be much larger than the number of unknown initial distribution parameters.

In conclusion the test of the validity of this model depends on the extent to which it can adequately explain experimental results and forecast new results.

2.2 Development of the Finite Difference Form of the Diffusion Kinetics Equations

Since the development of the partial differential equation describing the time and position behavior of reacting chemical species can be found in many references (1, 2), it will be sufficient to state in this report that the general form of the diffusion kinetics equation for second order reactions can be written as

$$\frac{\partial c_i(\underline{r}, t)}{\partial t} = D_i \nabla^2 c_i(\underline{r}, t) + \sum_{j=1}^N \sum_{k=1}^j k_{jk}^{ij} c_j(\underline{r}, t) c_k(\underline{r}, t)$$

$$-c_i(\underline{r}, t) \sum_{j=1}^N \bar{k}_{ij} c_j(\underline{r}, t), \quad i=1, 2, \dots, N \quad (1)$$

where $c_i(\underline{r}, t)$ = concentration of the i^{th} species,

D_i = diffusion coefficient for the i^{th} species,

k_{jk}^{ij} = rate constant for the second order reaction of species

j with species k to produce species i ,

\bar{k}_{ij} = 2nd order rate constant for the disappearance of species i by reaction of i with j ,

∇^2 = Laplacian operator,

N = number of reacting species.

The term on the left side of Eq. (1) is the time rate of change of the concentration of species i . The first term on the right side of Eq. (1) represents the change of concentration of species i due to diffusion, the second term represents the creation of species i due to reaction of species j and k ,

and the third term represents the disappearance of species i by reaction of species i and j .

The form of the Laplacian operator used is that for angularly-independent and axially-independent cylindrical tracks, and angularly-independent spherical spurs. This form can be written as

$$\nabla^2 = \frac{\partial^2}{\partial r^2} + \frac{\alpha}{r} \frac{\partial}{\partial r}, \quad (2)$$

where r = radial coordinate,

$\alpha = 1$ for cylindrical tracks; 2 for spherical spurs.

For the formation of free radicals by the radiolysis of liquids this report will follow the assumption given by Lea (3) that the initial radial distribution of the free radicals is Gaussian in form.

The boundary conditions are then given as

$$C_i(\infty, t) = 0 \text{ for free radicals,} \quad (3)$$

$$= C_0^i \text{ for solutes,} \quad (4)$$

$$\frac{\partial C_i(0, t)}{\partial r} = 0 \text{ for radicals and solutes,} \quad (5)$$

$$C_i(r, 0) = C_0^i \text{ for solutes,} \quad (6)$$

$$= \frac{N_0^i}{[2\pi(R_0^i)^2]^{3/2}} e^{-r^2/[2(R_0^i)^2]} \text{ for spherical spurs,} \quad (7)$$

$$= \frac{N_0^i}{\pi [2(R_0^i)^2]} e^{-r^2/[2(R_0^i)^2]} \text{ for cylindrical tracks,} \quad (8)$$

where N_o^i = number of free radicals in a spherical spur,

N_o^i/L = number of free radicals per unit track length in a cylindrical track,

C_o^i = spatially-constant solute concentration,

R_o^i = empirical constant.

Before choosing a finite difference scheme for the numerical solution of Eq. (1) it is first necessary to modify the form of Eq. (1) in order to remove some of the problems inherent in the numerical solution.

The first problem is in the choice of the time increments needed. Since, in general, the concentration of any species considered will decrease with time due to diffusion and reaction, the reaction rate associated with this species will also decrease. This makes it possible for the time increments chosen in the finite difference scheme to be increased with time without decreasing the accuracy obtained at each time step. This procedure is very desirable since it decreases the amount of computational time needed by a large factor.

There are two methods of increasing the time increments. The first method is to increase the time increment by some arbitrary factor several times throughout the computation. The points at which the time increments are increased also must be chosen, based upon some suitable criterion. It is difficult, however, to choose a criterion that satisfies all reaction possibilities, so that it is necessary to limit the criterion

to the particular reaction system chosen. Even with this limitation, a suitable criterion can only be found by a trial and error process.

The second method for increasing the time increments is analytical in nature. One attempts to find some suitable relationship between time and another variable such that constant increments in the second variable correspond to increasing increments in time. This relation is substituted into the original partial differential equation and a finite difference scheme used with the second variable. A relationship which is suitable for the reaction system considered in this report is that given by Dyne (4) as

$$t = t_0 e^x, \quad 0 \leq x \leq \infty, \quad t_0 \leq t \leq \infty, \quad (9)$$

where t = time,

x = dimensionless, independent variable,

t_0 = scaling factor corresponding to time.

The problem now becomes one of choosing the proper t_0 and x -increment such that the desired accuracy is obtained for the solution. This is once again a trial and error procedure.

The second problem that must be resolved is that of keeping pace with the expansion of the free radicals in the radial direction as time increases. An analytical solution to this problem is given by Dyne (4) as the introduction of a new variable, ρ , replacing the radial variable in such a fashion that a constant range in ρ corresponds to a time-increasing range in r , the radial variable. The range in r must increase

at the same rate that the radicals diffuse outward in order that significant information is not lost from the problem. It can be shown (see Appendix A.1) that the proper form for ρ for Gaussian spurs or tracks is given by

$$\rho = r/\sqrt{Dt}, \quad t_0 \leq t < \infty. \quad (10)$$

The constant, t_0 , is now given as (see Appendix A.1)

$$t_0 = R_0/(2D). \quad (11)$$

The substitution of Eq. (9) and Eq. (10) into Eq. (1) will give the required form for the diffusion kinetics equations provided that all the diffusion constants and initial Gaussian widths at half-maximum are the same. If this is not the case, then the problem arises of how to best follow all of the diffusing radical species with time. One method is to define a set of ρ_i , one for each diffusing free radical species, and to use an interpolation formula in computing the reaction terms. In this manner, the errors introduced in computation of the diffusion portion of the kinetics equation for each species will be minimized as much as possible, since each species will be followed independently in position. The error introduced by the use of an interpolation scheme in order to compute the reaction terms will also be minimal due to the well-behaved spatial forms for the concentrations. This method will tend to increase the problem computation time due to the need for interpolation, but at the same time the accuracy will be significantly increased.

If we now redefine Eqs. (9), (10), and (11)

$$t \equiv t_o^i [e^x - 1] ; \quad 0 \leq x \leq \infty , \quad (12)$$

$$\rho_i \equiv \frac{r}{\sqrt{D_i(t_o^i + t)}} , \quad (13)$$

$$t_o^i \equiv \frac{(R_o^i)^2}{2D_i} . \quad (14)$$

Substituting Eq. (13) into Eq. (1), we have for the various terms

$$\frac{\partial C_i(r, t)}{\partial r} = \frac{\partial C_i(\rho_i, t)}{\partial \rho_i} \frac{\partial \rho_i}{\partial r} = \frac{1}{\sqrt{D_i(t_o^i + t)}} \frac{\partial C_i(\rho_i, t)}{\partial \rho_i} , \quad (15)$$

$$\frac{\partial^2 C_i(r, t)}{\partial r^2} = \frac{1}{\sqrt{D_i(t_o^i + t)}} \frac{\partial}{\partial \rho_i} \frac{\partial \rho_i}{\partial r} \frac{\partial C_i(\rho_i, t)}{\partial \rho_i} = \frac{1}{D_i(t_o^i + t)} \frac{\partial^2 C_i(\rho_i, t)}{\partial \rho_i^2} , \quad (16)$$

$$\begin{aligned} \frac{\partial C_i(r, t)}{\partial t} &= \frac{\partial C_i(\rho_i, t)}{\partial t} + \frac{\partial C_i(\rho_i, t)}{\partial \rho_i} \frac{\partial \rho_i}{\partial t} \\ &= \frac{\partial C_i(\rho_i, t)}{\partial t} - \frac{r}{2(t_o^i + t)\sqrt{D_i(t_o^i + t)}} \frac{\partial C_i(\rho_i, t)}{\partial \rho_i} , \\ &= \frac{\partial C_i(\rho_i, t)}{\partial t} - \frac{\rho_i}{2(t_o^i + t)} \frac{\partial C_i(\rho_i, t)}{\partial \rho_i} . \end{aligned} \quad (17)$$

Eq. (1) becomes

$$(t_o^i + t) \frac{\partial C_i(\rho_i, t)}{\partial t} = \frac{\partial^2 C_i}{\partial \rho_i^2} + \left[\frac{\rho_i}{2} + \frac{\alpha}{\rho_i} \right] \frac{\partial C_i}{\partial \rho_i} + (t_o^i + t) \left[\sum_{\ell=1}^N \sum_{m=1}^{\ell} k_{\ell m}^i C_{\ell}(\rho_i, t) C_m(\rho_i, t) - C_i(\rho_i, t) \sum_{\ell=1}^N \bar{k}_{i\ell} C_{\ell}(\rho_i, t) \right]. \quad (18)$$

Substituting Eq. (12) into Eq. (18) gives

$$\frac{\partial C_i(\rho_i, \chi)}{\partial \chi} = \frac{1}{1 + e^{\frac{\chi}{t_o^i}} \left[\frac{t_o^i}{t_o^1} - 1 \right]} \cdot \frac{\partial^2 C_i}{\partial \rho_i^2} + \left[\frac{\rho_i}{2} + \frac{\alpha}{\rho_i} \right] \frac{\partial C_i}{\partial \rho_i} + t_o^i e^{\chi} \left[\sum_{\ell=1}^N \sum_{m=1}^{\ell} k_{\ell m}^i C_{\ell}(\rho_i, \chi) C_m(\rho_i, \chi) - C_i(\rho_i, \chi) \sum_{\ell=1}^N \bar{k}_{i\ell} C_{\ell}(\rho_i, \chi) \right]. \quad (19)$$

Eq. (19) is in the proper form such that a constant increment in χ will give an exponentially-increasing increment in time, and a constant increment in ρ will give time-increasing position increments such that the same portion of the Gaussian concentration for the free radicals will be utilized at each time step.

In order to solve the set of nonlinear partial differential equations given by Eq. (19), it is convenient to use some form of finite differences

for the various terms. The choice of the difference scheme used is determined by experience as there are many difference schemes available. The scheme used in this report is that of central differences in ρ and forward differences in X .

If we let $\Delta\rho$ be the finite increment chosen along the ρ axis, and j be the index associated with this axis, and if we let ΔX be the finite increment chosen along the X axis, and k be the index associated with this axis, the derivatives in Eq. (19) become

$$\frac{\partial C_i(\rho_j, X)}{\partial X} = \frac{C_i(j, k+1) - C_i(j, k)}{\Delta X}, \quad (20)$$

$$\frac{\partial C_i(\rho_i, X)}{\partial \rho_i} = \frac{C_i(j+1, k) - C_i(j-1, k)}{2\Delta\rho}, \quad (21)$$

$$\frac{\partial^2 C_i(\rho_i, X)}{\partial \rho_i^2} = \frac{C_i(j+1, k) - 2C_i(j, k) + C_i(j-1, k)}{(\Delta\rho)^2}. \quad (22)$$

where $C_i(j, k)$ = concentration of species i at the location $\rho = j\Delta\rho$
and $X = k\Delta X$.

It is to be noted that the truncation error caused by the approximations to the derivatives with respect to ρ_i is of order $(\Delta\rho)^2$, and the truncation error caused by the approximation to the derivative with respect to X is of order (ΔX) . There are several reasons why a better approximation scheme is not chosen for the derivative with respect to X , the first being that any other scheme makes the starting of the problem

solution difficult due to the lack of sufficient initial data. For instance, if a form for Eq. (20) were chosen similar to that for Eq. (21), it would still be necessary for the first step in χ to be computed using the form given by Eq. (20) in order to start the solution. The second reason for using the given form is that of limited computer core storage. Any other form for the derivative will require that additional values of C_i be stored in the computer as the problem is solved. The third reason for the form chosen is concerned with the stability of the solution and is discussed in the section of this report on stability.

Before substitution of Eqs. (20) through (22) is performed there is a problem that exists with Eq. (19) and that is the singularity at $\rho_i = 0$. Using L'Hospital's rule we have

$$\lim_{\rho_i \rightarrow 0} \left[\frac{1}{\rho_i} \frac{\partial C_i(\rho_i, \chi)}{\partial \rho_i} \right] = \lim_{\rho_i \rightarrow 0} \left[\frac{\partial^2 C_i(\rho_i, \chi)}{\partial \rho_i^2} \right] = \left. \frac{\partial^2 C_i(\rho_i, \chi)}{\partial \rho_i^2} \right|_{\rho_i=0}. \quad (23)$$

This limit is allowable since $\lim_{\rho_i \rightarrow 0} \frac{C_i(\rho_i, \chi)}{\partial \rho_i} = 0$ due to the symmetry of the concentrations around $r = 0$ (hence around $\rho_i = 0$, since ρ_i is a linear function of r).

Eqs. (20) through (23) allow Eq. (19) to be written in finite difference form as

For $\rho_i > 0$:

$$\begin{aligned}
 C_i(j, k+1) = & \left[C_i(j+1, k) \left[\frac{\Delta\chi}{(\Delta\rho)^2} + \frac{j\Delta\chi}{4} + \frac{\alpha\Delta\chi}{2j(\Delta\rho)^2} \right] + C_i(j-1, k) \right. \\
 & \left. \left[\frac{\Delta\chi}{(\Delta\rho)^2} - \frac{j\Delta\chi}{4} - \frac{\alpha\Delta\chi}{2j(\Delta\rho)^2} \right] - \frac{2\Delta\chi}{(\Delta\rho)^2} C_i(j, k) \right] \cdot \frac{1}{1+e^{-k\Delta\chi} \left[\frac{t_o^i}{t_o^1} - 1 \right]} \\
 & + C_i(j, k) + \Delta\chi t_o^1 e^{k\Delta\chi} \left[\sum_{\ell=1}^N \sum_{m=1}^{\ell} k_{\ell m}^i C_{\ell}(\rho_i, k) C_m(\rho_i, k) \right. \\
 & \left. - C_i(j, k) \sum_{\ell=1}^N \bar{k}_{i\ell} C_{\ell}(\rho_i, k) \right] + C_i(j, k) \tag{24}
 \end{aligned}$$

For $\rho_i = 0$:

$$\begin{aligned}
 C_j(0, k+1) = & \frac{2(1+\alpha)\Delta\chi}{1+e^{-k\Delta\chi} \left[\frac{t_o^i}{t_o^1} - 1 \right]} \left[\frac{C(1, k) - C(0, k)}{[\Delta\rho]^2} \right] \\
 & + t_o^1 e^{k\Delta\chi} \Delta\chi \left[\sum_{\ell=1}^N \sum_{m=1}^{\ell} k_{\ell m}^i C_{\ell}(0, k) C_m(0, k) - C_i(0, k) \sum_{\ell=1}^N \bar{k}_{i\ell} C_{\ell}(0, k) \right] \\
 & + C_i(0, k) . \tag{25}
 \end{aligned}$$

Inspection of Eq. (24) shows that another item must be considered, and that is the reaction terms of the form $C_{\ell}(\rho_i, k) C_m(\rho_i, k)$. In general,

unless the diffusion constants and initial Gaussian widths at half-maximum are the same for species ℓ and m as those for species i , no values for $C_\ell(\rho_i, k)$ and $C_m(\rho_i, k)$ will be obtainable at ρ_i due to the nature of the finite difference scheme. For this reason it is necessary to introduce some sort of interpolation scheme in order to compute the reaction terms.

Writing Eq. (13) for species i and ℓ we have

$$\rho_i = \frac{r}{\sqrt{D_i(t_o^i + t)}}, \quad (26)$$

$$\rho_\ell = \frac{r}{\sqrt{D_\ell(t_o^\ell + t)}}. \quad (27)$$

Combining Eqs. (26) and (27) to eliminate r

$$\rho_\ell = \rho_i \left[\frac{D_i(t_o^i + t)}{D_\ell(t_o^\ell + t)} \right]^{1/2}. \quad (28)$$

This last equation then essentially represents a spatial coordinate transformation from the i^{th} system to the ℓ^{th} system. Note that in general $\frac{\rho_\ell}{\Delta\rho}$ will not be an integer so that interpolation is necessary.

Since the spatial distributions encountered in this report are smoothly-varying functions, a simple second-order interpolation scheme is used. For those cases where the interpolated quantity falls outside the range considered in the numerical solution, the value is taken to be zero.

The final detail considered in this section of the report is that of how best to follow the solute concentrations in time and space. The requirements here are different from that for the radicals due to two facts: (1) solute concentration changes are primarily due to reaction rather than diffusion, and (2) the solute concentration does not go to zero far from the center of the spur or track. In order to insure that the solute concentrations are well followed in time and space, it is necessary that a spatially-increasing coordinate system be chosen for each solute. The system used in this report is

$$\rho_\ell = \frac{r}{\sqrt{D_i(t_o^i + t)}} , \quad (29)$$

where the i^{th} superscript here refers to species i. Species i is that species reacting with solute ℓ which has the largest diffusion coefficient.

If we use Eq. (29) and perform a derivation similar to the one done previously, we obtain the following finite difference equations for the solute concentrations.

For $\rho_l > 0$:

$$\begin{aligned}
 C_l(j, k+1) = & C_l(j, k) + \frac{D_l}{D_i} \frac{\Delta\chi}{1+e^{-k\Delta\chi} \left[\frac{t_o^i}{t_o^1} - 1 \right]} \cdot \left[C_l(j+1, k) \left[\frac{1}{(\Delta\rho)^2} \right. \right. \\
 & \left. \left. + \frac{j}{4} + \frac{\alpha}{2j(\Delta\rho)^2} \right] + C_l(j-1, k) \left[\frac{1}{(\Delta\rho)^2} - \frac{j}{4} - \frac{\alpha}{2j(\Delta\rho)^2} \right] - \frac{2}{(\Delta\rho)^2} C_l(j, k) \right] \\
 & + \Delta\chi t_o^1 e^{k\Delta\chi} \left[\sum_{m=1}^N \sum_{n=1}^m k_{mn}^i C_m(\rho_l, k) C_n(\rho_l, k) \right. \\
 & \left. - C_l(j, k) \sum_{m=1}^N \bar{k}_{lm} C_m(\rho_l, k) \right], \tag{30}
 \end{aligned}$$

For $\rho_l = 0$:

$$\begin{aligned}
 C_l(0, k+1) = & C_l(0, k) + \frac{D_l}{D_i} \frac{2(1+\alpha)\Delta\chi}{1+e^{-k\Delta\chi} \left[\frac{t_o^i}{t_o^1} - 1 \right]} \cdot \left[\frac{C_l(1, k) - C_l(0, k)}{(\Delta\rho)^2} \right] \\
 & + \Delta\chi t_o^1 e^{k\Delta\chi} \left[\sum_{m=1}^N \sum_{n=1}^m k_{mn}^i C_m(0, k) C_n(0, k) \right. \\
 & \left. - C_l(0, k) \sum_{m=1}^N \bar{k}_{lm} C_m(0, k) \right]. \tag{31}
 \end{aligned}$$

Note that the only difference between Eqs. (30) and (31) and Eqs. (24) and (25) is the addition of a factor $\frac{D_l}{D_i}$. In practice it is usually sufficient to set $D_i = D_l$ so that Eqs. (30) and (31) are identical with Eqs. (24) and (25) previously derived. This simplifies the programming somewhat, and will give sufficient accuracy unless D_i and D_l are quite different in value

2.3 Development of the Finite Difference Form of the Reaction Integrals

The reaction integrals give the total amount of a particular species formed or destroyed by a particular reaction and are important in calculating yields and checking the stability of the numerical solution. These integrals are given as

$$\bar{L}_{ij}(t) = \int_0^t dt \int_0^\infty dV \bar{k}_{ij} c_i(r,t) c_j(r,t) , \quad (32)$$

and

$$N_i(t) = \int_0^\infty dV c_i(r,t) , \quad (33)$$

in which $\bar{L}_{ij}(t)$ = the number of the i^{th} radicals created by reaction of species i with species j in a single spur up to time t . L_{jk}^i is the number of i^{th} radicals created with \bar{k}_{ij} replaced by k_{jk}^i ,

$N_i(t)$ = the number of radicals of species i present at time t in a single spur, or, the number of radicals per unit track length present at time t in a single track;

dV = differential volume,
 $= 4\pi r^2 dr$ for spurs,
 $= 2\pi r dr$ for tracks.

As a check on the solution obtained a material balance gives the following relationship which must hold at every time t :

$$N_i(0) = N_i(t) - \sum_{j=1}^N \bar{L}_{ij}(t) + \sum_{j=1}^N \sum_{k=1}^j L_{jk}^i(t). \quad (34)$$

Deviations from this equality are inherent in any numerical solution and the extent of deviation can only be used in a qualitative manner based upon experience to form an opinion on the actual accuracy of solution.

In order to put Eqs. (32) and (33) into a form consistent with the calculational procedure for the solution of the diffusion-kinetics equations Eqs. (12) and (13) are used in the form

$$dt = t_o^1 e^X d\chi, \quad (35)$$

$$dr = \sqrt{D_i \left[\frac{t^i}{t_o} + t_o^1 (e^X - 1) \right]} d\rho_i. \quad (36)$$

Substituting Eqs. (35) and (36) into Eqs. (32) and (33) gives

For spurs:

$$\begin{aligned} \bar{L}_{ij}(x) &= 4\pi t_o^1 (D_i)^{3/2} k_{ij} \int_0^x dx e^x \left[\frac{t^i}{t_o} + t_o^1 (e^x - 1) \right]^{3/2} \\ &\cdot \int_0^\infty d\rho_i \rho_i^2 C_i(\rho_i, x) C_j(\rho_i, x) \end{aligned} \quad (37)$$

$$N_i(\chi) = 4\pi D_i \left[t_o^i + t_o^1(e^\chi - 1) \right]^{3/2} \int_0^\infty d\rho_i \rho_i^2 C_i(\rho_i, \chi) , \quad (38)$$

For tracks:

$$\bar{L}_{ij}(\chi) = 2\pi D_i t_o^1 \bar{k}_{ij} \int_0^\chi d\chi e^\chi \left[t_o^i + t_o^1(e^\chi - 1) \right] \int_0^\infty d\rho_i \rho_i C_i(\rho_i, \chi) C_j(\rho_i, \chi) , \quad (39)$$

$$N_i(\chi) = 2\pi D_i \left[t_o^i + t_o^1(e^\chi - 1) \right] \int_0^\infty d\rho_i \rho_i C_i(\rho_i, \chi) . \quad (40)$$

In order to numerically evaluate these integrals they are written in the following form

$$\bar{L}_{ij} = \sum_{m=1}^M \Delta\chi \int_0^\infty d\rho_i F_i C_i(\rho_i, m\Delta\chi) C_j(\rho_i, m\Delta\chi) \bar{k}_{ij} t_o^1 e^{m\Delta\chi} , \quad (41)$$

$$N_i(\chi) = \int_0^\infty d\rho_i F_i C_i(\rho_i, \chi) , \quad (42)$$

where $M = \chi/\Delta\chi$, an integer,

$$F_i = 4\pi D_i \left[t_o^i + t_o^1(e^{m\Delta\chi} - 1) \right]^{3/2} \quad \text{for spurs,}$$

$$= 2\pi D_i \left[t_o^i + t_o^1(e^{m\Delta\chi} - 1) \right] \quad \text{for tracks .}$$

In order to evaluate the volume integrals, a second-order numerical scheme is used (see explanation of "FATES" subroutine elsewhere in this report) which gives a weighting factor WNR(ℓ) such that Eqs. (41) and (42) can be written as

$$\bar{L}_{ij}(x) = \sum_{m=1}^M \Delta x \sum_{\ell=1}^{\infty} F_i C_i(\ell, m) C_j(\rho_i, m) \bar{k}_{ij} t_o^1 e^{m \Delta x} WNR(\ell) , \quad (43)$$

$$N_i(x) = \sum_{\ell=1}^{\infty} F_i C_i(\ell, M) WNR(\ell) . \quad (44)$$

Once again we notice that in general the term $C_j(\rho_i, m)$ will not have tabulated values so that interpolation is necessary. In this case, however, the quantity $C_i(\ell, m) C_j(\rho_i, m)$ has previously been calculated in the solution of the diffusion-kinetics equations so that it is only necessary to use this value.

2.4 Stability of the Finite Difference Form
of the Diffusion-Kinetics Equations

Since the exact analysis of the stability of the given set of nonlinear partial differential equations used in this report is extremely difficult if not impossible, stability criteria will be determined only for the case where there are no reaction terms. The possible effects of the reaction terms will then be discussed in a qualitative fashion.

Writing Eqs. (24) and (25) in matrix form without reaction terms,

$$\bar{C}_i(k+1) = \bar{B}_i \bar{C}_i(k) , \quad (45)$$

where

$$\bar{C}_i(k) = \begin{bmatrix} C_i(0,k) \\ C_i(1,k) \\ C_i(2,k) \\ \vdots \\ \vdots \\ \vdots \end{bmatrix} \quad (46)$$

$$\bar{B}_i = \begin{bmatrix} -2(1+\alpha)\Delta\chi & 2(1+\alpha)\Delta\chi & 0 & \dots \\ \frac{(\Delta\rho)^2}{1+e^{-k\Delta\chi}} \begin{bmatrix} t_o^i & -1 \\ t_o^1 & \end{bmatrix} + 1 & \frac{(\Delta\rho)^2}{1+e^{-k\Delta\chi}} \begin{bmatrix} t_o^i & -1 \\ t_o^1 & \end{bmatrix} & & \\ \Delta\chi \left[\frac{1}{(\Delta\rho)^2} - \frac{1}{4} - \frac{\alpha}{2(\Delta\rho)^2} \right] & \frac{-2\Delta\chi/(\Delta\rho)^2}{1+e^{-k\Delta\chi}} \begin{bmatrix} t_o^i & -1 \\ t_o^1 & \end{bmatrix} + 1 & \frac{\Delta\chi \left[\frac{1}{(\Delta\rho)^2} + \frac{1}{4} + \frac{\alpha}{2(\Delta\rho)^2} \right]}{1+e^{-k\Delta\chi}} \begin{bmatrix} t_o^i & -1 \\ t_o^1 & \end{bmatrix} & 0 \dots \\ 1+e^{-k\Delta\chi} \begin{bmatrix} t_o^i & -1 \\ t_o^1 & \end{bmatrix} & & & \\ 0 & \frac{\Delta\chi \left[\frac{1}{(\Delta\rho)^2} - \frac{1}{2} - \frac{\alpha}{4(\Delta\rho)^2} \right]}{1+e^{-k\Delta\chi}} \begin{bmatrix} t_o^i & -1 \\ t_o^1 & \end{bmatrix} & \frac{-2\Delta\chi/(\Delta\rho)^2}{1+e^{-k\Delta\chi}} \begin{bmatrix} t_o^i & -1 \\ t_o^1 & \end{bmatrix} & \dots \\ & & & \\ & & & \\ & & & \end{bmatrix} \quad (47)$$

Now a necessary and sufficient condition for stability of the given set of equations is that all of the eigenvalues, λ , of the matrix \bar{B}_i satisfy the relationship $|\lambda| \leq 1$. In order to obtain bounds on the eigenvalues we can use the Gershgorin theorem which states that the largest eigenvalue is equal to or less than the maximum value of the sum of the magnitudes of the elements in any row. That is, if $\bar{B}_i = (b_{jk})_i$,

then

$$[\lambda_{\max}]_i \leq \max_j \sum_k [b_{jk}]_i . \quad (48)$$

Applying this theorem to the first row we have

$$\frac{\Delta X}{(\Delta\rho)^2} \leq \frac{1}{2(1+\alpha) \left[1 + e^{-k\Delta X} \left[\begin{matrix} t_o^i & -1 \\ t_o^1 & -1 \end{matrix} \right] \right]^{-1}} . \quad (49)$$

Applying this theorem to the j^{th} row we have

$$\frac{\Delta X}{(\Delta\rho)^2} \leq \frac{1}{2 \left[1 + e^{-k\Delta X} \left[\begin{matrix} t_o^i & -1 \\ t_o^1 & -1 \end{matrix} \right] \right]^{-1}} . \quad (50)$$

In order to obtain Eqs. (49) and (50) it was necessary to assume that

$$t_o^i \geq t_o^1 . \quad (51)$$

It is also easily seen that the most limiting requirement is that given by Eq. (49) so that this is the criterion used.

Now it is obvious that the smallest value for the term on the right-hand-side of Eq. (49) is obtained when the value of k is infinite. This gives the criterion that must be met as

$$\frac{\Delta x}{(\Delta \rho)^2} \leq \frac{1}{2(1+\alpha)} . \quad (52)$$

For the case where $\alpha = 2$, this requirement may be too restrictive. This can be seen by noting that in this case, the magnitude of the first term in the second row of matrix \bar{B}_i will become $= \Delta x / 4$ which will be of the order 0.01 or so. If we take this value to be identically zero in comparison to the magnitudes of the rest of the quantities in the matrix, the stability criterion becomes

$$\frac{\Delta x}{(\Delta \rho)^2} \leq \frac{1}{3} . \quad (53)$$

The criterion given by Eq. (53) is probably more realistic than that given by Eq. (52) for spur calculations.

It is also of interest to compare the criteria obtained here with that obtained by Kuppermann (5) for the case where finite differences were used directly with the original diffusion-kinetics equations in time, t , and space, r . From Eqs. (12) and (13) we obtain the following transformation

$$\frac{D_i dt}{(dr)^2} = \frac{t_o^1 e^X}{t_o^i - t_o^1 + t_o^1 e^X} \frac{dx}{(d\rho_i)^2} . \quad (54)$$

If we let $i = 1$ and replace the derivatives with finite difference approximations we have

$$\frac{D_1 \Delta t}{(\Delta r)^2} \approx \frac{\Delta x}{(\Delta p)^2} . \quad (55)$$

Since the equality given by Eq. (55) is approximately true, it follows that the criterion given by Eqs. (52) and (53) should be very nearly the same as that given by Kuppermann for the quantity $\frac{D_1 \Delta t}{(\Delta r)^2}$. This would probably not be the case, however, if the type of finite difference scheme used by Kuppermann was significantly different than that used here.

It can be seen by referring to Kuppermann's paper that the set of criteria are in fact identical for the case where $i = 1$, thus further substantiating the validity of using Eq. (53) for spur calculations.

Before proceeding to a general discussion of stability with reaction terms present, it is necessary to show the change in the stability criteria obtained if the following more accurate approximation to the time derivative were used:

$$\frac{\partial C_i(p_i, x)}{\partial x} \approx \frac{C_i(j, k+1) - C_i(j, k-1)}{2\Delta x} . \quad (56)$$

This approximation will cause two changes in Eqs. (24) and (25). All of the terms on the right side of these equations will be multiplied by two except for the $C_i(j, k)$ term, which will be replaced by $C_i(j, k-1)$. If we

now assume that the following relation holds everywhere

$$C_i(j,k-1) = \beta_{jk} C_i(j,k) , \quad (57)$$

where β_{jk} is a number very close to one, we have a set of equations of the form given by Eq. (45) and can obtain the stability criterion as

$$\frac{\Delta x}{(\Delta \rho)^2} \leq \frac{1}{4(1+\alpha)} . \quad (58)$$

Comparison of Eq. (58) with Eq. (52) shows that the more accurate approximation effectively doubles the number of time mesh points needed for a given spatial increment in order for the stability criterion to be satisfied. This is a major reason for using the less accurate finite difference approximation.

Concerning the influence of the reaction terms on the stability of the solution, a few generalities can be obtained if the reaction terms are written in the form

$$C_i(j,k) G_i(j,k) = \Delta x t_o^1 e^{k \Delta x} \sum_{\ell=1}^N \sum_{m=1}^{\ell} k_{\ell m}^i C_{\ell}(\rho_i, k) C_m(\rho_i, k) - C_i(j,k) \sum_{\ell=1}^N \bar{k}_{i\ell} C_{\ell}(\rho_i, k) , \quad (59)$$

where it is assumed that it possible somehow to determine $G_i(j,k)$.

The stability criterion obtained for this case is given as:

$$\frac{\Delta x}{(\Delta \rho)^2} \leq \frac{2 - \max |G_i(j,k)|}{4(1+\alpha)} \left[1 + e^{-k\Delta x} \begin{bmatrix} \frac{t^i_0}{t^1_0} & -1 \\ t^1_0 & 1 \end{bmatrix} \right] \quad (60)$$

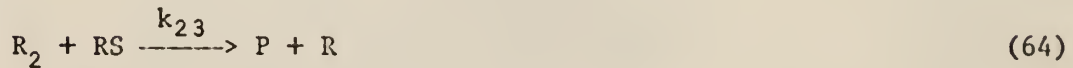
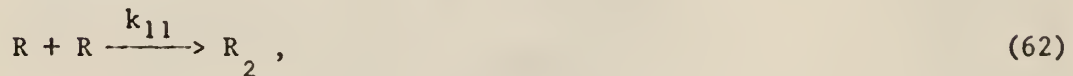
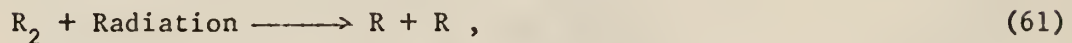
From Eq. (60) it is easy to see that in order to keep the original stability criterion valid, $\max |G_i(j,k)|$ must remain small in comparison to unity. Physically this means that the change in the spatial concentration profile from one time step to the next caused by reaction must be small, at least in the regions where the concentrations of the various species are large so that the possible growth of errors can cause a significant error in the final answer. The maximum allowable value for $G_i(j,k)$ is determined once a value is chosen for $\frac{\Delta x}{(\Delta \rho)^2}$. In actual practice, however, it is usually sufficient to set a value for $\Delta \rho$ and determine Δx from Eq. (60) for the case of $j = k = 0$ (that is, from the given initial conditions in the center of the spur or track where the reaction rate is greatest). This procedure will be sufficient generally for the entire solution for the case where the reaction rates continually cause decreases in the values of the concentrations of all the species since the absolute value of $G_i(j,k)$ will generally decrease. Unfortunately, the opposite is also generally true for the case where the reaction rates cause the concentration of one or more species to increase. For this case, it may become mandatory to change the value of Δx several times

during the course of the solution in order to keep the errors within a desired level. The decision about what type of computation scheme to use for any particular reaction scheme can only be reached after much consideration and experimentation.

For the reaction scheme considered in this report, it is sufficient to determine a value for Δx from Eq. (60) for $j = k = 0$ and to leave this value unchanged throughout the entire calculation.

2.5 The Reaction Scheme Considered and
 Development of the Equations Describing the
 Rate of Product Formation as a Function of
 Dose Rate

The reaction mechanism considered in this report is given by the following set of equations



where R = a free radical,

R_2 = a solute,

S = a solute,

P = a final product,

RS = an intermediate product,

k_{11} = rate constant for reaction (62),

k_{14} = rate constant for reaction (63),

k_{23} = rate constant for reaction (64).

The first equation represents the formation of free radicals by radiolysis of the solute, R_2 , to give the initial Gaussian distribution of free

radicals used in the calculations. The consequences of this reaction appear in the initial conditions. The second equation describes the radical recombination, or chain-breaking, reaction. The last two equations describe the chain propagation step.

Letting a bracket denote the concentration of each of the species, the diffusion kinetic equations to be solved are

$$\frac{\partial [R]}{\partial t} = D_R \nabla^2 [R] - k_{11}[R]^2 - k_{14}[R][S] + k_{23}[R_2][RS], \quad (65)$$

$$\frac{\partial [R_2]}{\partial t} = D_{R_2} \nabla^2 [R_2] + \frac{1}{2}k_{11}[R]^2 - k_{23}[R_2][RS], \quad (66)$$

$$\frac{\partial [S]}{\partial t} = D_S \nabla^2 [S] - k_{14}[R][S], \quad (67)$$

$$\frac{\partial [RS]}{\partial t} = D_{RS} \nabla^2 [RS] + k_{14}[R][S] - k_{23}[R_2][RS], \quad (68)$$

$$\frac{d[P]}{dt} = D_P \nabla^2 [P] + k_{23}[R_2][RS]. \quad (69)$$

In order to describe the formation-of-product rate as a function of dose rate for the reaction scheme considered it is necessary to integrate over spatial dependence of Eqs. (65) through (69). Applying the spherical volume integral to the diffusion term in Eq. (65) we have

$$\int_V dV D_R \nabla^2 [R] = 4\pi D_R \int_0^\infty dr r^2 \frac{\partial^2 [R]}{\partial r^2} + 8\pi D_R \int_0^\infty dr r \frac{\partial [R]}{\partial r} . \quad (70)$$

Integrating the first integral on the right side of Eq. (70) gives

$$\int_0^\infty dr r^2 \frac{\partial^2 [R]}{\partial r^2} = r^2 \frac{\partial [R]}{\partial r} \Big|_0^\infty - 2 \int_0^\infty r dr \frac{\partial [R]}{\partial r} . \quad (71)$$

Substituting Eq. (71) into (70) gives

$$\int_0^\infty dV D_R \nabla^2 [R] = 4\pi D_R r^2 \frac{\partial [R]}{\partial r} \Big|_0^\infty . \quad (72)$$

For the cases of either Gaussian conditions or solutes it is seen that

$$\lim_{r \rightarrow 0} r^2 \frac{\partial [R]}{\partial r} = \lim_{r \rightarrow \infty} r^2 \frac{\partial [R]}{\partial r} = 0 \quad (73)$$

Therefore Eq. (72) becomes

$$\int_V dV D_R \nabla^2 [R] = 0. \quad (74)$$

For each of the reaction terms we make the following definition for brace notation

$$\{[R][S]\} \equiv \int_V dV [R][S] . \quad (75)$$

This gives for the set of differential equations

$$\frac{d\{[R]\}}{dt} = -k_{11}\{[R]^2\} - k_{14}\{[R][S]\} + k_{23}\{[R_2][RS]\} , \quad (76)$$

$$\frac{d\{[R_2]\}}{dt} = \frac{1}{2}k_{11}\{[R]^2\} - k_{23}\{[R_2][RS]\} , \quad (77)$$

$$\frac{d\{[S]\}}{dt} = -k_{14}\{[R][S]\} , \quad (78)$$

$$\frac{d\{[RS]\}}{dt} = k_{14}\{[R][S]\} - k_{23}\{[R_2][RS]\} , \quad (79)$$

$$\frac{d\{[P]\}}{dt} = k_{23}\{[R_2][RS]\} . \quad (80)$$

For the case of low dose rates we will assume that the chain length is large so that a near steady state position will be reached with respect to the intermediate product, RS. This means that the radical recombination is negligible and a balance is reached where the total number of radicals and intermediate product, RS, remain nearly unchanged with time. For this case we set

$$\frac{d\{[RS]\}}{dt} = 0 = k_{14}\{[R][S]\} - k_{23}\{[R_2][RS]\} . \quad (81)$$

Substituting into Eq. (69) gives

$$\frac{d\{[P]\}}{dt} = k_{14}\{[R][S]\}. \quad (82)$$

If we now assume that the total amount of solute, S, remains approximately spatially constant at a concentration $[S]_0$ we have

$$\frac{d\{[P]\}}{dt} = k_{14}[S]_0\{[R]\}. \quad (83)$$

This gives the rate of production of the product as a function of the solute concentration and the total number of radicals present when steady state is reached. Since $\{[R]\}$ is not a function of time at steady state it follows that the total rate for a system containing n spurs will simply be n times the rate for one spur. Letting I be the dose rate (energy absorbed by the system per unit mass per unit time), $2w$ be the energy required to produce a radical pair, μ be the density of the system, and α be the ratio of the number of unrecombined radicals in a spur at steady state (steady state here referring to the time at which the radical recombination reaction becomes negligible in comparison to the other reactions) to the number initially present, we have for the total rate of production of product species per unit volume

$$\frac{d}{dt}\{[P]\}_T = k_{14} \frac{\alpha \mu I}{w} [S]_0, \quad (84)$$

where t = time since beginning of irradiation.

This shows that for low dose rates the rate of product formation is proportional to the total dose, I_t , received up to time t , since we have assumed that the chain reactions in each spur are unterminating. In actuality, the chains will be terminated at some time, giving a total number of product molecules for each spur. For this case, the product formation rate would be proportional to the dose rate.

Another method for treating this case which is somewhat more valid is to consider the reaction as consisting of a diffusion-kinetics portion followed by homogeneous kinetics. For the diffusion-kinetics portion, if \bar{t} is the time at which $N_R(t)$ levels off, at which time we have the defined quantities $N_P^T \equiv N_P^T(\bar{t})$, $\bar{N}_R \equiv N_R(\bar{t})$, $\bar{N}_{RS} \equiv N_{RS}(\bar{t})$. If ϵ is defined as the energy deposited per spur then the number of spurs per cm^3 per second is equal to $\mu I / \epsilon$, and if N_A is Avagadro's number, so the product rate of formation for the spur reaction is given by

$$\frac{d[P]}{dt} = 10^3 \frac{\mu I}{\epsilon N_A} \bar{N}_P^T \equiv K \bar{N}_P^T . \quad (85)$$

For the subsequent homogeneous reaction we have the rate equations

$$\frac{d[R]}{dt} = K \bar{N}_R - k_{11} [R]^2 - k_{14} [R][S] + k_{23} \frac{[R][RS]}{2} , \quad (86)$$

$$\frac{d[RS]}{dt} = \bar{N}_{RS} + k_{14}[R][S] - k_{23}[R_2][RS]. \quad (87)$$

Since at steady state $\frac{d[R]}{dt} = 0$ and $\frac{d[RS]}{dt} = 0$ Eqs. (86) and (87) lead to

$$[R] = \left[\frac{K}{k_{11}} (\bar{N}_R + \bar{N}_{RS}) \right]^{\frac{1}{2}}. \quad (88)$$

Substituting this into the product rate equation given analogously to Eq. (83) but for homogeneous reaction as

$$\frac{d[P]}{dt} = k_{14}[S][R], \quad (89)$$

we have

$$\frac{d[P]}{dt} = k_{14}[S] \left[\frac{K}{k_{11}} (\bar{N}_R + \bar{N}_{RS}) \right]^{\frac{1}{2}} \quad (90)$$

The overall rate is then equal to the sum of the rates from the homogeneous reaction and the spur reactions

$$\frac{d[P]}{dt} = \bar{N}_P^T + k_{14}[S] \left[\frac{K}{k_{11}} (\bar{N}_R + \bar{N}_{RS}) \right]^{\frac{1}{2}} \quad (91)$$

The important observation from Eq. (91) is that at low dose rates,

the product rate of formation is equal to the sum of a term linearly-dependent on the dose rate and a term with a square root dependence on the dose rate and a linear dependence on the solute concentration. This derivation is only valid, however, where the depletion of R_2 and S is negligible.

For the case of high dose rates, the radiation can be considered as distributed uniformly so that homogeneous kinetics alone apply. The equations describing the system are the same as those given previously without the brackets. When steady state is reached in this case, the time rate of change of radical concentration and the time rate of change of intermediate concentration will be zero. The losses in radicals will be balanced by the production from radiation initiation with a rate $\mu I/w$. Setting the rate of radical production equal to zero

$$\mu I/w - k_{11}[R]^2 - k_{14}[R][S] + k_{23}[R_2][RS] = 0. \quad (92)$$

Setting the intermediate product rate of formation equal to zero

$$k_{14}[R][S] - k_{23}[R_2][RS] = 0. \quad (93)$$

Combining Eqs. (80), (92) and (93) gives (with braces deleted)

$$\frac{d[P]}{dt} = k_{14}[S] \left[\frac{\mu I}{w k_{11}} \right]^{\frac{1}{2}} . \quad (94)$$

In this case we see that the rate of product formation is proportional to the square root of the radiation intensity, and is also proportional to the solute concentration.

3.0 DISCUSSION AND RESULTS

The parameters that may be varied in the solution of Eqs. (65) through (69) are

- 1) geometry,
- 2) initial solute concentrations,
- 3) initial free radical spatial distribution,
- 4) rate constants,
- 5) diffusion coefficients,
- 6) initial number of radicals.

In this report only variations of initial solute concentrations, rate constants, and initial number of radicals are considered. The geometry is taken to be spherically-symmetric, the initial free radical distribution is taken as Gaussian of a fixed size, and the same value is used for all the diffusion coefficients. Even with these simplifications, the variations of the other parameters must be severely restricted because of the magnitude of computer time necessary for the numerical solution of Eqs. (65) through (69). For this reason, care must be used in selection of values for the parameters so that the maximum amount of information can be obtained. A table of the parameters used in this study is given in Table I. For all the runs, the values of the diffusion coefficients were taken as

$$D = 2 \times 10^{-5} \text{ cm}^2/\text{sec}, \quad (95)$$

and the value of the parameter representing the size of the spur initially is taken as

$$R_o = 7.07 \text{ } \text{\AA} . \quad (96)$$

These particular values are chosen as being representative of those encountered in many reaction schemes.

For the set of parameters listed in Table I, a digital computer

TABLE I. LIST OF RUNS AND THE VALUES OF THE PARAMETERS

Run Number	k_{11}	k_{14}	k_{23}	N_o	$[R_2]_o$	$[S]_o$
1	10^{-11}	10^{-11}	10^{-11}	6	10^{-2}	10^{-2}
2	"	"	"	"	10^{-1}	10^{-1}
3	"	"	"	"	1	1
4	"	"	"	"	10	10
5	"	"	"	"	10^{-1}	1
6	"	"	"	"	1	10^{-1}
7	"	"	"	9	10^{-1}	"
8	"	"	"	12	"	"
9	10^{-13}	"	"	6	"	"
10	10^{-11}	10^{-13}	"	"	"	"
11	"	10^{-11}	10^{-9}	"	"	"
12	"	10^{-9}	10^{-11}	"	"	"

Note: The units for k are $\text{cm}^3/\text{molecule-sec}$; the units for N_o are radicals; the units for R_2 and S are moles/liter.

solution of Eqs. (65) through (69) lists spatially-distributed values of the concentrations of the various species as well as values for the reaction losses and total number of radicals at various times. As the computer output contains thousands of values, the best method of representing the data is graphically. Figures 1 through 12 show plots of the following quantities versus time:

$2N_{R_2}^T(t)$: twice the total number of R_2 molecules that have been formed by radical recombination up to time t ,

$N_{RS}^T(t)$: the total number of RS molecules that have been formed by reaction up to time t ,

$N_P^T(t)$: the total number of P molecules that have been formed by reaction up to time t ,

$N_R(t)$: the total number of radicals that exist at time t ,

$\Sigma_R(t)$: the sum of the reaction loss terms and the number of radicals existing at time t .

Figures 13 through 16 show sample plots of the spatial variation of the concentrations of the diffusing species as a function of time. Note that these quantities are plotted versus the dimensionless quantity ρ , rather than radial distance. Also note that, since all of the diffusion coefficients are the same and there is only one radical species, there is a one-to-one correspondence between the radial position determined by the same value for ρ for each plot.

The information given by Figures 13 through 16 is useful in understanding the physical process of the reaction system. Figure 13 shows

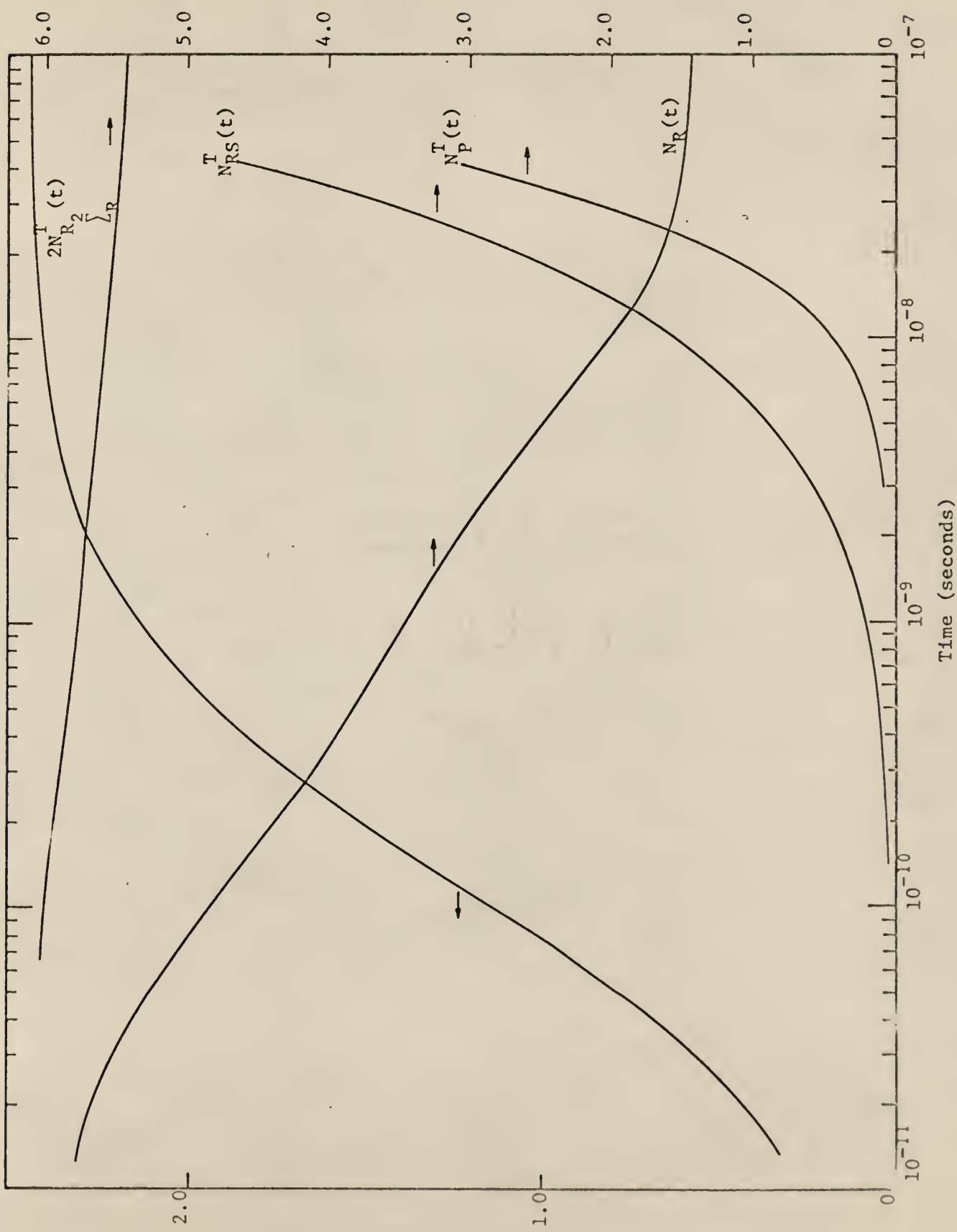


Fig. 1. Variation of $2N_{R_2}^T(t)$, $\sum_R N_{RS}^T(t)$, $N_p^T(t)$, and $N_R(t)$ with time for the parameters given for Run 1

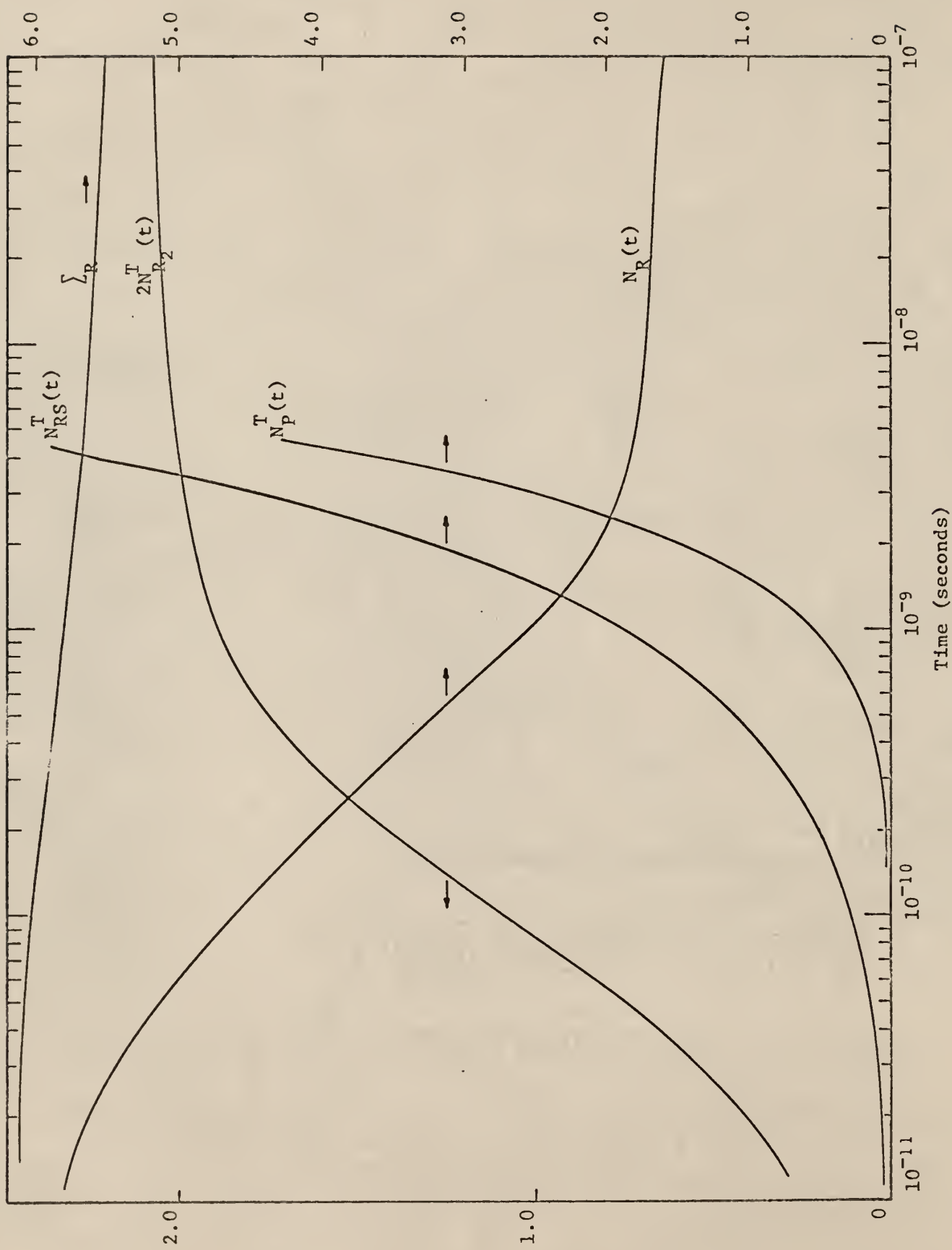


Fig. 2. Variation of $2N_{R_2}^T(t)$, \sum_R , $N_{RS}^T(t)$, $N_P^T(t)$, and $N_R(t)$ with time for the parameters given for Run 2

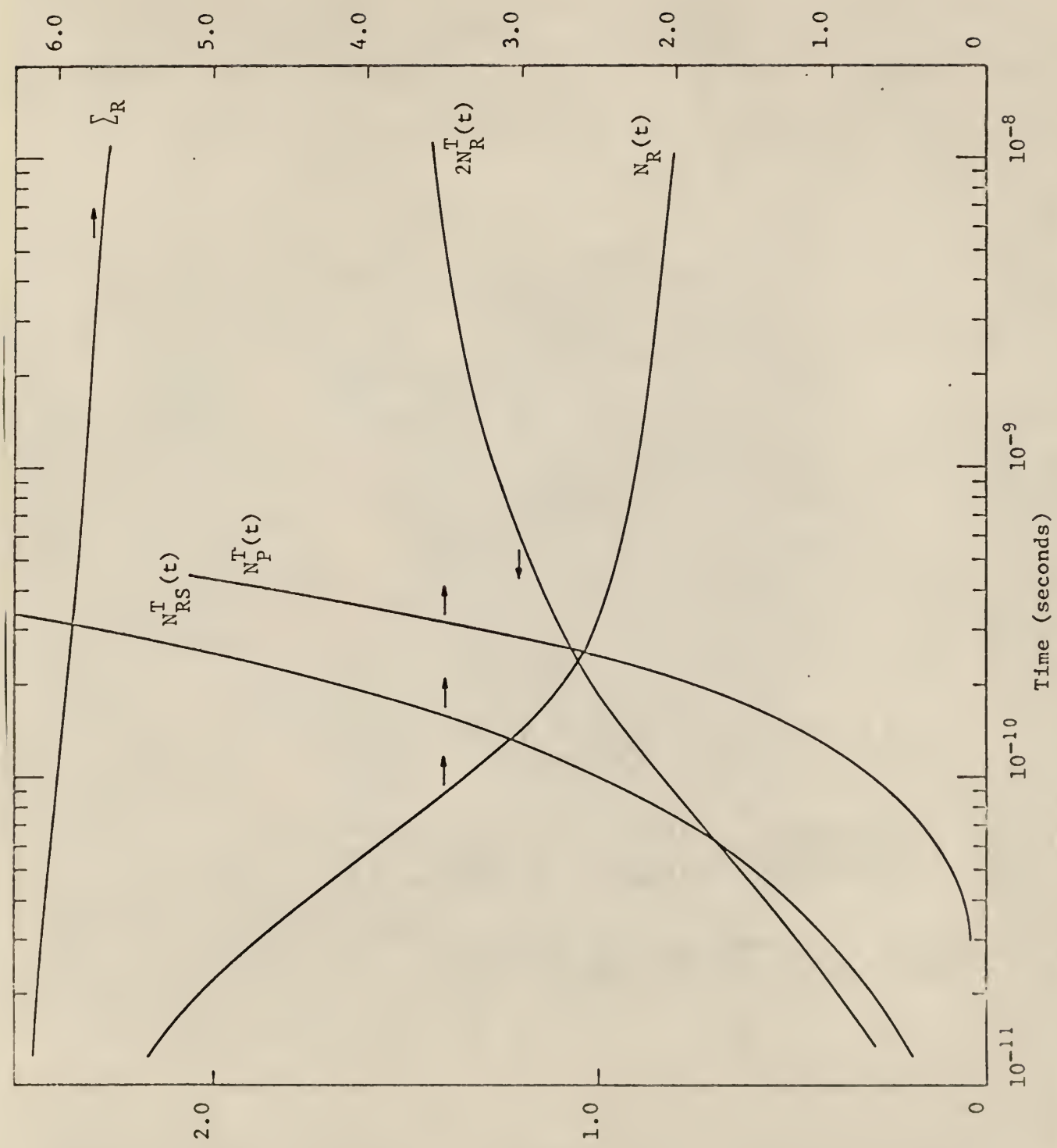


Fig. 3. Variation of $2N_{R_2}^T(t)$, $\sum_R N_{RS}^T(t)$, $N_P^T(t)$, and $N_R(t)$ with time for the parameters given for Run 3.

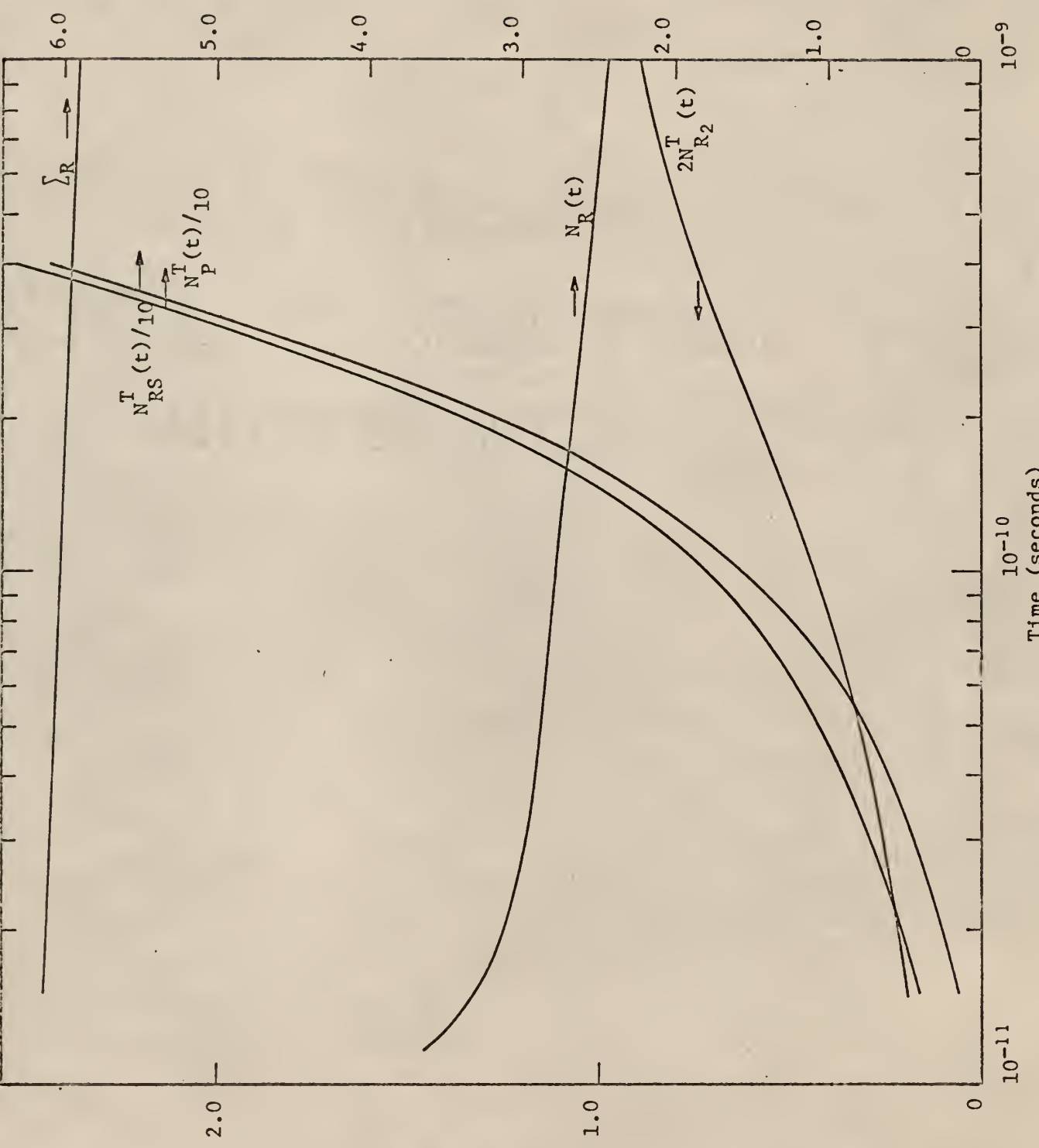


Fig. 4. Variation of $2N_{R_2}^T(t)$, Σ_R , $N_{RS}^T(t)$, $N_P^T(t)$, and $N_R(t)$ with time for the parameters given for Run 4

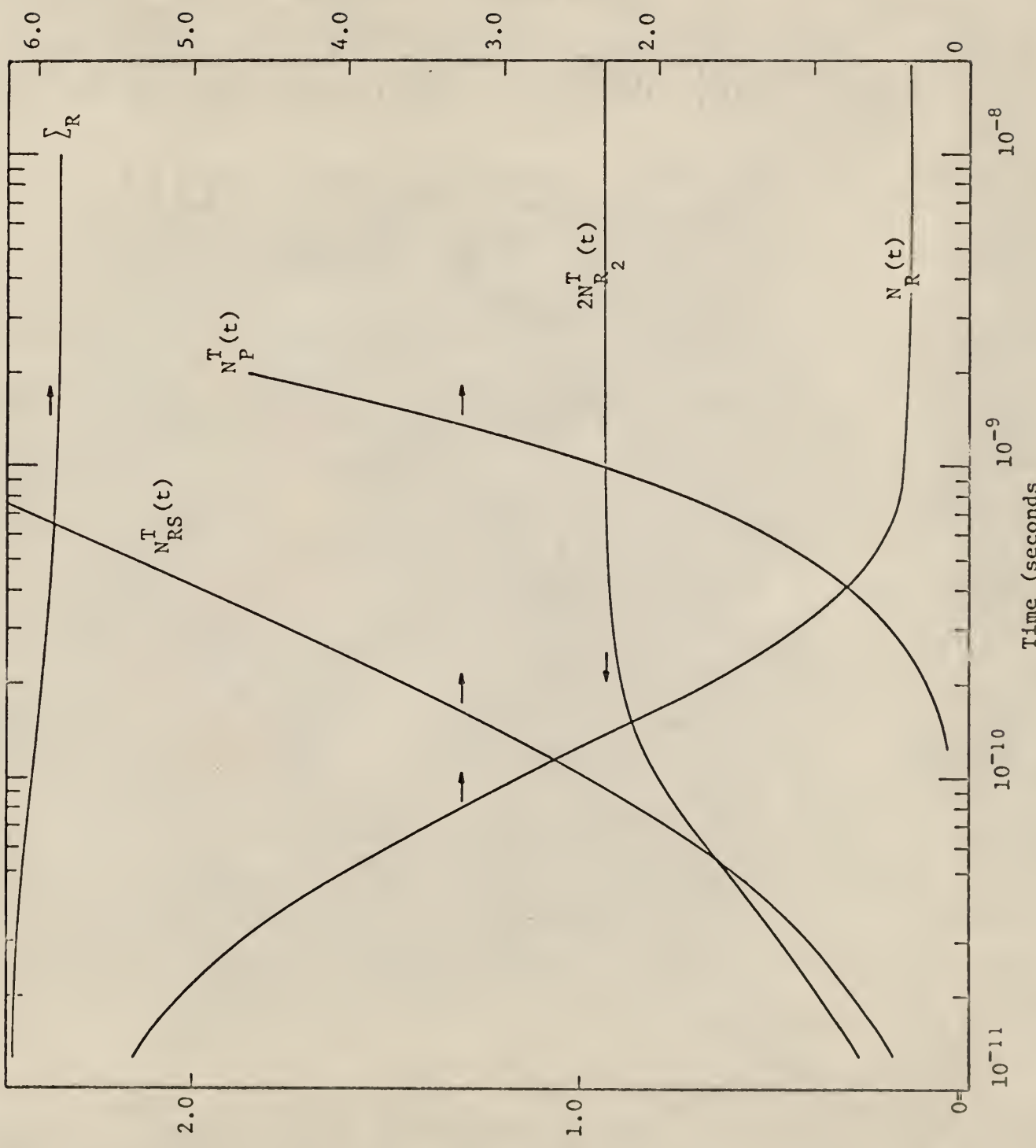
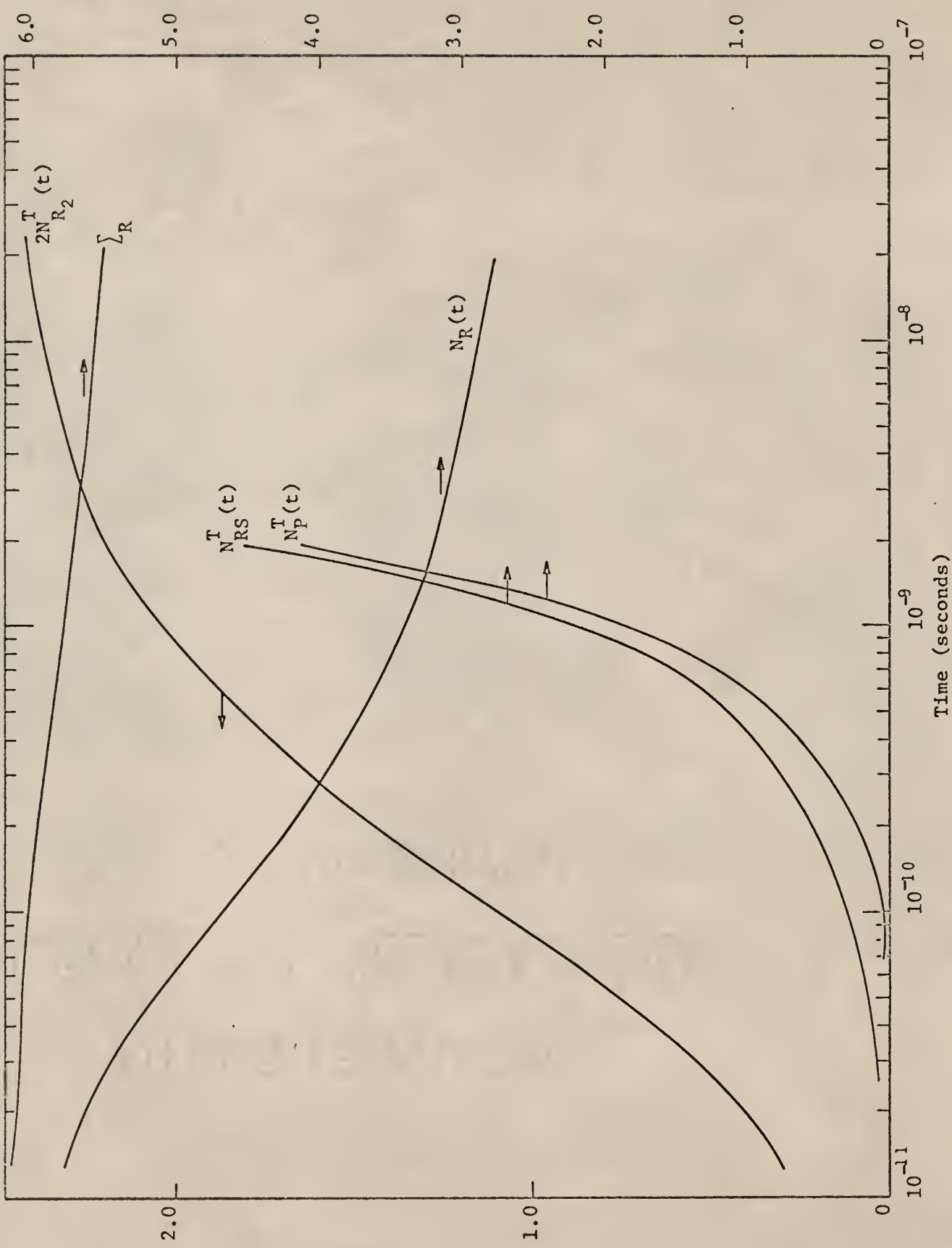


Fig. 5. Variation of $2N_{R_2}^T(t)$, \sum_R , $N_{RS}^T(t)$, $N_P^T(t)$, and $N_R(t)$ with time for the parameters given for Run 5

Fig. 6. Variation of $2N_{R_2}^T(t)$, $\sum_R N_{RS}(t)$, $N_p^T(t)$, and $N_R(t)$ with time for the parameters given for



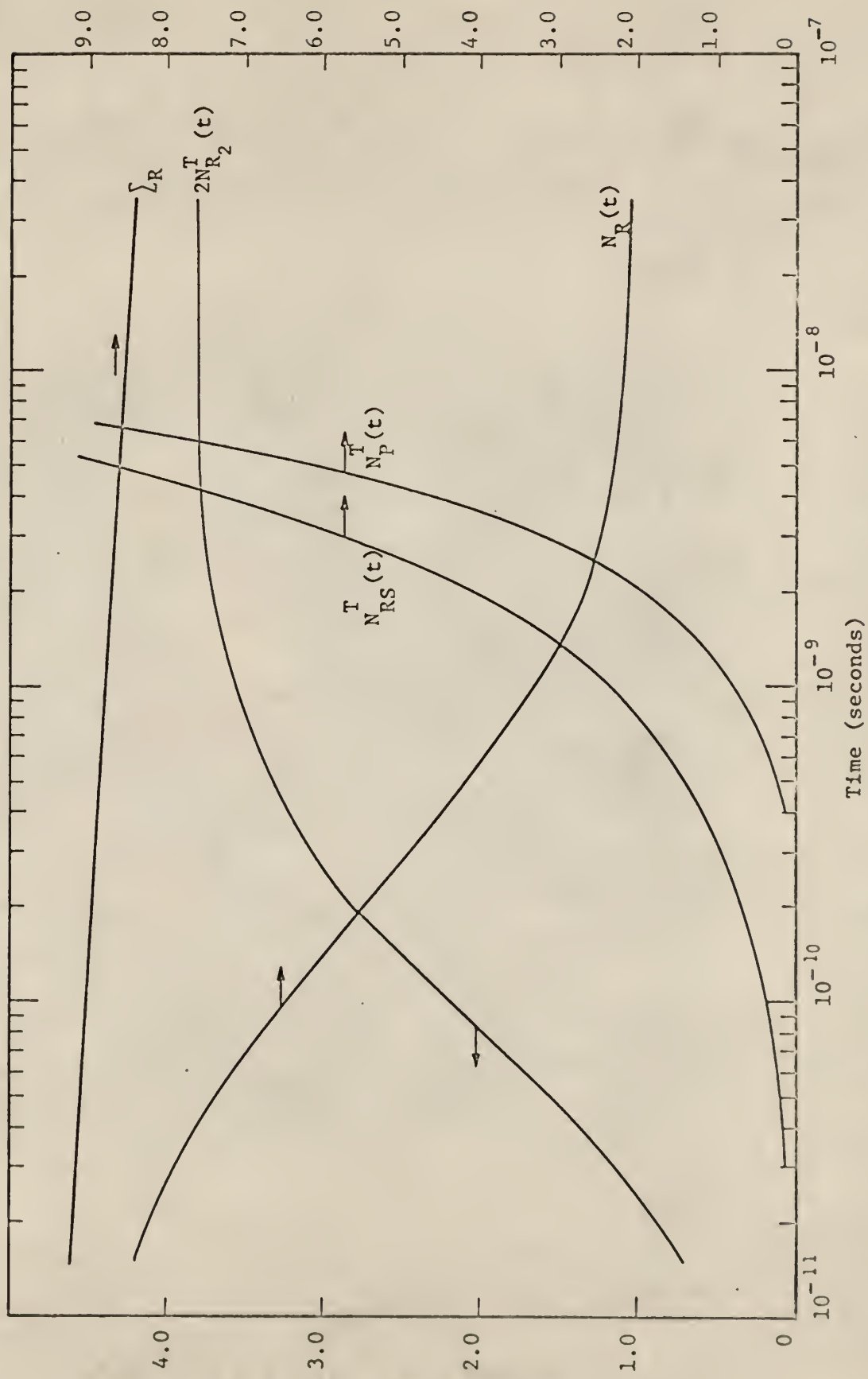
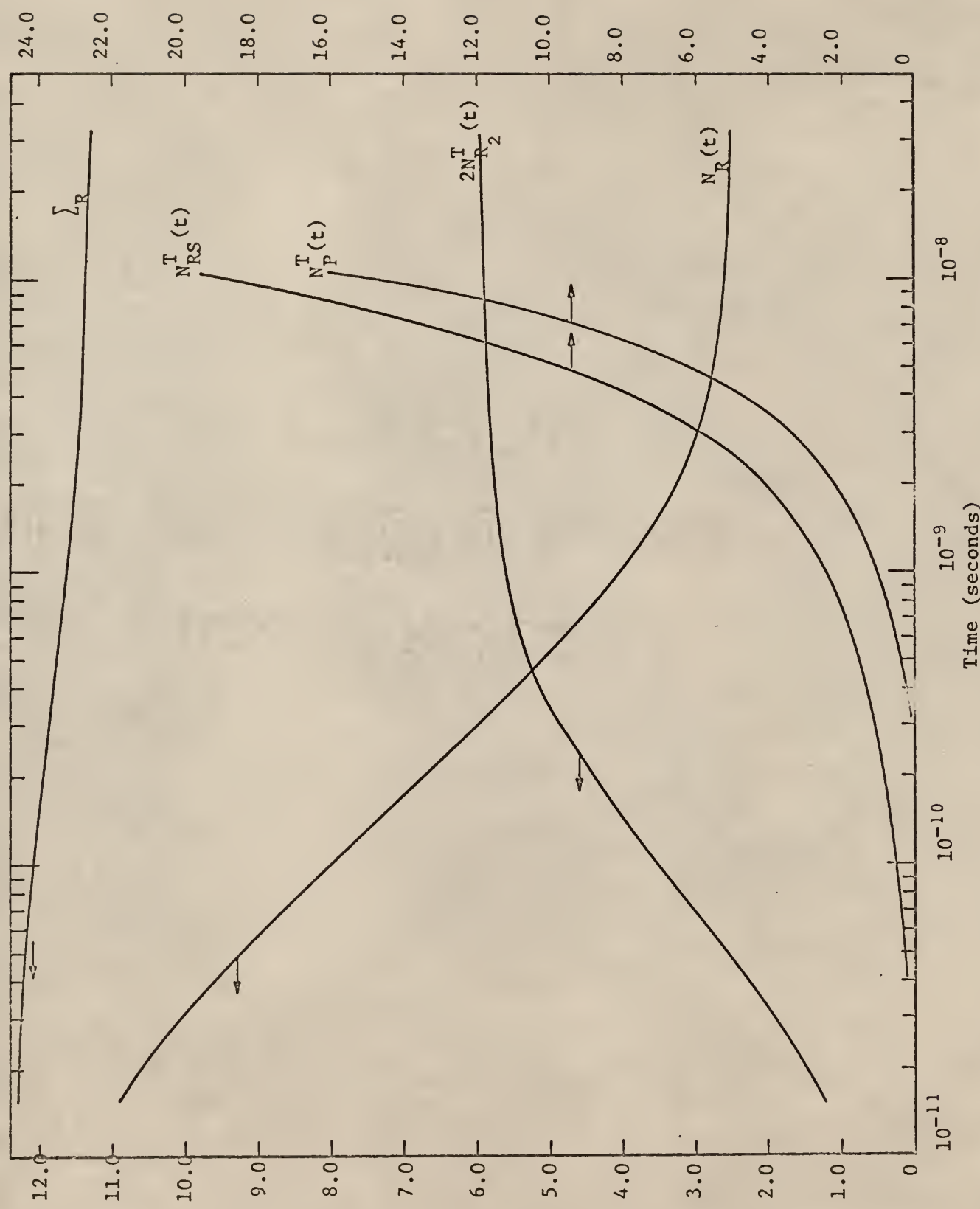


Fig. 7. Variation of $2N_{R2}^T(t)$, \sum_R , $N_{RS}^T(t)$, $N_p^T(t)$, and $N_R(t)$ with time for the parameters given for Run 7

Run 8

Fig. 8. Variation of $2N_{R_2}^T(t)$, $\sum_R N_{RS}^T(t)$, $N_P^T(r)$, and $N_R(t)$ with time for the parameters given for



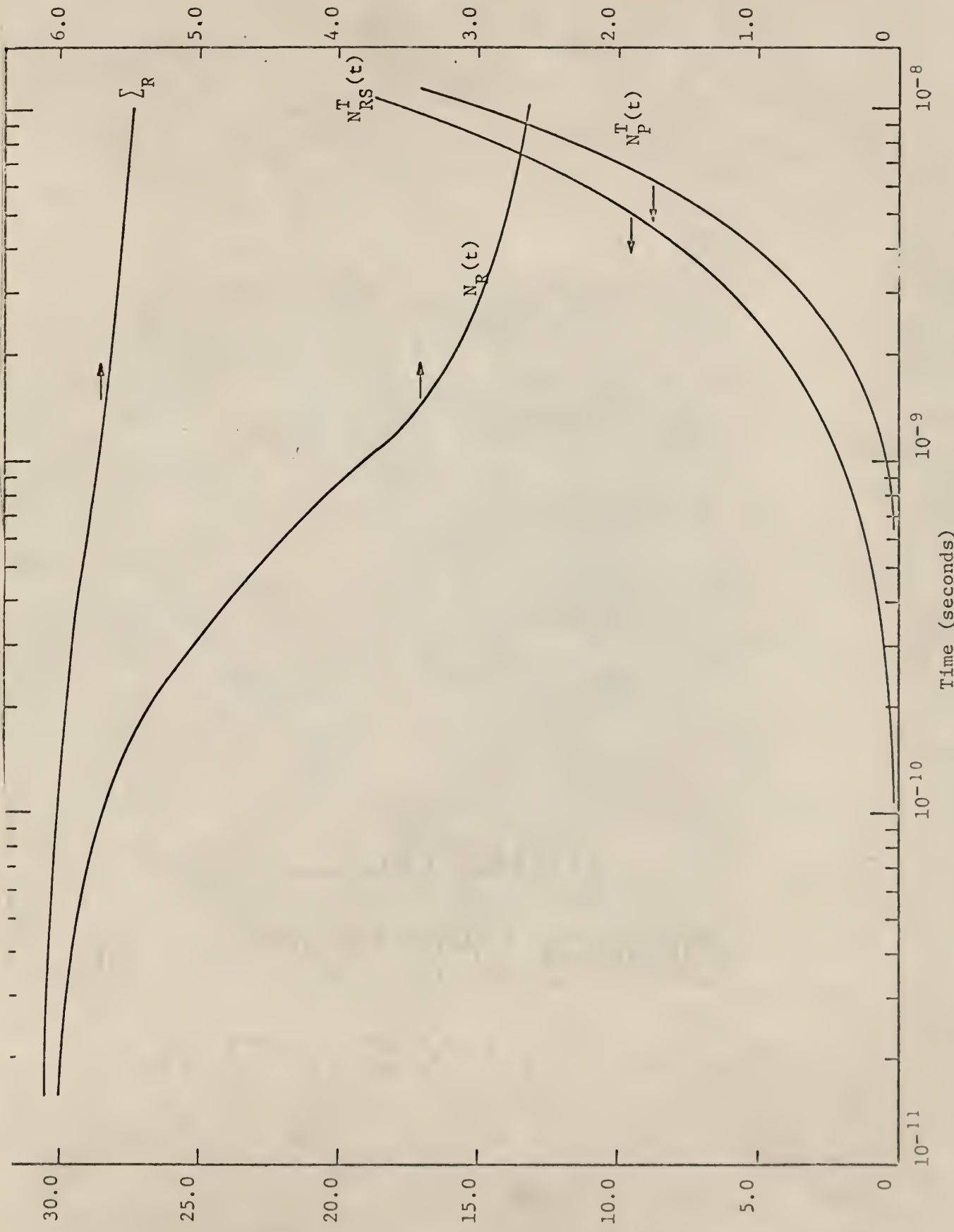


Fig. 9. Variation of \sum_R , $N_{RS}^T(t)$, $N_P^T(t)$, and $N_R(t)$ with time for the parameters given for Run 9

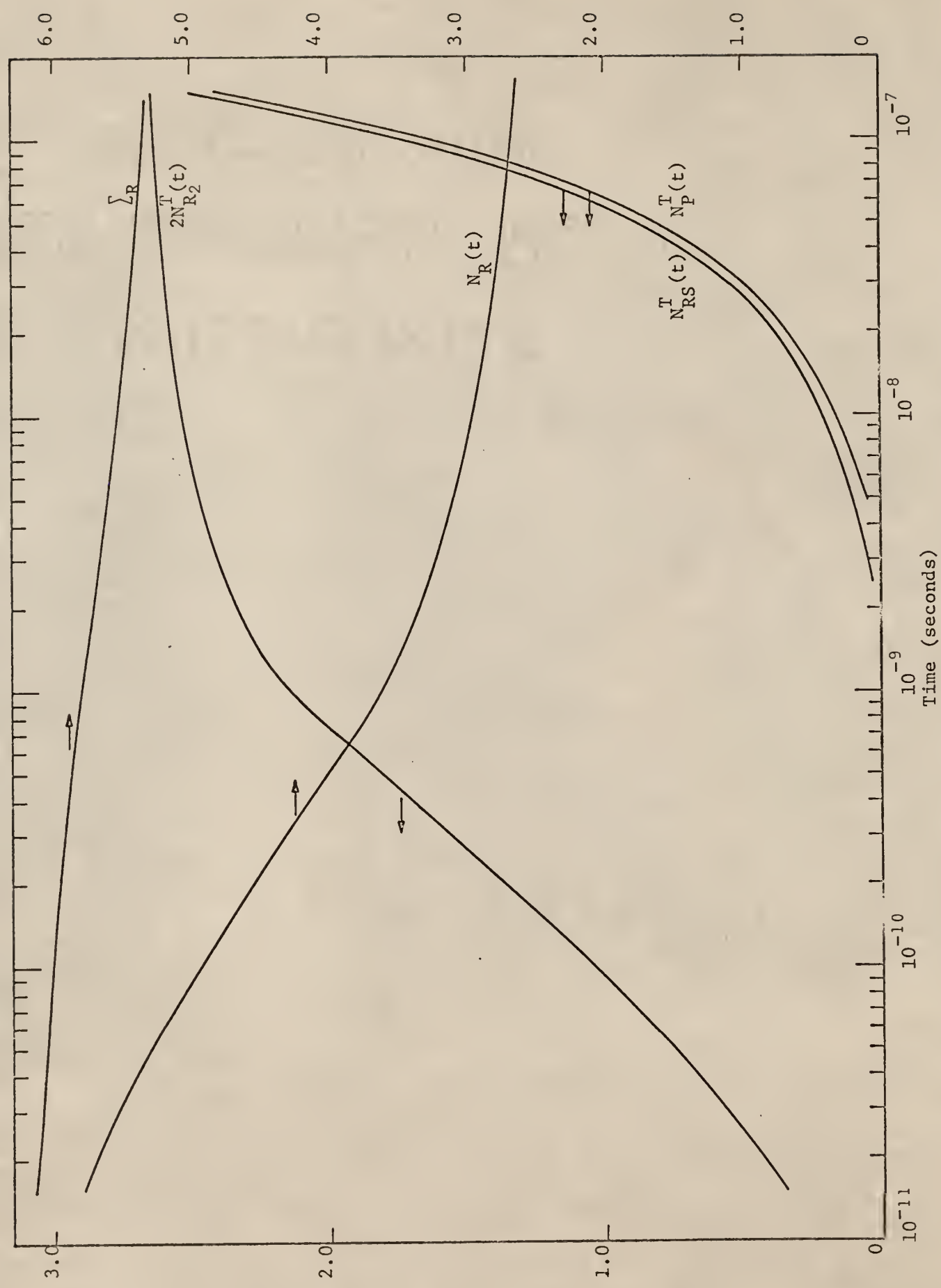


Fig. 10. Variation of $2N_{R_2}^T(t)$, Σ_R , $N_{RS}^T(t)$, $N_P^T(t)$, and $N_R(t)$ with time for the parameters given for Run 10

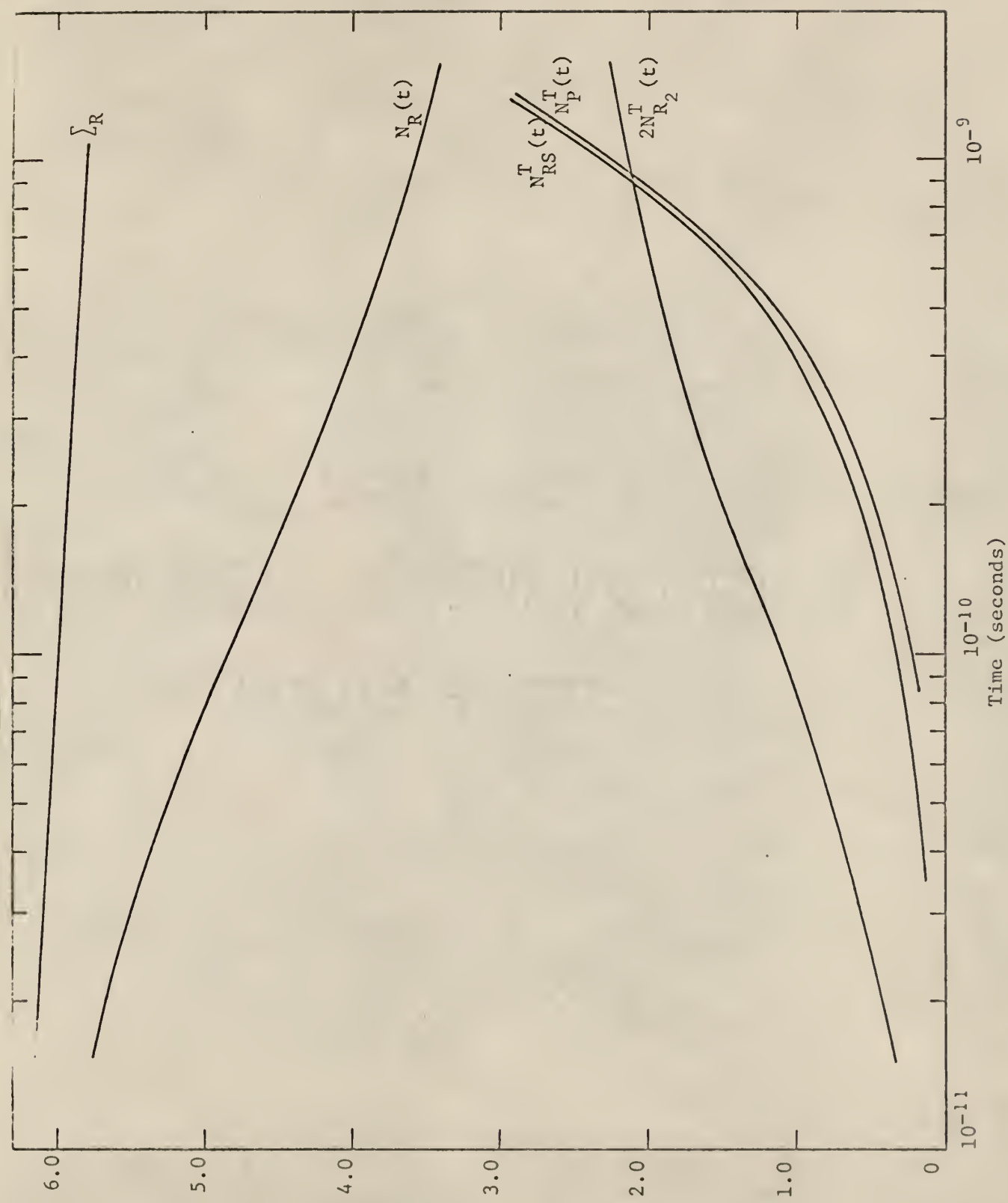


Fig. 11. Variation of $2N_{R_2}^T(t)$, \sum_R , $N_{RS}^T(t)$, $N_p^T(t)$, and $N_R(t)$ with time for the parameters given for Run 11

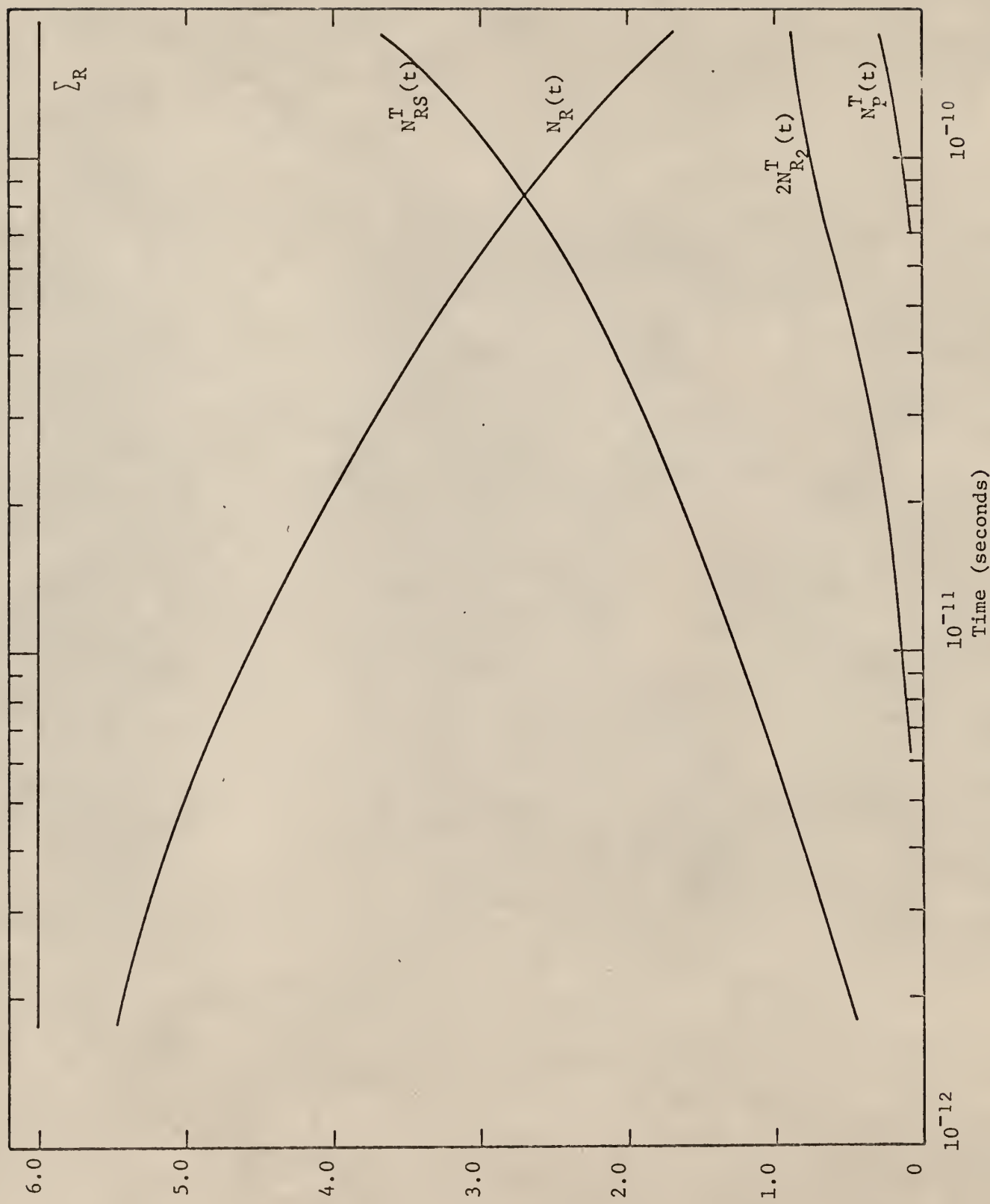


Fig. 12. Variation of $2N_{R_2}^T(t)$, Σ_R , $N_{RS}^T(t)$, $N_P^T(t)$, and $N_R(t)$ with time for the parameters given for Run 12

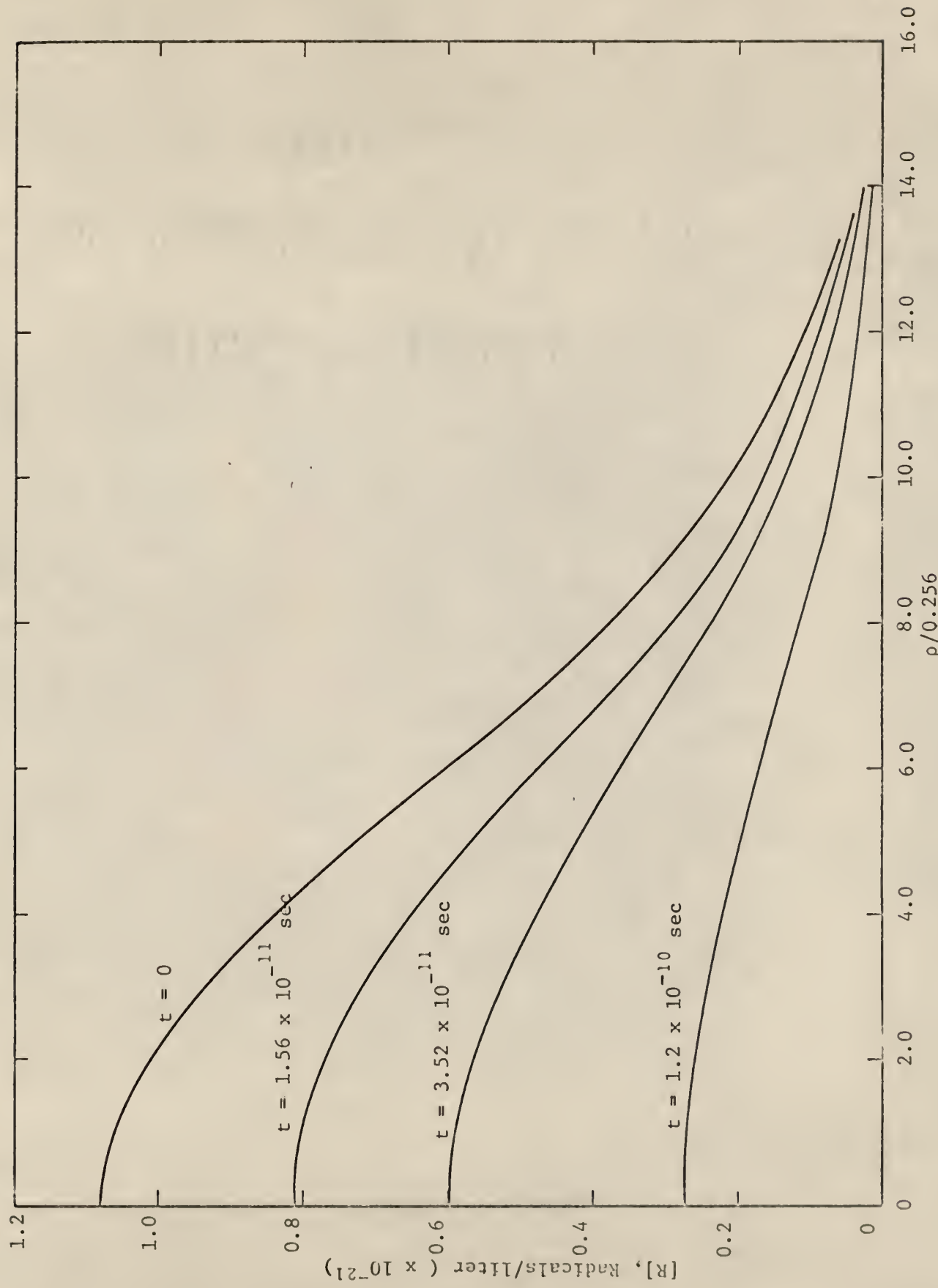


Fig. 13. Variation of the radical concentration, $[R]$, with distance from the center of the spur with time as a parameter. Data for Run 1

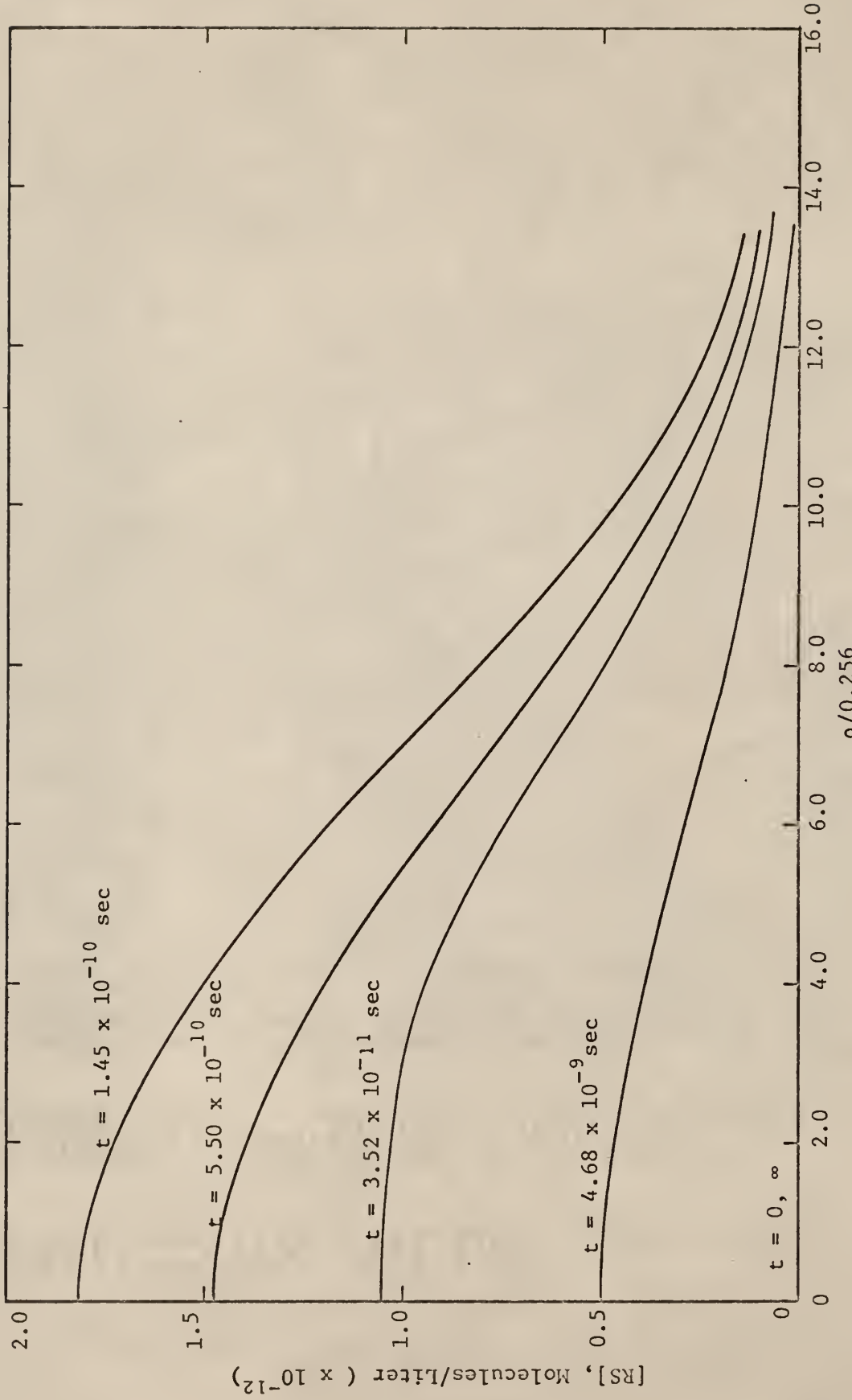


Fig. 14. Variation of the intermediate product concentration $[RS]$, with distance from the center of the spur with time as a parameter. Data for Run 1

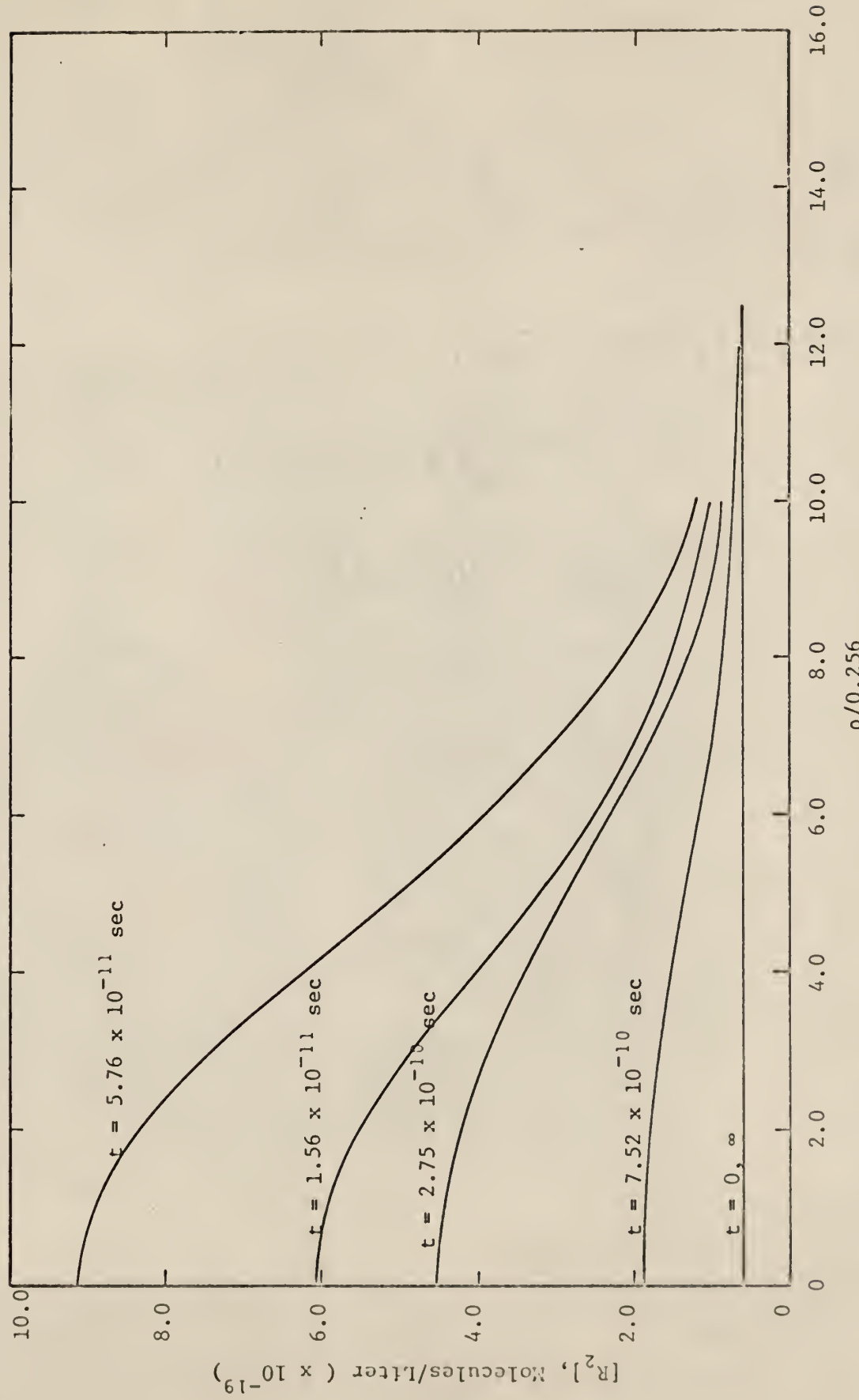


Fig. 15. Variation of R_2 concentration with distance from the center of the spur with time as a parameter. Data for Run 1

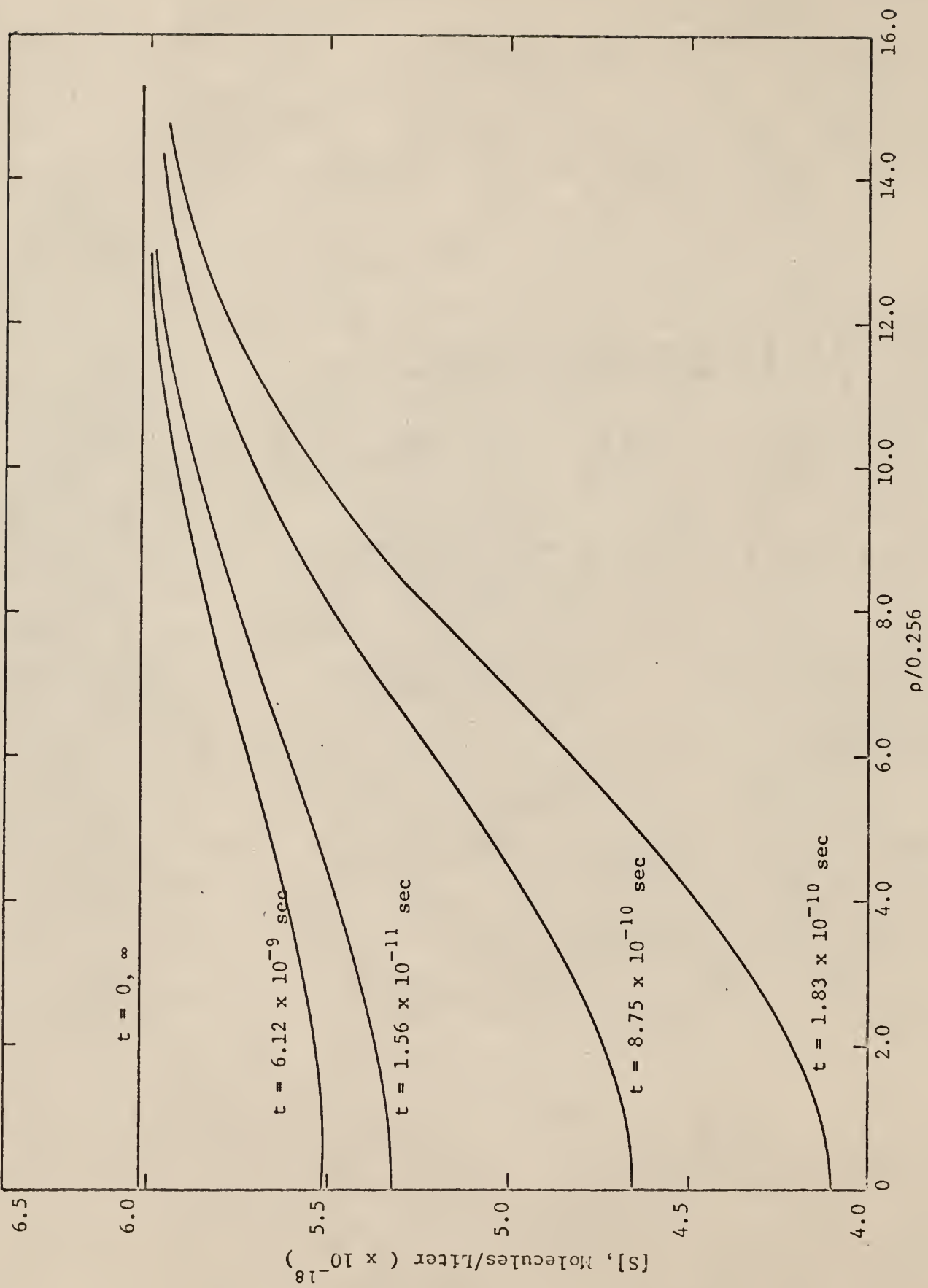


Fig. 16. Variation of the solute concentration, $[S]$, with distance from the center of the spur with time as a parameter, Data for Run 1

that the radicals have an initial Gaussian distribution which is maintained to some degree with a decrease in amplitude to zero as the radicals diffuse and are lost through reaction. During this time, the size of the spur is increasing (remember that a constant value for ρ corresponds to time-increasing radial distance) to many times its original size.

Figure 14 shows that the concentration of the intermediate product is initially zero, builds up to some maximum value, and then returns to zero. The buildup is caused by the reaction of radicals with the solute, S, and the subsequent decay is caused by diffusion and reaction of the intermediate product with the solute, R_2 . It is interesting to note that the shape of the curve is approximately Gaussian.

Figure 15 shows that the concentration of the solute, R_2 , is initially constant at some value, builds up to some maximum value, and then returns to its initial value. The buildup is caused by radical recombination, and the decay is caused by the reaction of R_2 with the intermediate product and by diffusion. This spatial distribution is approximately that of a Gaussian plus a constant.

Figure 16 shows that the concentration of the solute, S, is initially constant at some value, decreases to some minimum value in the spur center, and then returns to its initial value. The decrease is caused by the reaction of the solute with the radicals, and the buildup is caused by diffusion. This curve has the approximate shape of a constant minus a Gaussian.

Referring to Figures 1 through 12 it is possible to describe the

results in a general fashion by discussion of the following eight types of parameter variations

- 1) Increasing both solute concentrations,
- 2) Increasing the concentration of R_2 ,
- 3) Increasing the concentration of S,
- 4) Increasing the initial number of radicals,
- 5) Decreasing the rate constant for the radical recombination reaction,
- 6) Decreasing the rate constant for the radical-solute reaction,
- 7) Increasing the rate constant for the chain propagation reaction,
- 8) Increasing the rate constant for the radical-solute reaction.

The effect of increasing both solute concentrations may be seen from Figures 1 through 4. The effect on the current amount of radicals present is to cause a more rapid initial decrease due to higher reaction rates with the solute, S, and a leveling off at greater amounts of radicals. The effect on the total amounts of intermediate and final product formed is to cause a more rapid increase due to the higher concentrations of intermediate product achieved coupled with the higher concentration of solute, R_2 . The effect on the amount of R_2 formed by radical recombination is to cause a leveling off at lower amounts due to the decrease in the radical concentration caused by radical-solute reaction.

The effect of increasing the concentration of solute R_2 can be seen by comparison of Figure 6 with Figure 2. The effect on the current amount

of radicals present is to cause an increase due to the higher reaction rate between R_2 and RS causing fewer radicals to be bound up with the solute, S. The effect on the intermediate and final product is to cause an increase in their rates of formation and to cause the difference between their respective amounts to be smaller, this latter effect being caused by a more rapid reaction rate between R_2 and RS. The effect on the amount of R_2 formed is to cause an increase. This is the result of a higher concentration of radicals present since fewer are retained in the form of RS molecules.

The effect of increasing the concentration of solute S can be seen by comparison of Figure 5 with Figure 2. The effect on the current amount of radicals present is to cause a more rapid decrease to a lower value before leveling-off is achieved. This is due to the higher reaction rate between the radical and the solute, S. The effect on the intermediate product is to cause a large increase in amount formed, the same being true for the final product to a lesser degree since the amount of final product has a higher-order dependence on the concentration of the solute, S. The effect on the amount of R_2 formed is to cause a decrease. This is due to the concentration of radicals being lowered by reaction with the solute, S.

The effect of increasing the initial number of radicals can be seen by comparison of Figures 2, 7, and 8. The effect on the current amount of radicals present is to cause a similar rate of decrease to a relatively smaller leveling-off value (in comparison to their initial values). This

is due primarily to an increase in the radical recombination rate. The effect on the intermediate and final product is small due to the high radical recombination rate decreasing the amount of radicals available for chain propagation. The effect on the amount of R_2 formed is to cause a relative increase due to the higher radical recombination rate.

The effect of decreasing the rate constant for the radical recombination reaction can be seen by comparison of Figures 9 and 2. These curves show the expected results of higher amount of radicals present, smaller amount of R_2 formed, and greater amounts of intermediate and final product formed, this last being the consequence of higher radical concentrations.

The effect of decreasing the rate constant for the radical-solute reaction can be seen from Figures 10 and 2. The effect on the current amount of radicals is to cause an increase since the radical-solute reaction rate is slower. The effect on the intermediate and final product is to lower their values and cause the relative differences between these products to be smaller. The latter is caused by the R-S reaction being slow in comparison to the R_2 -RS reaction. The effect on the amount of R_2 formed is to cause an increase since the radical concentration is high due to little reaction with the solute, S.

The effect of increasing the rate constant for the chain propagation step can be seen by comparison of Figures 11 and 2. The effect on the current amount of radicals present is to cause an increase since fewer are being retained in the form of the intermediate product. This is offset

somewhat by the higher concentrations of radicals causing more radical recombination. The effect on the intermediate and final product is to increase the amounts formed. This is due to the higher radical concentration causing a faster chain reaction. The major effect is to cause the amount of P formed to be very nearly that of RS formed since the R_2 -RS reaction is much faster than the R-S reaction.

The effect of increasing the rate constant for the radical-solute reaction can be seen from Figures 12 and 2. These curves show the expected results of smaller amount of radicals present and R_2 formed, and greater amounts of intermediate and final products formed.

Having formed the above general observations, it is important to obtain a qualitative understanding of the effects that spur overlap should have on the rate of product formation. Here we will only consider the case where overlap occurs before the amount of radicals reaches the leveling-off region shown in Figures 1 through 12, as little radical recombination occurs after this time. Also necessary is a knowledge of the spur size increase with time so that one can estimate the spur separation distances that would be necessary for the effects of overlap to become important. Table II gives approximate values for the factor by which the Gaussian width at half-maximum has increased as a function of time. These values were determined from the computer solution data for Run 1 and are fairly representative values for all the runs. The deviations from these values for the other runs does not exceed approximately five percent.

TABLE II. SPUR SIZE AS A FUNCTION OF TIME

Time (seconds)	$r_{\frac{1}{2}}(t)/r_{\frac{1}{2}}(o)$
1.5×10^{-11}	1.1
1.8×10^{-10}	1.7
1.4×10^{-9}	3.6
1.2×10^{-8}	10
1.1×10^{-7}	30

The basic effects that overlap will have are as follows. The overlapping of the radicals in the spurs will cause the recombination reaction to increase, decreasing the radical concentration and increasing the R_2 concentration. The decrease of the radical concentration will cause a decrease in the rate of production of the intermediate product. It would be expected that initially, the rate of production of the final product would increase because of the increased concentration of the intermediate product in the overlap region, along with the increased concentration of R_2 from the increased recombination occurring. The rate will subsequently fall below the value without overlap because of depletion of available intermediate product.

Having established that the basic effects of spur overlap depend primarily on the radical recombination, the important question is then how the presence of a chain reaction affects the concentration of the

radicals as a function of position and time. In order to simplify the analysis it is necessary to assume that the spatial concentration profile of the radicals remains of a Gaussian shape at all times so that the important information is represented by values of the radical concentration at the half-maximum position. This assumption is quite good for the runs made in this report. The values obtained are listed in Table III and plotted in Figure 17. The concentrations have been normalized to their respective initial values in the center of the spur.

In order to obtain an upper limit for these curves for the case of no radical recombination and infinite propagation rate (that is, for $k_{11} = 0$ and $k_{23} = \infty$) we note that this would correspond to the case for radical diffusion with no reaction for which we have the analytical solution

$$[R(r,t)] = \frac{N_0}{\left[\pi(2R_o^2 + 4Dt)\right]^{3/2}} e^{-r^2/\left[2R_o^2 + 4Dt\right]}, \quad (97)$$

Noting that

$$[R(0,0)] \approx [R]_o = \frac{N_0}{\left[2\pi R_o^2\right]^{3/2}}. \quad (98)$$

we have for Eq. (97)

$$\frac{[R(r_z, t)]}{[R]_o} = \left[\frac{2R_o^2}{2R_o^2 + 4Dt} \right]^{3/2} e^{-r_z^2/[2R_o^2 + 4Dt]}. \quad (99)$$

TABLE III. RADICAL CONCENTRATIONS AT HALF-MAXIMUM POSITION AS
 A FUNCTION OF HALF-MAXIMUM POSITION

RUN	$[R]_{\frac{1}{2}}/[R]_0$				
	$r_{\frac{1}{2}}(t)$				
1	0.376	0.796×10^{-1}	0.619×10^{-2}	0.175×10^{-3}	0.480×10^{-5}
	9.21	14.4	30.0	81.4	246
2	0.374	0.751×10^{-1}	0.462×10^{-2}	0.158×10^{-3}	0.544×10^{-5}
	9.20	14.3	29.2	81.0	248
3	0.350	0.564×10^{-1}	0.451×10^{-2}	0.158×10^{-3}	
	9.20	13.6	29.0	90.3	
4	0.230	0.566×10^{-1}	0.812×10^{-2}		
	9.05	13.5	23.9		
5	0.348	0.399×10^{-1}	0.814×10^{-3}	0.348×10^{-4}	
	9.14	13.3	29.6	82.6	
6	0.374	0.778×10^{-1}	0.634×10^{-2}	0.254×10^{-3}	
	9.21	14.5	29.8	81.7	
7	0.352	0.640×10^{-1}	0.399×10^{-2}	0.136×10^{-3}	0.460×10^{-5}
	9.40	14.7	29.4	81.1	251
8	0.334	0.557×10^{-1}	0.354×10^{-2}	0.120×10^{-3}	0.386×10^{-5}
	9.56	15.1	29.6	81.2	260
9	0.424	0.120	0.774×10^{-2}	0.245×10^{-3}	0.358×10^{-5}
	8.84	13.0	28.0	80.4	254
10	0.376	0.801×10^{-1}	0.652×10^{-2}	0.262×10^{-3}	0.870×10^{-5}
	9.21	14.5	30.1	82.1	256
11	0.375	0.801×10^{-1}	0.653×10^{-2}		
	9.20	14.5	30.1		
12	0.346	0.682×10^{-1}			
	8.75	11.7			

where $r_{\frac{1}{2}}$ = radial position at a concentration equal to half the maximum value.

To obtain $r_{\frac{1}{2}}(t)$ we have

$$\frac{[R(r_{\frac{1}{2}}, t)]}{[R(0, t)]} = \frac{1}{2} = e^{-\frac{r_{\frac{1}{2}}^2}{2R_0^2 + 4Dt}} \quad (100)$$

so that

$$r_{\frac{1}{2}}^2(t) = [2R_0^2 + 4Dt]\ln(2) . \quad (101)$$

Substituting Eq. (101) into Eq. (99) gives

$$\left. \frac{[R]}{[R]_0} \right|_{r=r_{\frac{1}{2}}} = 0.816 \left[\frac{R_0}{r_{\frac{1}{2}}} \right]^3 . \quad (102)$$

Equation (102) is the relation for the maximum $\frac{[R]_{\frac{1}{2}}}{[R]_0}$ that could be obtained from the chain reaction scheme considered, for any value of $r_{\frac{1}{2}}(t)$. This equation is plotted as the dashed line in Figure 17. A log-log plot was used in order to investigate deviations of the numerical solution values from a straight line. The only serious deviations occurred for Runs 3 and 4 so these were omitted from the plot. The deviations from a straight line are caused by deviations in the spatial distribution of the concentration of radicals from a Gaussian form. The

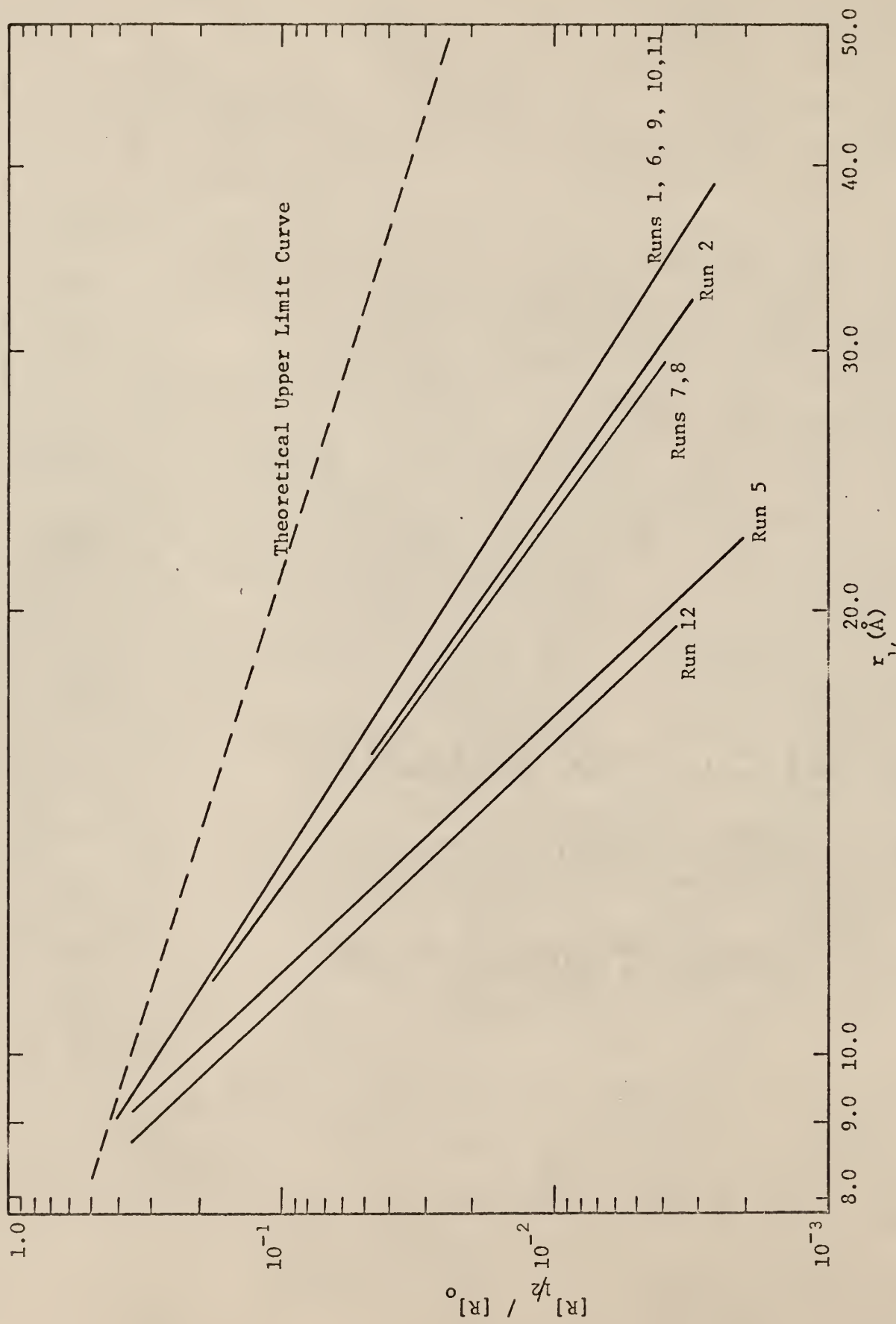


Fig. 17. Plot of radical concentrations at the half-maximum position vs. the half-maximum position

form was flattened in the center of the spur for these cases due to the high reaction rates caused by large solute concentrations.

In order to draw useful conclusions from Figure 17 we must keep in mind that the purpose here is to attempt to determine qualitatively whether reaction can increase the importance of overlap effects. Thus, the larger $[R]_{12}/[R]_0$ is for a given r_{12} , the more important overlap effects become. We notice from Figure 17 that the run which would have least importance for overlapping is Run 12. Comparing Run 12 with Run 2, and comparing the parameters that produced these runs, we notice that we could interpret Run 2 as the chain reaction and Run 12 as the non-chain reaction. The reason why it is possible to treat one reaction as a chain reaction and the other as the non-chain reaction is basically that in one reaction, the chain propagation step is more pronounced than in the other reaction. Thus, although both reactions are actually chain reactions, it is feasible for comparative purposes to term the one with the greater chain length the chain reaction and the other the non-chain reaction. Of course, the actual non-chain reaction would be the one for which the reaction rate constant for the chain propagation step was identically zero, but this would reduce the problem to one of recombination only. Since the values for Run 2 from Figure 17 are higher than those for Run 12, the conclusion is that overlap effects should be more important for chain reactions than for non-chain reactions due to the higher concentrations of radicals present. A more realistic comparison can be obtained by interpreting Run 2 as the non-chain reaction and Run 11 as the chain reaction. This comparison, also, shows that the radical concentrations are higher for the

chain reaction case.

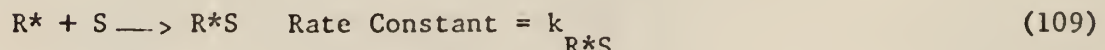
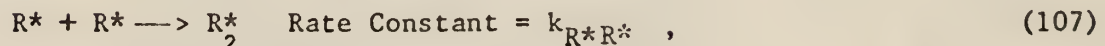
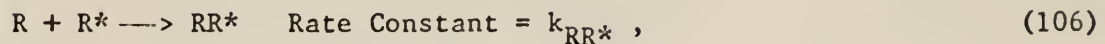
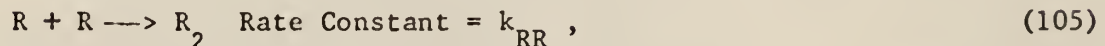
The runs which gave the highest radical concentrations are 1, 6, 9, 10, and 11. It is not possible to draw general conclusions from these runs except to note that in comparison to Run 2, higher concentrations were obtained by decreasing the recombination rate constant; by decreasing the radical-solute rate constant; and by increasing the chain propagation rate constant.

An interesting feature is noticed by comparing Runs 2, 7, and 8. These cases correspond to an increase in the initial number of radicals in the spur and it can be seen that although there was some decrease in relative concentration when the initial number of radicals was increased from 6 to 9, there was no further decrease in relative concentration when the number was increased from 9 to 12 radicals per spur. Therefore it may be concluded that the effect of increasing the radical concentration has only a minor effect on the relative concentration as a function of width at half-maximum, although, of course, the actual radical concentration is higher.

A further substantiation that a chain reaction significantly increases the radical concentration is seen by comparison of Run 5 with Run 6. Because of the initial concentrations involved, Run 5 favors the solute reaction step and Run 6 favors the chain propagation step, so that we may interpret Run 5 as the non-chain reaction and Run 6 as the chain reaction. Once again we see that effect of a chain reaction is to significantly increase the radical concentration, so that overlap will be more important.

4.0 ACCURACY OF THE FINITE DIFFERENCE SOLUTION
AND ANALYSIS OF ERRORS FOR THE RUNS

In order to estimate the accuracy of "and determine the sources of error in" the finite difference solution values two other runs were performed. The first was a solution of the two-radical, non-depletion of solute, model used by Dyne and Kennedy (4) with the reaction scheme given as



The values of the parameters used in the solution were

$$\frac{D}{S} = \infty ,$$

$$k_{RS} = 10^{-11} \text{ cm}^3/\text{sec-radical} ,$$

$$k_{RR} = 1.2 \times 10^{-11} \text{ cm}^3/\text{sec-radical} ,$$

$$k_{RR^*} = 3.0 \times 10^{-11} \text{ cm}^3/\text{sec-radical} ,$$

$$k_{R^*R^*} = 0.9 \times 10^{-11} \text{ cm}^3/\text{sec-radical} ,$$

$$D_R = 8.0 \times 10^{-5} \text{ cm}^2/\text{sec} ,$$

$$D_R^* = 2.0 \times 10^{-5} \text{ cm}^2/\text{sec} ,$$

$$N_o = 6.0 \text{ radicals} ,$$

$$N_o^* = 6.0 \text{ radicals} ,$$

$$R_o = 7.07 \text{ } \overset{\circ}{\text{A}} ,$$

$$R_o^* = 7.07 \text{ } \overset{\circ}{\text{A}} ,$$

$$[S]_o = 10^{-3} \text{ mole/liter} .$$

The results of the computer solution compared to those published by Dyne and Kennedy and those computed by F. E. Haskin (6) using the prescribed diffusion hypothesis are listed in Table V. In this table, N_o and N_o^* are the initial number of R and R* radicals respectively, N_{R_2} , $N_{R_2^*}$, and N_{RR^*} are the final numbers of R_2 , R_2^* , and RR^* molecules formed by radical recombination respectively, and N_R and N_{R^*} are the final numbers of radicals which reacted with the solute.

TABLE V. COMPARISON OF THE TWO-RADICAL MODEL RESULTS

Quantity	This Work	Dyne and Kennedy	Haskin
$2N_{R_2}/N_o$	0.115	0.093	0.127
$2N_{R_2^*}/N_o^*$	0.217	0.183	0.233
N_{RR^*}/N_o	0.389	0.417	0.431
N_R/N_o	0.496	0.490	0.439
N_{R^*}/N_o^*	0.394	0.400	0.333

Since Dyne and Kennedy's results are supposed to be accurate to 1% or so, it is seen that for the number of spatial mesh points used in this work, only an accuracy of 10% or so can be expected. A higher accuracy was not sought after in this work since it was not the numerical value that was important but the trend of the solutions. To obtain a higher accuracy, a smaller mesh size, and therefore more mesh points, would have to be used, thus significantly increasing computation time. For instance, if the mesh size in the spatial coordinates were halved, the computation time would have increased by a factor of eight since the stability relation forces a factor of four decrease in time mesh size. This added computation time was not deemed necessary in this work. Another estimate of the accuracy is given by Kuppermann (7) as being the percent error in the Σ_R calculated for the runs. Kuppermann states that in the runs he performed, the percent error in Σ_R was a good estimate of the percent error in the values determined. For the run described above, the percent error in the Σ_R value was about 10%, tending to agree with the numerical results listed in Table V.

In order to show that these magnitudes of errors do not alter the general shapes of the time plots, as well as indicating the validity of using the prescribed diffusion hypothesis even in this complex reaction system, the results obtained from this work are plotted in Figure 18 along with those obtained by Haskin (dashed lines). It is seen that even though the percent error in the final values is large, the general shapes of the curves do not change much in a qualitative sense, and it is these

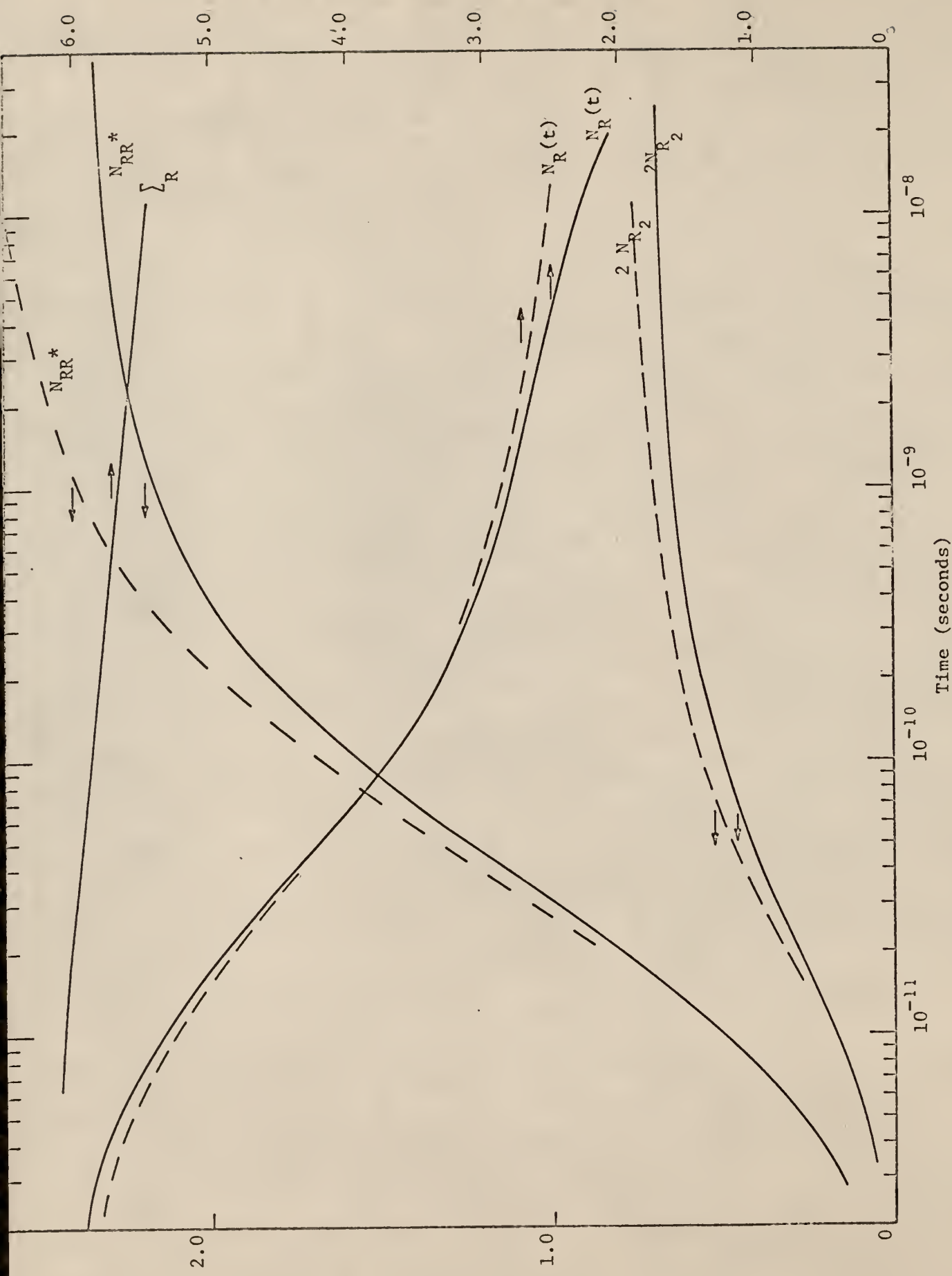


Fig. 18. Variation of N_{RR}^* , $\sum R$, and $N_R(t)$ with time for the data given in Section 3.0

trends that are important in this work.

Since, in general, the only method for locating the sources of errors in any numerical solution is to change the mesh sizes, Run 3 was recalculated in Run 3-A using a time mesh size that was decreased by a factor of two. Since the results obtained were so close to the original, it is necessary to show the differences in tabular form. The results are given in Table VI.

TABLE VI. EFFECT OF THE TIME MESH SIZE ON THE NUMERICAL RESULTS

Problem Time (sec)	Quantity	Run 3	Run 3-A
8.35×10^{-11}	$N_{RS}^T(t)$	2.17	2.20
	$N_P^T(t)$	0.522	0.533
	$2N_{R_2}^T(t)$	0.775	0.782
	$N_R(t)$	3.58	3.58
	$\Sigma_R(t)$	6.00	6.01
5.55×10^{-10}	$N_{RS}^T(t)$	9.08	9.04
	$N_P^T(t)$	6.73	6.70
	$2N_{R_2}^T(t)$	1.18	1.19
	$N_R(t)$	2.36	2.35
	$\Sigma_R(t)$	5.89	5.88
5.35×10^{-9}	$N_{RS}^T(t)$	70.0	69.9
	$N_P^T(t)$	67.8	67.6
	$2N_{R_2}^T(t)$	1.40	1.40
	$N_R(t)$	2.11	2.07
	$\Sigma_R(t)$	5.77	5.73

Since this table shows that the decrease in the time mesh size had little effect on the results, the source of error must lie in the spatial portion of the finite difference solution. The two possible regions of error here are the effect of only using a finite portion of the Gaussian and the finite difference error in the computation of the spatial derivatives. Since the program used includes more than 99.99% of the Gaussian in its calculations, the main source of error must lie in the computation of the derivatives. This is a reasonable conclusion since only thirty spatial mesh points were used. Therefore, to obtain higher accuracy, it is necessary to use a larger number of spatial mesh points.

Concerning the analysis of errors in the runs there is only one major correction that could be made, and this is for the curves showing the time behavior of the current amounts of radicals present at any time. If one plots Σ_R and $N_R(t)$ for any run on an expanded scale near the end of the runs as is done in Figure 19 for Run 2, it is noticed that their respective slopes are very nearly the same. If one then plots $N_{RS}^T(t)$ and $N_P^T(t)$ for any run, as was done in Figure 20 for Run 1, it is seen that these quantities are very linear with time near the end of the computation. Since [S] at the times considered is quite constant, it is seen from Eq. (83) that in order for the time rate of change of product formed to be constant, then $N_R(t)$ must be constant. If we then can assume that $N_R(t)$ is nearly constant, we have the conclusion that the major portion of the slope of Σ_R is due to spurious losses of radicals, that is, losses due to the numerical method employed. Therefore, in all

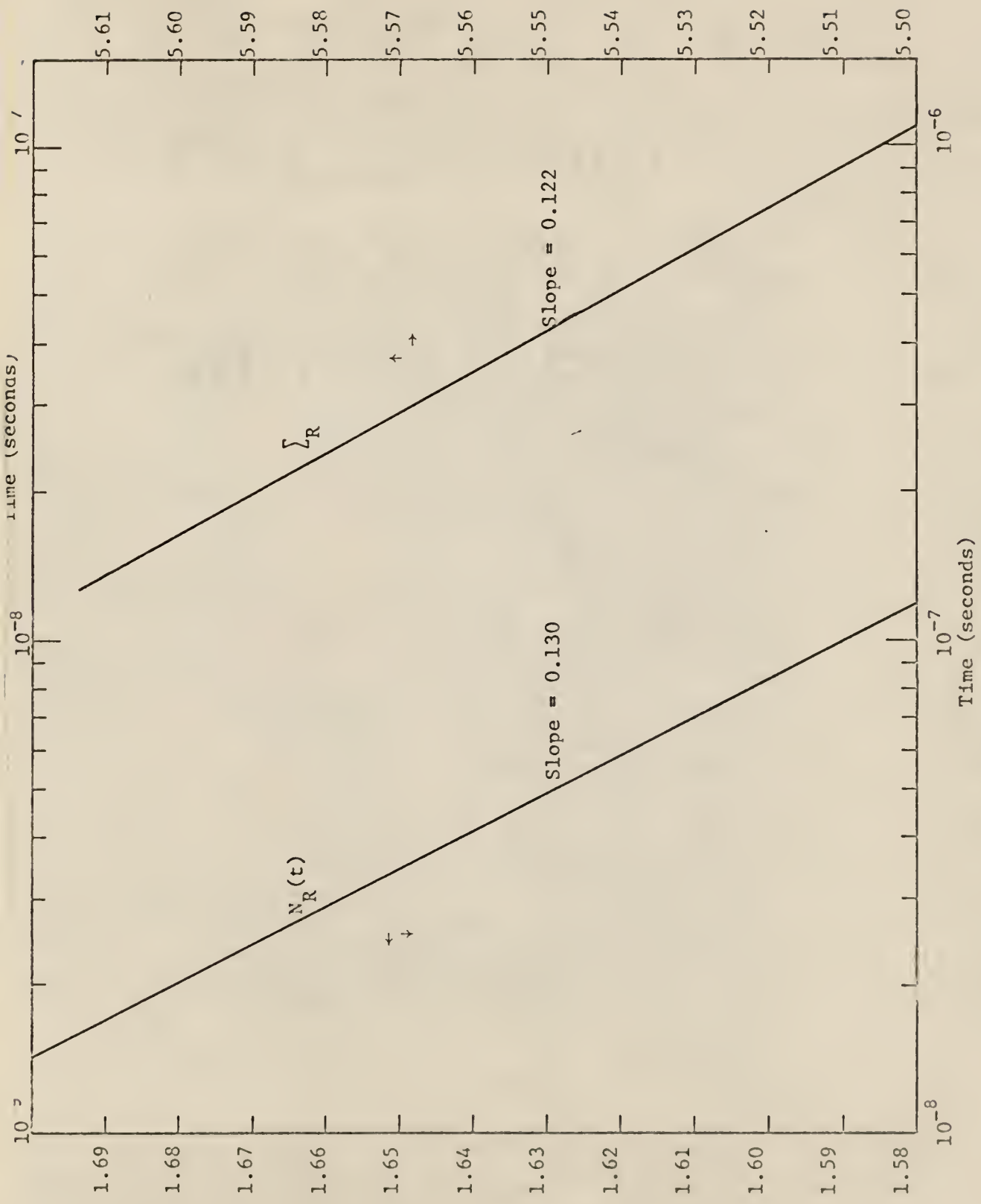


Fig. 19. Variation of $N_R(t)$ and \sum_R with time. Data for Run 2

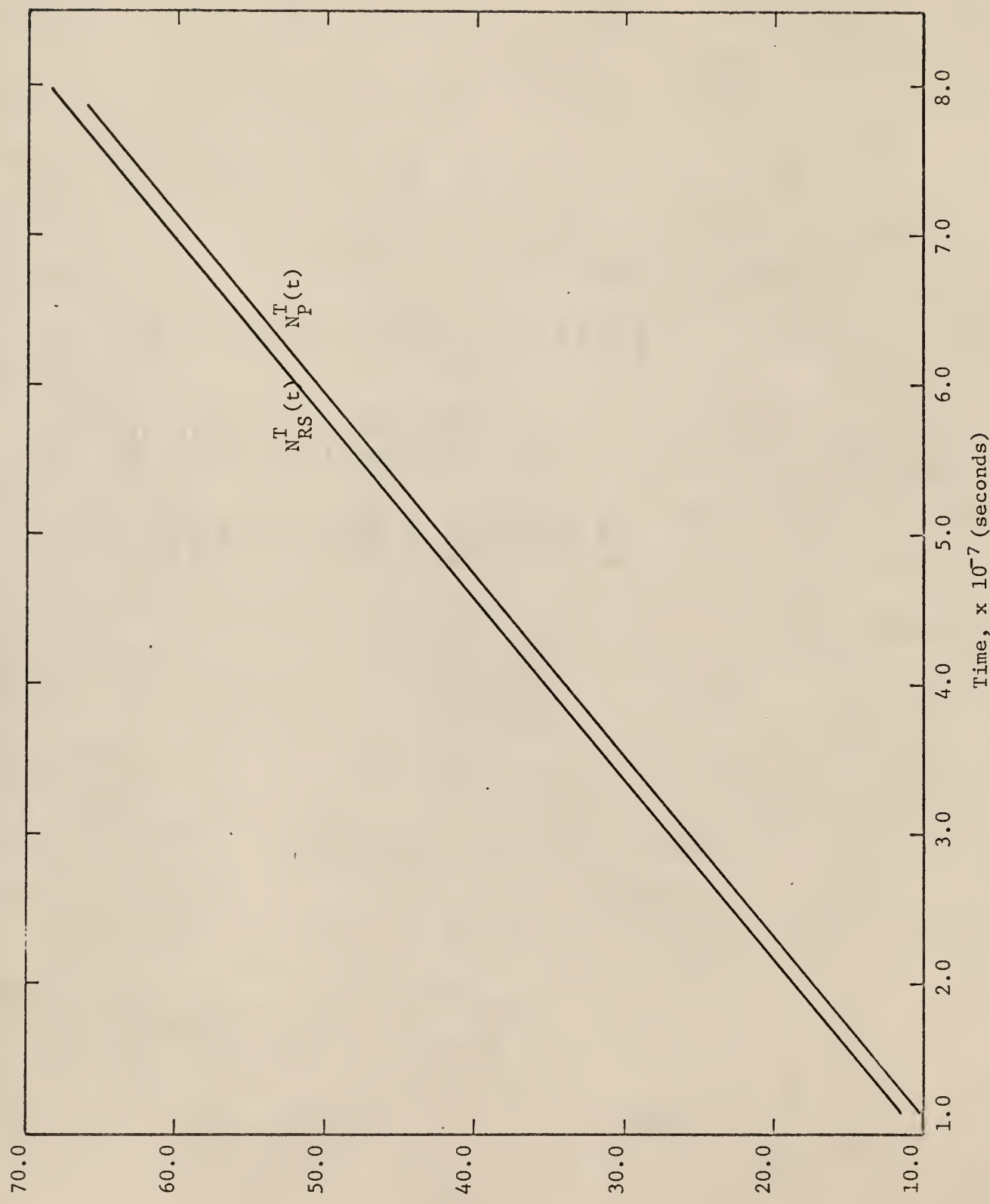


Fig. 20. Variation of $N_{RS}^T(t)$ and $N_P^T(t)$ with time. Data for Run 1.

the runs made, $N_R(t)$ is actually much more constant towards the end of the runs than indicated by the figures.

5.0 CONCLUSIONS

The results of this work have led to the major qualitative conclusion that effects of spur overlap will be important at lower dose rates for chain reactions than for non-chain reactions. This conclusion is based on the fact that for the runs made for the reaction scheme considered, there was a significant increase in the radical concentration throughout the history of the spur for chain reactions as opposed to non-chain reactions, indicating that radical interactions between neighboring spurs would be greater for the same dose rates for the chain reaction. It has also been shown that the overall reaction rate for the system considered should be lower than that predicted from homogeneous kinetics for the case of high dose rates. This decrease in the overall reaction rate is caused by radical recombination in each spur before complete spatial uniformity of the radical concentrations is reached. This inhomogeneity will also cause the overall reaction rate to depend on more of the reaction parameters than predicted from homogeneous kinetics.

One other conclusion that was reached from an examination of the space-time histories of each of the species for each of the runs is that a modified form of the prescribed diffusion hypothesis should give good results for the reaction scheme considered except for very high solute concentrations, where the original Gaussian form is flattened in the center of the spur.

6.0 SUGGESTIONS FOR FURTHER STUDY

This study was intended to serve as a basis to establish the importance of spur overlap for chain reactions and the only calculations performed were those for a single cluster of reacting species. This work can be extended by obtaining numerical solutions for the case of spur overlap for a chain of equally-spaced spurs with the addition of one more spatial variable, thus creating a partial differential equation in three variables to be solved. It is estimated that increase in computation time for this case would be a factor of ten to thirty over that for the two-variable equation used in this work. This amount of computation time is not prohibitive if the parameters used in the study are chosen carefully.

A further extension of this work is to perform the same calculations used in this work with the use of a modified form of the prescribed diffusion hypothesis. This modification would involve the use of a Gaussian shape for the radicals throughout their history, a constant plus a Gaussian for the shape of the species formed by radical recombination, a constant minus a Gaussian for the solute, and a Gaussian for the intermediate product. This type of system would reduce the solution of the partial differential equation to the solution of an ordinary differential equation, amounting to a tremendous savings in computation time.

7.0 ACKNOWLEDGMENT

The author is grateful for support given by the National Defense Education Act Fellowship granted through the Nuclear Engineering Department at Kansas State University. Appreciation goes to the computing center at Argonne National Laboratory for their assistance in using the CDC-3600 computer facility. Authorization and funding for time at this facility was through Associated Midwestern Universities - Argonne National Laboratory.

The author greatly appreciates the encouragement and assistance given by Dr. Richard E. Faw. Sincere gratitude is also given to Dr. William R. Kimel for making this study possible.

8.0 LITERATURE CITED

1. J.W.T. Spinks and R. J. Woods
An Introduction to Radiation Chemistry
John Wiley and Sons, Inc. (1964).
2. R. B. Bird, et al.
Transport Phenomena
John Wiley and Sons, Inc. (1960).
3. D. E. Lea
Actions of Radiations on Living Cells
Cambridge University Press, Cambridge, England (1946).
4. P. J. Dyne and J. M. Kennedy
Canadian Journal of Chemistry, 36, 1518 (1958).
5. A. Kuppermann
J. Chem. Ed., 36, 279 (1959).
6. F. E. Haskin, Graduate Fellow, Nuclear Engineering Dept.
Kansas State University, Manhattan, Kansas.
(Private Communication).
7. A. Kuppermann and G. G. Belford
Diffusion Kinetics in Radiation Chemistry.
J. Chem. Physics, 36, No. 6, (1962).

9.0 SELECTED REFERENCES

Allen, A. O.

The Radiation Chemistry of Water and Aqueous Solutions
Van Nostrand (1961).

Chapiro, A.

Radiation Chemistry of Polymeric Systems
Interscience, N. Y. (1962).

Faw, R. E.

Spur Coalescence in Radiation Chemistry, Kansas Engineering Experiment Station, Special Report Number 44, Manhattan, Kansas (1963).

Faw, R. E. and L. F. Miller

Track Effects in Radiation - Induced Chemical Reactions, Proceedings of the A.I. Ch.E. Symposium on Photoreactor Design, (1966).

Fox, L.

Numerical Solution of Ordinary and Partial Differential Equations
Pergamon Press (1962).

Frost, A. A.

Kinetics and Mechanism
Wiley, N. Y. (1961).

Haissinsky, M.

The Chemical and Biological Action of Radiations
Academic Press, Inc., Ltd., London (1961).

Hamming, R. W.

Numerical Methods for Scientists and Engineers
McGraw-Hill Book Company, Inc., N. Y. (1962).

Hansen, A. G.

Similarity Analyses of Boundary Value Problems in Engineering
Prentice-Hall, Inc. (1964).

Hochanadel, C. J.

Radiation Chemistry of Water, in "Comparitive Effects of Radiation.",
M. Burton, J. S. Kirby-Smith and J. L. Magee (eds.), Wiley, N.Y. (1960).

Kondrat'ev, V.N.

Chemical Kinetics of Gas Reactions
Pergaman Press, Ltd. (1964).

Samuel, A. H. and J. L. Magee

J. Chem. Phys., 21, 1080 (1953).

Semenov, N. N.

Some Problems in Chemical Kinetics and Reactivity
Pergamon Press, Vols. I, II (1958).

Spinkes, J.W.T. and R. J. Woods

An Introduction to Radiation Chemistry
Wiley, N. Y. (1964).

Wissler, E. H. and R. S. Schechter

A Diffusion Problem with Chemical Reaction
Appl. Sci. Res. Sect. A, 10, 198-204 (1961).

Wylie, C. R.

Advanced Engineering Mathematics
McGraw-Hill Book Company, Inc., N. Y. (1960).

A.0 APPENDIX

A.1 Justification for the Variable Transformation

$$\rho_i = \frac{r}{\sqrt{D_i(t_0^i + t)}}$$

Consider the case where free radicals diffuse outward from a point source with no reaction. The diffusion equation is given as

$$\frac{\partial C_i(r,t)}{\partial t} = D_i \frac{\partial^2 C_i(r,t)}{\partial r^2} + \frac{2}{r} D_i \frac{\partial C_i(r,t)}{\partial t}, \quad (110)$$

with boundary conditions

$$C_i(r,0) = N_o^i \delta(r) / 4\pi r^2, \quad (111)$$

$$C_i(\infty, t) = 0, \quad (112)$$

$$\frac{\partial C_i(0,t)}{\partial r} = 0, \quad (113)$$

where $\delta(r)$ = Dirac delta function,

r = radial distance,

$C_i(r,t)$ = concentration of free radicals of species i ,

t = time,

N_o^i = number of free radicals present of species i .

The solution to Eq. (110) with the given boundary conditions yields

$$C_i(r,t) = \frac{N_o^i e^{-r^2/4D_i t}}{[4\pi D_i t]^{3/2}} \quad (114)$$

If the time scale is shifted so that time zero in a new scale is equal to time t_o^i in the old scale and a new quantity, R_o^i , is defined by $4D_i t_o^i = 2[R_o^i]^2$ Eq. (114) becomes

$$C_i(r,t) = \frac{N_o^i e^{-r^2/[4D_i t + 2(R_o^i)^2]}}{[\pi\{4D_i t + 2(R_o^i)^2\}]^{3/2}}, \quad (115)$$

which has the initial condition

$$C_i(r,o) = \frac{N_o^i e^{-r^2/2(R_o^i)^2}}{\left[2\pi(R_o^i)^2\right]^{3/2}}. \quad (116)$$

Eq. (115) therefore gives the solution to the diffusion-kinetics equation in the absence of reaction for the type on initial condition considered for free radicals in this report.

Defining the new variable $N_i(R)$ as the number of radicals present in the volume bounded by $r = R$

$$N_i(R) = \int_0^R 4\pi r^2 dr C_i(r,t). \quad (117)$$

Defining the variable transformation

$$\rho_i = \frac{r}{\sqrt{D_i(t_0^i + t)}} . \quad (118)$$

Substituting Eq. (118) and Eq. (115) into Eq. (117) gives

$$N_i(P) = \frac{N_o^i}{(2\pi)^{3/2}} \int_0^P d\rho_i \rho_i^2 = \frac{N_o^i P^3}{24(\pi)^{3/2}} . \quad (119)$$

The result obtained in Eq. (119) shows that a fixed, finite range in ρ produces a time-independent determination of the number of radicals for the case of Gaussian initial conditions and absence of reaction. Therefore the introduction of this transformation into the diffusion-kinetics equation will allow a fixed, finite range in ρ to include the same amount of information about the free radical concentration at every time step. It can also be shown that the same type of result is obtained for the case of cylindrical tracks with the transformation given by Eq. (118).

A.2 Explanation of the Computer Program Used in This Work

The computer program discussed here numerically solves the diffusion-kinetics equations for spherically-symmetric geometry with either Gaussian-initial free radical spurs and diffusing solutes or Gaussian-initial free radical spurs and non-diffusing solutes. The program is written in Fortran language for the CDC-3600 computer and the output data include concentration profiles and values of the reaction integrals at spaced time intervals during the calculation. This program is separated into several subprograms for ease of understanding. The following list indicates the program division:

DIFFUSE Main Program

SPURCYL
INTMULT } . . . Subroutines
INTG1D }
FATES }

DIFFUSE Program

The function of this program is to read and write the input data, initialize all variables used, calculate initial free radical and solute concentration profiles, and determine the spatial and time increments such that stability of the finite difference solution is initially assured.

Input Data

Symbol	Explanation
NUMBER	Number of separate solutions to the diffusion-kinetics equations to be run
TTIME	Length of time considered for the reaction
NUMRAD	Number of free radical species
NUMSOL	Number of solute species
NUMRPTS	Number of spatial grid points used
ITYPESOL	Code number for type of solute diffusion = 1 for solute diffusion = 0 for lack of solute depletion assumption
RZERO(I)	Initial Gaussian width at half-maximum for species I
D(I)	Diffusion constant for species I
NRXNTERM(I)	Number of reaction terms appearing in the diffusion-kinetics equation for species I
IC(I,J), JC(I,J)	Index identifiers associated with the reaction terms. For example, if in the diffusion-kinetics equation for species 1 the fourth reaction term involves reaction between species 2 and species 3, the values of the index identifiers become IC(1,4) = 2 and JC(1,4) = 3.
S(I,L,M)	Rate constant for the reaction of species L with species M in the diffusion-kinetics equation for the I th species
C(1,I)	Initial number of free radicals of species I present or initial concentration of the I th solute in atoms/unit volume

Other Important Symbols Used

Symbol	Explanation
C(J,I)	Spatial concentration profiles for species I at position J
DELTAR	Spatial increment, $\Delta\phi$
DELTAT	Time increment, $\Delta\chi$
WNR(J)	Weight factor to be used in evaluation of volume integrals
TAU(I)	Initial time parameter, t_0^i

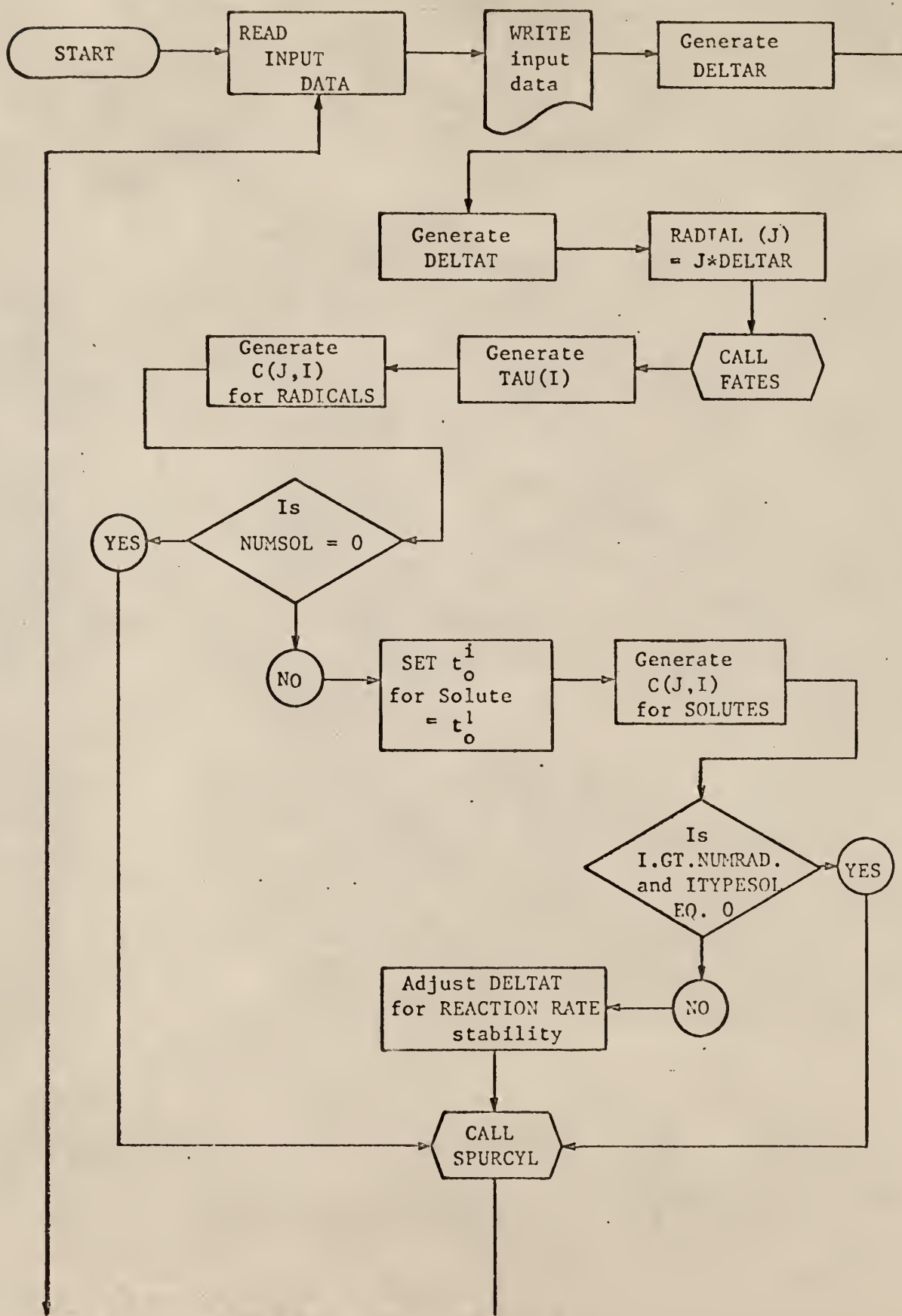
The subprograms used by this program are:

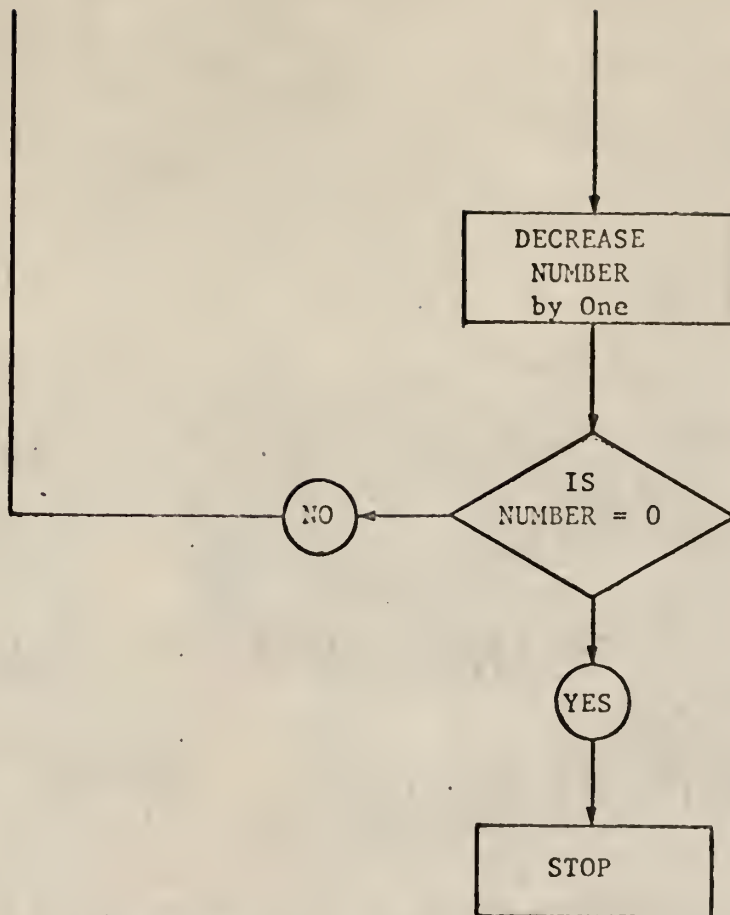
SUBROUTINE FATES (I, NUMRPTS, RADIAL, WNR)

SUBROUTINE SPURCYL

These subprograms are explained in a later section.

Logic Diagram for Program DIFFUSE





```

PROGRAM DIFFUSE
DIMENSION RZERO(5),D(5),C(50,10)    ),NRXNTERM(5),IC(5,5),JC(5,5)
DIMENSION S(5,5,5),A(5),              CZERO(5),CLEFT(5),RADIAL(50)
DIMENSION WNR(50),WTR(5,50),AXIAL(50),WNZ(50),MARG(5,5),CZLEFT(5)
DIMENSION COEFF1(5),COEFF2(5),COEFF3(5),COEFF4(50,5),COEFF5(5,50)
DIMENSION SUM(5),CMULT(5,50),CZTLOSS(5,5),CLOSS(5,5),DLTM(5)
COMMON CZLOSS(5,5)
COMMON TAU(5)
COMMON TIMFB(5)
COMMON TTIME
COMMON SPUR,NUMRAD,NUMSCL,NUMRPTS,RZERO,D,NRADSCL,C,NRXNTERM,IC,JC
1,S,NUMZPTS,SPURSEP,ALPHA,TINIT,DELTAZ,A,DELTAR,DELTAT,CZERO,CLEFT,
1Q,RADIAL,WNR,WTR,AXIAL,WNZ,PI,ITYPESOL,MARG,COEFF1,COEFF2,COEFF3,
1COEFF4,COEFF5,TIME,DELTIME,SUM,CMULT,CZTLOSS,CLOSS,DLTM,CZLEFT
1 FORMAT(4E15.8)
2 FORMAT(10I5)
3 FORMAT(I5,E15.8)
4 FORMAT(2X,8E16.8)
READ 2,NUMBER
PRINT 2,NUMBER
DC 643 I=1,10
DC 643 J=1,50
643 C(J,I)=0.
DC 644 I=1,5
DC 644 J=1,5
644 CLOSS(I,J)=0.
READ 1,TTIME
PRINT 1,TTIME
NUMZPTS=1
READ 2,NUMRAD,NUMSCL,NUMRPTS
PRINT 2,NUMRAD,NUMSCL,NUMRPTS
READ 2,ITYPESOL
PRINT 2,ITYPESOL
READ 1,(RZERO(I),I=1,NUMRAD)
PRINT 1,(RZERO(I),I=1,NUMRAD)
NRADSCL=NUMRAD+NUMSCL*ITYPESOL
READ 1,(D(I),I=1,NRADSCL)
PRINT 1,(D(I),I=1,NRADSCL)
READ 2,(NRXNTERM(I),I=1,NRADSCL)
PRINT 2,(NRXNTERM(I),I=1,NRADSCL)
DC 100 I=1,NRADSCL
N=NRXNTERM(I)
DC 100 J=1,N
READ 2, IC(I,J),JC(I,J)
PRINT 2,IC(I,J),JC(I,J)
II=IC(I,J)
JJ=JC(I,J)
READ 1, S(I,II,JJ)
100 PRINT 4,S(I,II,JJ)
NRADSCL=NUMRAD+NUMSCL
READ 1,(C(1,I),I=1,NRADSCL)

```

```

PRINT 1,(C(1,I),I=1,NRADSCL)
ALPHA=2.
Z=NUMRPTS-1
DELTAR=((55.)**0.5)/Z
DELTAT=0.2*(DELTAR**2)
DO 112 I=1,NUMRAD
CZERO(I)=C(1,I)
112 CLEFT(I)=CZERO(I)
DO 108 J=1,NUMRPTS
Z=J-1
108 RADIAL(J)=Z*DELTAR
CALL FATES(1,NUMRPTS,RADIAL,WNR)
PI=3.1415926
NR=NUMRPTS-1
DO 113 I=1,NUMRAD
C(NUMRPTS,I)=0.
TAU(I)=(RZERO(I)**2)/(2.*D(I))
DO 113 J=1,NR
Z=J-1
113 C(J,I)=(CZERO(I)/((2.*PI*(RZERO(I)**2.))**1.5))*EXP(-(Z*
1DELTAR)**2)/4.)
N=NUMRAD+1
IF(NUMSOL.EQ.0) GO TO 177
NBC=NUMRPTS+2
DO 114 I=N,NRADSCL
TAU(I)=TAU(1)
IE=I+NRADSCL
DO 114 J=2,NBC
C(J,IE)=C(1,I)
114 C(J,I)=C(1,I)
DO 106 I=1,NRADSCL
IF(I.GT.NUMRAD.AND.ITYPESOL.EQ.0) GO TO 180
N=NRXNTERM(I)
DO 106 L=1,N
II=IC(I,L)
JJ=JC(I,L)
IF(S(I,II,JJ).GE.0.) GO TO 106
IF(C(1,I).EQ.0.) GO TO 106
IF(C(1,II).EQ.0.) GO TO 106
IF(C(1,JJ).EQ.0.) GO TO 106
G=0.1*C(1,I)/(TAU(1)*ABSF(S(I,II,JJ))*C(1,II)*C(1,JJ))
IF(DELTAT.GT.G) DELTAT=G
106 CONTINUE
180 CONTINUE
177 CONTINUE
PRINT 4,DELTAZ,DELTAT,TINIT
PRINT 4,DELTAR
PRINT 4,((C(J,I),J=1,NUMRPTS),I=1,NRADSCL)
CALL SPURCYL(K,LL,IS)
NUMBER=NUMBER-1
IF(NUMBER.NE.0) GO TO 1211
STOP
END

```

SUBROUTINE SPURCYL

The function of this subprogram is to perform the finite difference calculations for the set of diffusion-kinetics equations and to call the subroutines that perform the interpolation and calculation of the reaction integrals. All the input data needed in this program are brought in by the use of a COMMON area from Program DIFFUSE.

Important Program Variables

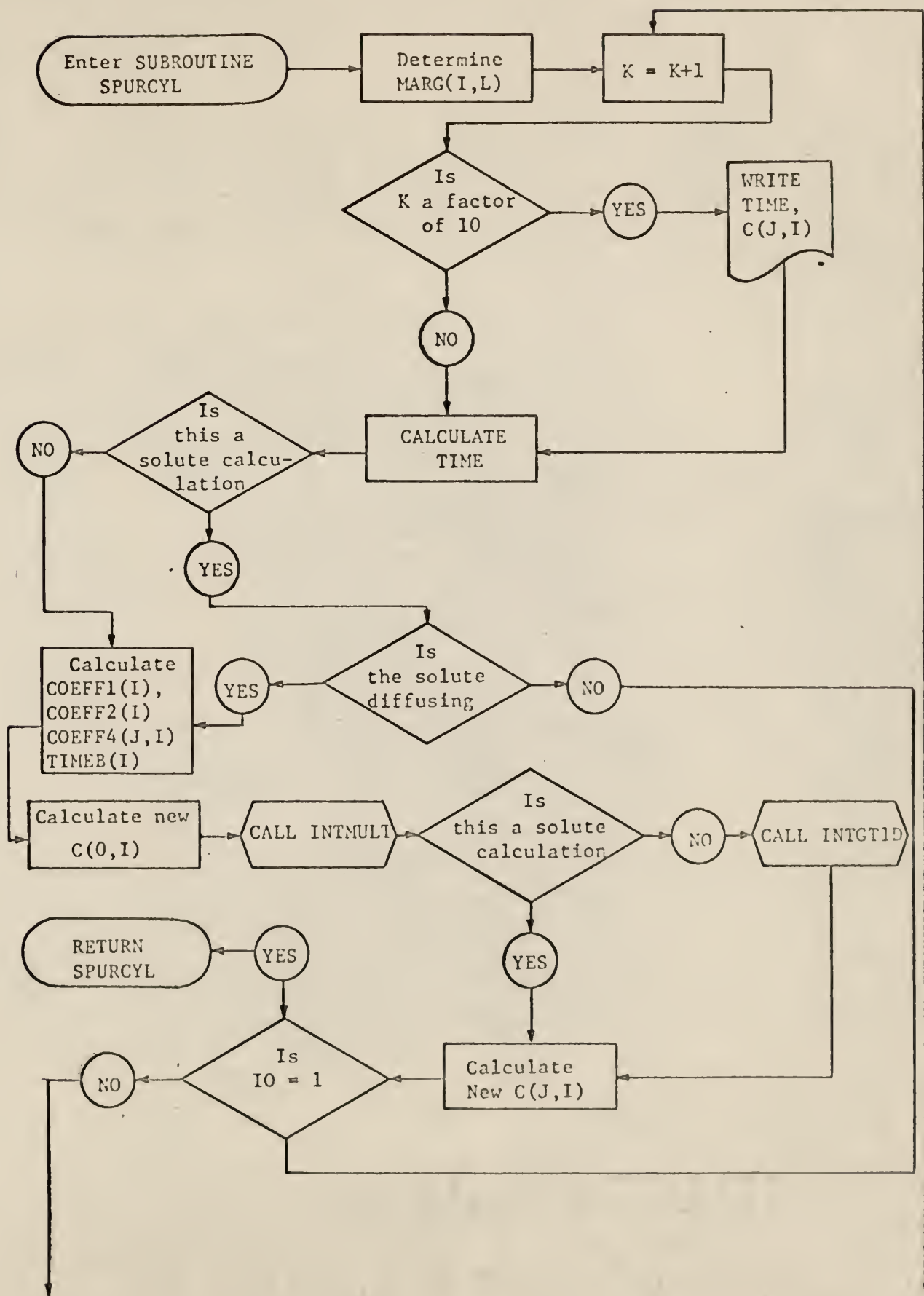
Symbol	Explanation
MARG(I,L)	Control variable determining the type of interpolation needed, if any
K	Index of the time loop
NRADL, NRADLL	Indices controlling the storage location of the concentrations
TIME	Current reaction time
COEFF1(I), COEFF2(I), COEFF4(J,I), TIMEB(I)	Factors used in the numerical solution of the finite difference equations
CZERO(I)	Initial amount of radicals of species I present
CLEFT(I)	Amount of radicals of species I present at time t

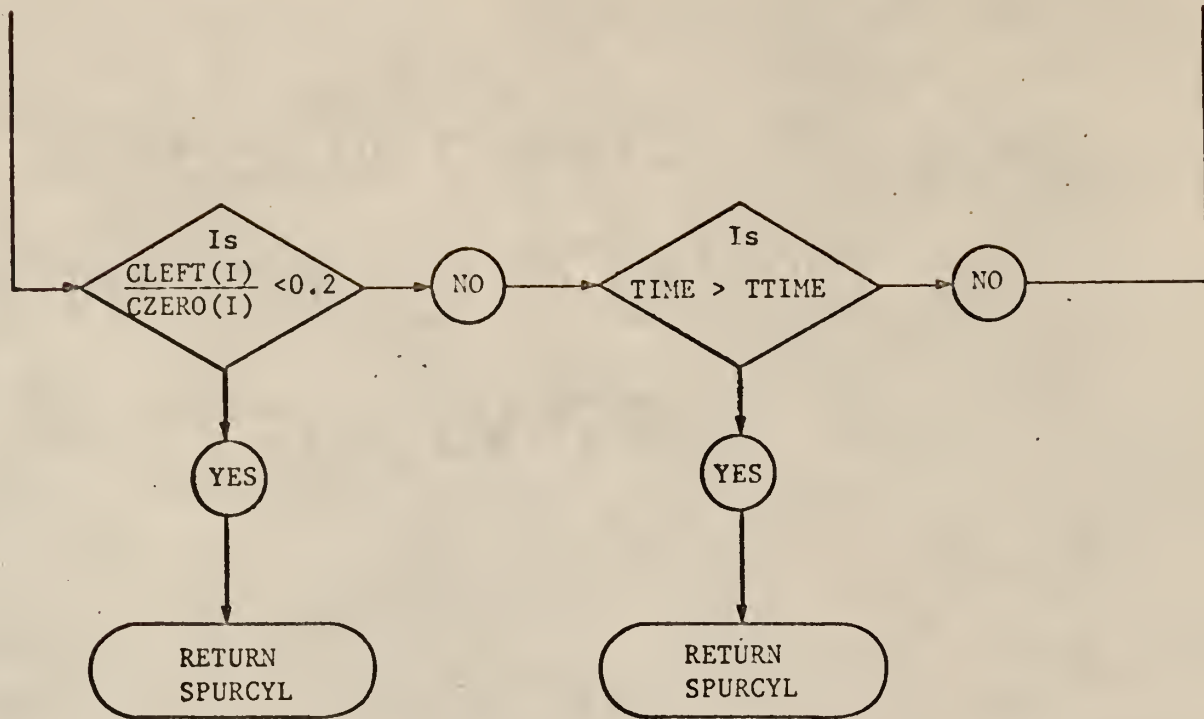
The subprograms used by this program are:

SUBROUTINE INTMULT(I,L,M,LL)

SUBROUTINE INTGT1D(I,LL,K,IO)

Logic Diagram for Subroutine SPURCYL





```

SUBROUTINE SPURCYL(K,LL,IS)
DIMENSION RZERO(5),D(5),C(50,10)      ),NRXNTERM(5),IC(5,5),JC(5,5)
DIMENSION S(5,5,5),A(5),                  CZERO(5),CLEFT(5),RADIAL(50)
DIMENSION WNR(50),WTR(5,50),AXIAL(50),WNZ(50),MARG(5,5),CZLEFT(5)
DIMENSION CCOEFF1(5),CCOEFF2(5),CCOEFF3(5),CCOEFF4(50,5),CCOEFF5(5,50)
DIMENSION SUM(5),CMULT(5,50),CZTLOSS(5,5),CLOSS(5,5),DLTM(5)
COMMON CZLOSS(5,5)
COMMON TAU(5)
COMMON TIMEB(5)
COMMON TTIME
COMMON SPUR,NUMRAD,NUMSCL,NUMRPTS,RZERO,D,NRADSCL,C,NRXNTERM,IC,JC
1,S,NUMZPTS,SPURSEP,ALPHA,TINIT,DELTAZ,A,DELTAR,DELTAT,CZERO,CLEFT,
1Q,RADIAL,WNR,WTR,AXIAL,WNZ,PI,ITYPESCL,MARG,CCOEFF1,CCOEFF2,CCOEFF3,
1CCOEFF4,CCOEFF5,TIME,DELTIME,SUM,CMULT,CZTLOSS,CLOSS,DLTM,CZLEFT
2 FORMAT(44H0 THE TIME-INCREASING RADIAL COEFFICIENTS ARE)
3 FORMAT(2X,8E16.8)
7 FORMAT(30H0 THE CONCENTRATIONS OF SPECIES,I2,4H ARE,/)
DC 1111 I=1,NRADSCL
N=NRXNTERM(I)
DC 1111 L=1,N
IF(I.GT.NUMRAD.AND.ITYPESCL.EQ.0) GO TO 173
II=IC(I,L)
JJ=JC(I,L)
IF(ITYPESCL.EQ.0.AND.II.GT.NUMRAD) D(II)=D(I)
IF(ITYPESCL.EQ.0.AND.II.GT.NUMRAD) TAU(II)=TAU(I)
IF(ITYPESCL.EQ.0.AND.JJ.GT.NUMRAD) D(JJ)=D(I)
IF(ITYPESCL.EQ.0.AND.JJ.GT.NUMRAD) TAU(JJ)=TAU(I)
IF(D(I).NE.D(II).OR.TAU(I).NE.TAU(II)) GO TO 40
39 IF(D(I).EQ.D(JJ).AND.TAU(I).EQ.TAU(JJ)) MARG(I,L)=1
IF(D(I).NE.D(JJ).OR.TAU(I).NE.TAU(JJ)) MARG(I,L)=2
GO TO 1111
40 IF(D(I).EQ.D(JJ).AND.TAU(I).EQ.TAU(JJ)) MARG(I,L)=3
IF(D(I).NE.D(JJ).OR.TAU(I).NE.TAU(JJ)) MARG(I,L)=4
1111 CONTINUE
173 LL=1
DC 105 K=1,1300
AN=K
NA=(AN/10.-.01)
NB=(AN/10.+.01)
IF(NA.EQ.NB) GO TO 3433
6 FORMAT(20H0 THE PROBLEM TIME IS,E10.4,8H SECONDS,///)
PRINT 6,TIME
DC 3432 I=1,NRADSCL
PRINT 7,I
PRINT 3, (C(J,I),J=1,NUMRPTS)
3432 CONTINUE
3433 CONTINUE
NRADL=NRADSCL*LL
NRADLL=NRADSCL*(1-LL)
Z=K
TIME=TAU(1)*(EXP(Z*DELTAT)-1.)

```

```

DC 100 I=1,NRADSOL
IF(I.GT.NUMRAD.AND.ITYPESOL.EQ.0) GO TO 174
TIMEB(I)=TIME+TAU(1)
CCEFF1(I)=DELTAT*TIMEB(I)/((DELTAR**2)*(TIME+TAU(I)))
CCEFF2(I)=CCEFF1(I)*2.*(1.+ALPHA)
DC 100 J=2,NUMRPTS
Z=J-1
100 CCEFF4(J,I)=(0.5*ALPHA/Z+0.25*Z*DELTAR**2)*CCEFF1(I)
174 CONTINUE
143 Z=K-1
IC=0
DC 102 I=1,NRADSOL
IF(I.GT.NUMRAD.AND.ITYPESOL.EQ.0) GO TO 175
SUMM=0.
N=NRXNTERM(I)
DC 101 J=1,N
II=IC(I,J)
JJ=JC(I,J)
MI=II+NRADLL
MJ=JJ+NRADLL
101 SUMM =SUMM +S(I,II,JJ)*C(1,MI )*C(1,MJ )
MJ=I+NRADL
MI=I+NRADLL
102 C(1,MJ)=C(1,MI)+CCEFF2(I)*(C(2,MI)-C(1,MI))+TIMEB(I)*SUMM*DELTAT
175 CONTINUE
IC=0
NR=NUMRPTS-1
DC 104 I=1,NRADSOL
IF(I.GT.NUMRAD.AND.ITYPESOL.EQ.0) GO TO 176
N=NRXNTERM(I)
DC 106 L=1,N
M=MARG(I,L)
106 CALL INTMULT(I,L,M,LL,1)
IF(I.GT.NUMRAD) GO TO 927
CALL INTGT1D(I,LL,K,IC)
927 CONTINUE
MI=I+NRADLL
MJ=I+NRADL
DC 104 J=2,NR
SUMM=0.
DC 115 L=1,N
115 SUMM =SUMM +CMULT(L,J)
104 C(J,MJ)=C(J,MI)+CCEFF1(I)*(C(J+1,MI)-2.*C(J,MI)+C(J-1,MI))
1+CCEFF4(J,I)*(C(J+1,MI)-C(J-1,MI))+TIMEB(I)*SUMM*DELTAT
176 CONTINUE
IF(IC.EQ.1) RETURN
Z=0.
DC 120 I=1,NUMRAD
IF(CLEFT(I)/CZERO(I).LT.0.02) Z=Z+1.
120 CONTINUE

```

```
Y=NUMRAD
IF(Z.EQ.Y) RETURN
IF(LL.EQ.1) GO TO 330
LL=1
GO TO 105
330 LL=0
IF(TIME.GE.TTIME) RETURN
105 CONTINUE
RETURN
END
```

SUBROUTINE INTMULT(I,L,M,LL)

The function of this subprogram is to perform the interpolation and multiplication necessary for calculation of the reaction terms in the finite difference equations and for the calculation of the reaction integrals.

The interpolation scheme used is the second order forward Gregory-Newton interpolation formula given as

$$f(x) \approx f(x_0 + rh) = f_0 + r\Delta f_0 + \frac{r(r-1)}{2!} \Delta^2 f_0 \quad (80)$$

where: x_0 = the tabulated value of position just below the interpolation point

h = the magnitude of the grid spacing

r = a number between zero and one such that $x_0 + rh$ is the value of the interpolation point

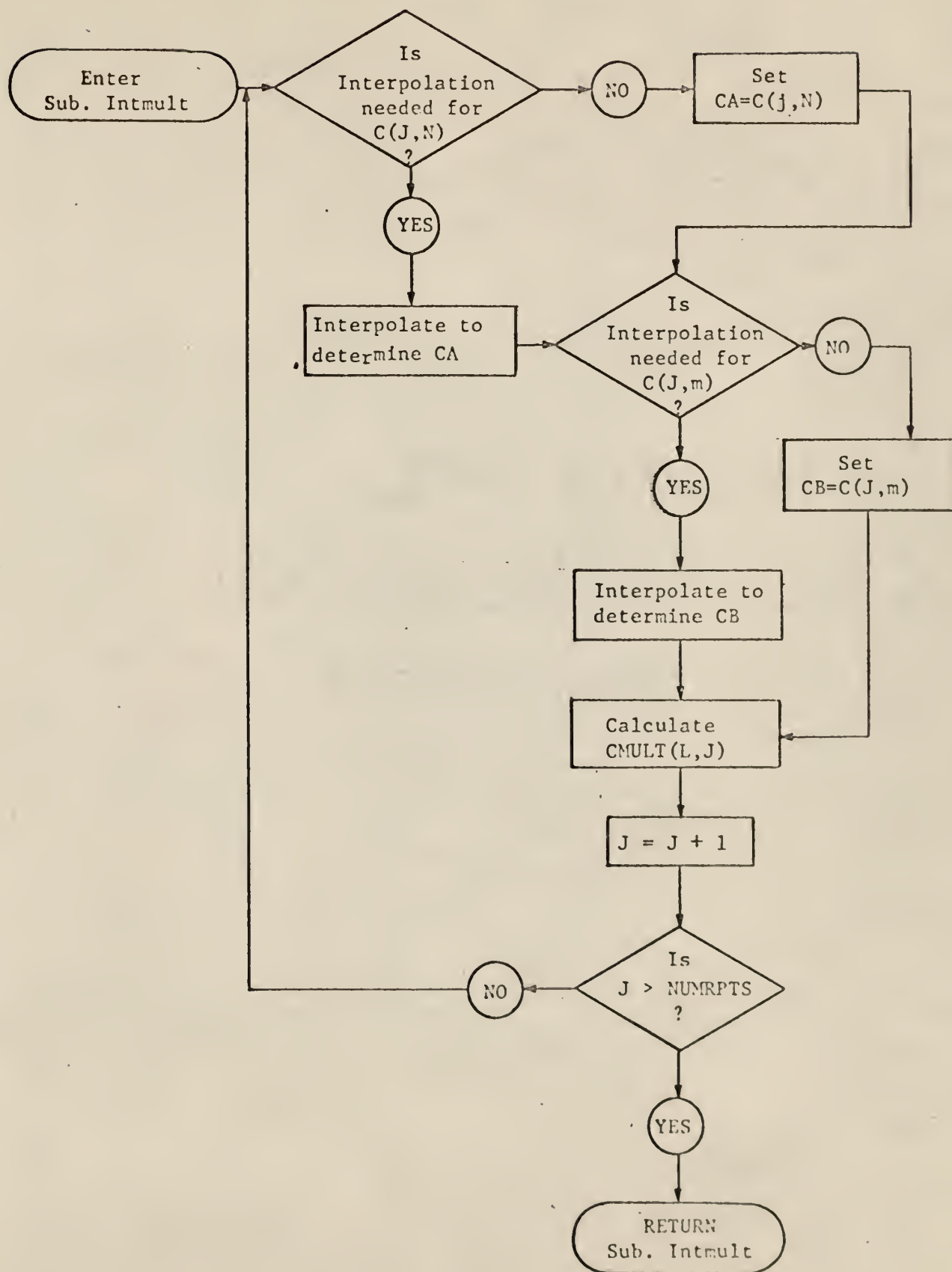
Δf_0 = first forward difference

$\Delta^2 f_0$ = second forward difference

Important Program Variables

Symbol	Explanation
M	Control variable equal to MARG(I,L) which determines the type of interpolation needed
H	Number corresponding to r in Eq. (80)
CA, CB	Values of the interpolated concentrations
CMULT(I,L)	Value of the interpolated reaction term

Logic Diagram for Subroutine INTMULT



```

SUBROUTINE INTMULT(I,L,M,LL,JZ)
DIMENSION RZERO(5),D(5),C(50,10)      ,NRXNTERM(5),IC(5,5),JC(5,5)
DIMENSION S(5,5,5),A(5),               CZERO(5),CLEFT(5),RADIAL(50)
DIMENSION WNR(50),WTR(5,50),AXIAL(50),WNZ(50),MARG(5,5),CZLEFT(5)
DIMENSION CCOEFF1(5),CCOEFF2(5),CCOEFF3(5),CCOEFF4(50,5),CCOEFF5(5,50)
DIMENSION SUM(5),CMULT(5,50),CZTLOSS(5,5),CLOSS(5,5),DLTM(5)
COMMON CZLOSS(5,5)
COMMON TAU(5)
COMMON TIMEB(5)
COMMON TTIME
COMMON SPUR,NUMRAD,NUMSCL,NUMRPTS,RZERO,D,NRADSOL,C,NRXNTERM,IC,JC
1,S,NUMZPTS,SPURSEP,ALPHA,TINIT,DELTAZ,A,DELTAR,DELTAT,CZERO,CLEFT,
1Q,RADIAL,WNR,WTR,AXIAL,WNZ,PI,I TYPESOL,MARG,CCOEFF1,CCOEFF2,CCOEFF3,
1CCOEFF4,CCOEFF5,TIME,DELTIME,SUM,CMULT,CZTLOSS,CLOSS,DLTM,CZLEFT
2 FORMAT(I5)
NR=NUMRPTS-1
II=IC(I,L)
JJ=JC(I,L)
LI=NRADSOL*(1-LL)
MI=II+LI
MJ=JJ+LI
R=((D(I)*(TAU(I)+TIME)/(D(II)*(TAU(II)+TIME)))**0.5)*DELTAR
RR=((D(I)*(TAU(I)+TIME)/(D(JJ)*(TAU(JJ)+TIME)))**0.5)*DELTAR
DO 100 J=2, NR
CA=0.
CB=0.
   GO TO (302,301,300,300),M
300 Z=J-1
RINTERP=Z*R
N=(RINTERP/DELTAR      )
IF(N.GT.NUMRPTS) GO TO 307
Z=N
Z=Z*DELTAR
H=(RINTERP-Z)/DELTAR
N=N+1
CA=H*(2.-H)*C(N+1,MI      )+0.5*(H-1.)*(H*C(N+2,MI      )+(H-2.)*
1C(N,MI      ))
   GO TO 305
307 CA=C(NUMRPTS,MI)
305 IF(M.EQ.3) GO TO 303
301 Z=J-1
RINTERP=Z*RR
N=(RINTERP/DELTAR      )
IF(N.GT.NUMRPTS) GO TO 308
Z=N
Z=Z*DELTAR
H=(RINTERP-Z)/DELTAR
N=N+1
CB=H*(2.-H)*C(N+1,MJ      )+0.5*(H-1.)*(H*C(N+2,MJ      )+(H-2.)*
1C(N,MJ))
   GO TO 306

```

```
308 CB=C(NUMRPTS,MJ)
306 IF(M.EQ.2) GO TO 304
      CMULT(L,J)=S(I,II,JJ)*CA*CB
      GO TO 100
303 CMULT(L,J)=S(I,II,JJ)*CA*C(J,MJ    )
      GO TO 100
304 CMULT(L,J)=S(I,II,JJ)*C(J,MI    )*CB
      GO TO 100
302 CMULT(L,J)=S(I,II,JJ)*C(J,MI    )*C(J,MJ    )
100 CONTINUE
      RETURN
      END
```

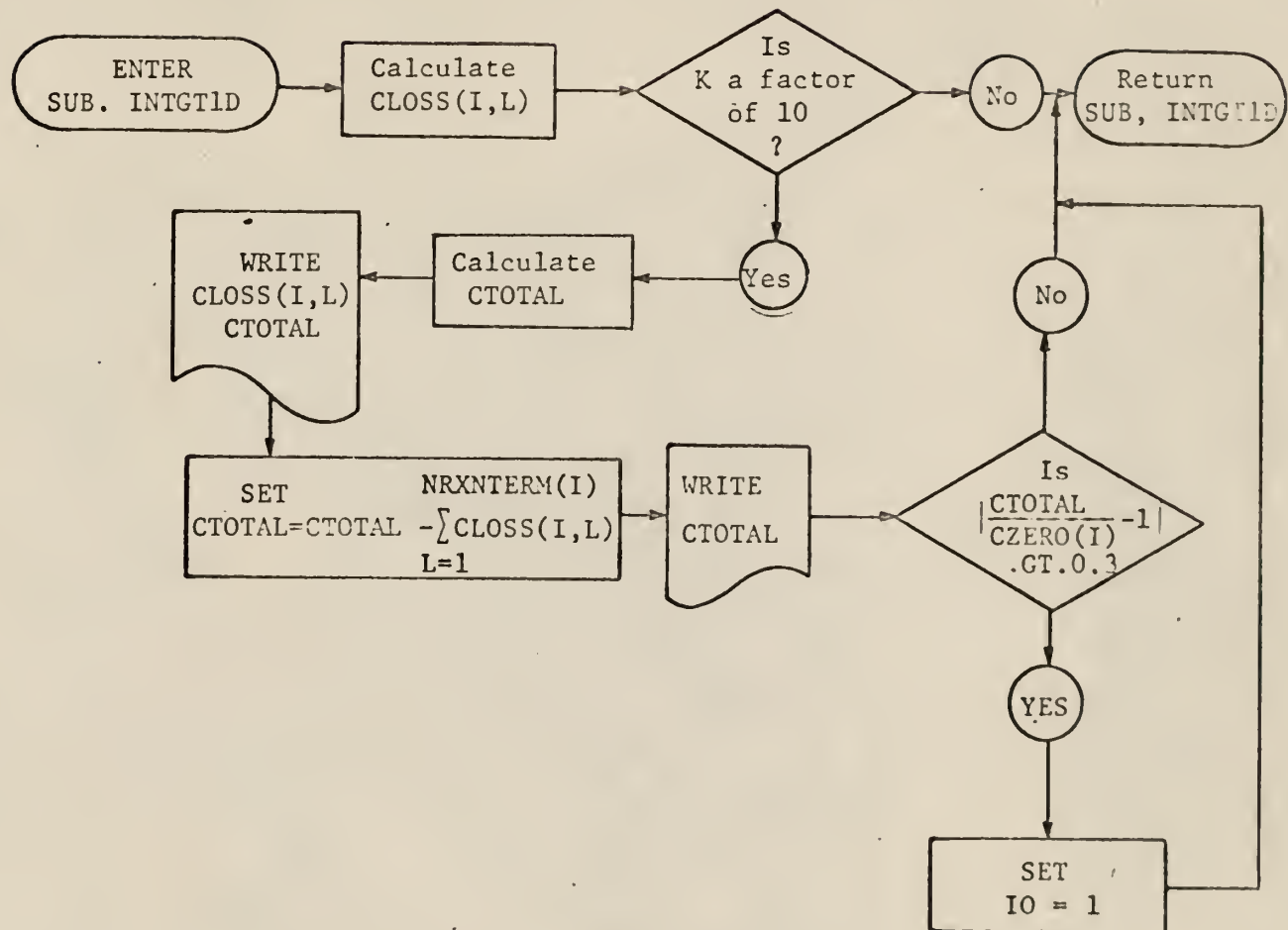
SUBROUTINE INTGT1D(I,LL,K,IO)

The function of this subroutine is to calculate the reaction loss integrals and the current amounts of free radicals present. These results are then printed out at every tenth time step. The volume integrals are determined numerically by a Simpson's Integration scheme with weights given by the FATES subprogram.

Important Program Variables

Symbol	Explanation
CLOSS(I,L)	Cumulative amount of the I^{th} species created by the L^{th} reaction term
CTOTAL	The first value determined is that for the amount of the I^{th} species present at time t. The second value determined is that for the sum of the amount of the I^{th} species present and the total amount lost by reaction. This value should remain close to the value for the initial amount of the I^{th} species present. If too large a deviation develops this subprogram will cause the main program to terminate this particular calculation.

Logic Diagram for Subroutine INTGT1D



```

SUBROUTINE INTGT1D(I,LL,K,IC)
DIMENSION RZERO(5),D(5),C(50,10      ),NRXNTERM(5),IC(5,5),JC(5,5)
DIMENSION S(5,5,5),A(5),          CZERO(5),CLEFT(5),RADIAL(50)
DIMENSION WNR(50),WTR(5,50),AXIAL(50),WNZ(50),MARG(5,5),CZLEFT(5)
DIMENSION CCEFF1(5),CCEFF2(5),CCEFF3(5),CCEFF4(50,5),CCEFF5(5,50)
DIMENSION SUM(5),CMULT(5,50),CZTLOSS(5,5),CLOSS(5,5),DLTM(5)
COMMON CZLOSS(5,5)
COMMON TAU(5)
COMMON TIMEB(5)
COMMON TTIME
COMMON SPUR,NUMRAD,NUMSCL,NUMRPTS,RZERO,D,NRADSCL,C,NRXNTERM,IC,JC
1,S,NUMZPTS,SPURSEP,ALPHA,TINIT,DELTAZ,A,DELTAR,DELTAT,CZERO,CLEFT,
1Q,RADIAL,WNR,WTR,AXIAL,WNZ,PI,ITYPESCL,MARG,CCEFF1,CCEFF2,CCEFF3,
1CCEFF4,CCEFF5,TIME,DELTIME,SUM,CMULT,CZTLOSS,CLOSS,DLTM,CZLEFT
3 FORMAT(2X,8E16.8)
4 FORMAT(24H THE REACTION LOSSES ARE,/)
5 FORMAT(35H THE CURRENT NUMBER OF PARTICLES IS,E15.8,/)
6 FORMAT(11H THE SUM IS,E15.8)
II=I+NRADSCL*(1-LL)
AN=K
NA=(AN/10.+.01)
NB=(AN/10.-.01)
Z=4.*PI*TIMEB(I)*((D(I)*(TAU(I)+TIME))**1.5)*DELTAT*DELTAR**2
N=NRXNTERM(I)
DC 102 L=1,N
SUMM=0.
DC 100 J=2,NUMRPTS
Y=J-1
100 SUMM=SUMM+CMULT(L,J)*WNR(J)*(Y**2)
102 CLOSS(I,L)=CLOSS(I,L)+SUMM*Z
IF(NA.EQ.NB) GO TO 301
Z=Z/(TIMEB(I)*DELTAT)
SUMM=0.
DC 101 J=2,NUMRPTS
Y=J-1
101 SUMM=SUMM+C(J,II)*WNR(J)*(Y**2)
CTOTAL=Z*SUMM
Z=0.
DC 103 L=1,N
103 Z=Z+CLOSS(I,L)
PRINT 4
PRINT 3,(CLOSS(I,L),L=1,N)
302 PRINT 5,CTOTAL
CTOTAL=CTOTAL-Z
PRINT 6,CTOTAL
IF(ABSF(CTOTAL/CZERO(I)-1.)>.0.30) IC=1
301 RETURN
END

```

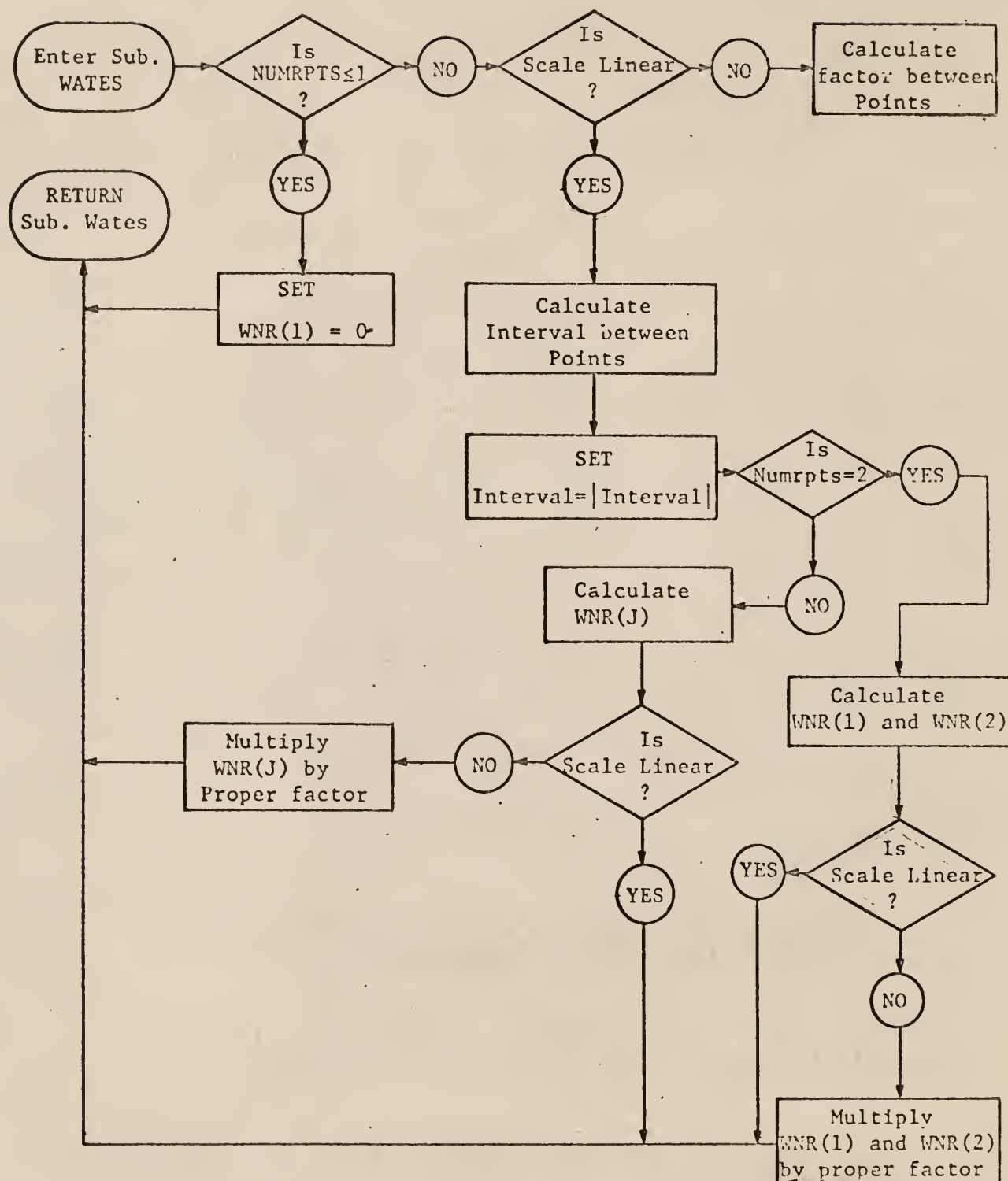
SUBROUTINE WATES(L,NUMRPTS,RADIAL,WNR)

The function of this subprogram is to generate the necessary weights for a Simpson-type numerical integration for either a linear or a logarithmic scale. If the number of points is even, a cubic approximation is used to subtract out the area of the center portion of the curve since the Simpson integration counts this area twice. If there are only two points, the area is determined using the trapezoidal rule. If there is only one point the area is set to zero.

Important Program Variables

Symbol	Explanation
L	Control integer = 1 for a linear scale > 1 for a logarithmic scale
NUMRPTS	Number of points considered for the integration
RADIAL(J)	Variable which locates the abscissa points for the integration
WNR(J)	Value of the weights determined by this subprogram to be used in the numerical integration

Logic Diagram for Subroutine WATES



```

SUBROUTINE FATES(IWT,NWT,WTAB,WATES)
DIMENSION WTAB(50),WATES(50)
819 WTA=NWT
  IF(NWT-2.GE.0) GO TO 39
19  WATES(1)=0.
  GO TO 259
39  IF(IWT-2.GE.0) GO TO 79
59  WTDEL=(WTAB(1)-WTAB(NWT))/(WTA-1.)
  GO TO 99
79  IF(IWT.EQ.3) GO TO 3333
      WTDEL=ALOG(WTAB(1)/WTAB(NWT))/(WTA-1.)
99  IF(WTDEL.GE.0.) GO TO 990
119 WTDEL=-WTDEL
  GO TO 990
3333 WTDEL=EXP(WTAB(1)/WTAB(NWT))/(WTA-1.)
990 IF(NWT-2) 259,1190,139
1190 WATES(1)= .5*WTDEL
      WATES(2)=WATES(1)
  GO TO 199
139 NWTA=(WTA/2.+.1)
      NWTB=(WTA/2.-.1)
      NWTC=(WTA/4.+.1)
      NWTD=(WTA/4.-.1)
      WATES(1)=WTDEL/3.
      WTC=WATES(1)
      WATES(NWT)=WATES(1)
      DO 159 I=1,NWTB
      WATES(I+1)=WTDEL+WTC
      INDX=NWT-I
      WATES(INDX)=WTDEL+WTC
159  WTC=-WTC
      WTD=1./24.
      IF(NWTC-NWTD.LE.0) GO TO 1790
1590 WTD=-WTD
1790 IF(NWTA-NWTB.LE.0) GO TO 199
179  WATES(NWTB)=WATES(NWTB)-WTD*WTDEL
      WATES(NWTB+1)=WATES(NWTB+1)+5.*WTD*WTDEL
      WATES(NWTB+3)=WATES(NWTB)
      WATES(NWTB+2)=WATES(NWTB+1)
199  IF(IWT-2.LT.0) GO TO 259
210  DO 239 I=1,NWT
239  WATES(I)=WATES(I)*WTAB(I)
259  RETURN
      END

```

A.2.1 Sample Input Data for Program Diffuse

```
12
•10000000E-04
 1   3   30
 1
•70700000E-07
•20000000E-04 •20000000E-04 •20000000E-04 •20000000E-04
 3   2   2   1
 1   4
-.10000000E-10
 2   3
•10000000E-10
 1   1
-.10000000E-10
 1   4
•10000000E-10
 2   3
-.10000000E-10
 1   1
•50000000E-11
 2   3
-.10000000E-10
 1   4
-.10000000E-10
•60000000E+01 •00000000E+00 •60235000E+19 •60235000E+19
```

Note: Each line represents one computer card.

A.3 Selected Data for Figures 1-12

Time (sec)	<u>Run 1</u>				
	$N_{RS}^T(t)$	$N_P^T(t)$	$2N_{R_2}^T(t)$	$N_R(t)$	Σ_R
1.561×10^{-11}	.006	---	.345	5.771	6.122
3.525×10^{-11}	.012	---	.620	5.456	6.088
5.764×10^{-11}	.019	---	.846	5.193	6.058
8.316×10^{-11}	.026	---	1.035	4.970	6.031
1.122×10^{-10}	.034	---	1.197	4.776	6.006
2.262×10^{-10}	.062	.002	1.566	4.314	5.940
4.676×10^{-10}	.115	.005	1.887	3.867	5.865
6.448×10^{-10}	.152	.007	2.002	3.684	5.831
1.015×10^{-9}	.226	.013	2.134	3.437	5.784
2.067×10^{-9}	.420	.031	2.280	3.048	5.712
4.090×10^{-9}	.755	.106	2.364	2.635	5.648
6.988×10^{-9}	1.174	.250	2.402	2.275	5.601
1.040×10^{-8}	1.610	.467	2.420	2.007	5.570
2.013×10^{-8}	2.663	1.232	2.436	1.655	5.522
4.427×10^{-8}	4.922	3.376	2.446	1.485	5.477
6.560×10^{-8}	6.834	5.284	2.449	1.458	5.458
1.108×10^{-7}	10.818	9.268	2.453	1.431	5.433
2.131×10^{-7}	19.672	18.123	2.456	1.399	5.404
4.100×10^{-7}	36.345	34.798	2.458	1.369	5.374
6.920×10^{-7}	59.784	58.237	2.459	1.345	5.352

Time (sec)	<u>Run 2</u>				
	$N_{RS}^T(t)$	$N_P^T(t)$	$2N_{R_2}^T(t)$	$N_R(t)$	$\sum R$
1.561×10^{-11}	.061	---	.343	5.723	6.126
3.525×10^{-11}	.123	.002	.610	5.359	6.091
5.764×10^{-11}	.188	.004	.826	5.051	6.061
8.316×10^{-11}	.257	.009	1.004	4.781	6.033
1.122×10^{-10}	.330	.015	1.153	4.540	6.008
2.262×10^{-10}	.590	.052	1.478	3.928	5.943
4.676×10^{-10}	1.060	.170	1.731	3.252	5.872
6.448×10^{-10}	1.936	.569	1.892	2.539	5.798
1.015×10^{-9}	3.301	1.574	1.966	2.044	5.737
2.067×10^{-9}	5.583	3.730	2.006	1.821	5.689
4.090×10^{-9}	8.699	6.838	2.026	1.771	5.658
6.988×10^{-9}	12.313	10.456	2.038	1.740	5.636
1.040×10^{-8}	22.412	20.561	2.053	1.695	5.599
2.013×10^{-8}	46.907	45.060	2.065	1.646	5.557
4.427×10^{-8}	68.173	66.329	2.069	1.624	5.536

Run 3

Time (sec)	$N_{RS}^T(t)$	$N_P^T(t)$	$2N_{R_2}^T(t)$	$N_R(t)$	\sum_R
1.561×10^{-11}	.586	.029	.318	5.284	6.159
3.525×10^{-11}	1.137	.126	.529	4.567	6.107
5.764×10^{-11}	1.673	.294	.677	4.010	6.067
8.316×10^{-11}	2.206	.536	.786	3.576	6.033
1.122×10^{-10}	2.751	.855	.869	3.240	6.005
2.262×10^{-10}	4.565	2.306	1.032	2.650	5.942
4.676×10^{-10}	7.924	5.579	1.163	2.380	5.889
6.448×10^{-10}	10.030	7.960	1.211	2.320	5.868
1.015×10^{-9}	15.165	12.848	1.270	2.252	5.838
2.067×10^{-9}	28.725	26.438	1.341	2.164	5.791
4.090×10^{-9}	54.227	51.963	1.390	2.093	5.746
6.988×10^{-9}	90.068	87.817	1.417	2.043	5.711

Time (sec)	<u>Run 4</u>				
	$N_{RS}^T(t)$	$N_P^T(t)$	$2N_{R_2}^T(t)$	$N_R(t)$	\sum_R
1.561×10^{-11}	4.440	1.810	.193	3.304	6.127
3.525×10^{-11}	7.938	5.116	.278	2.938	6.038
5.764×10^{-11}	11.678	8.874	.350	2.866	6.020
8.316×10^{-11}	15.819	13.044	.414	2.812	6.007
1.122×10^{-10}	20.434	17.686	.473	2.774	5.994
2.262×10^{-10}	37.899	35.221	.620	2.661	5.959
4.676×10^{-10}	73.428	70.819	.763	2.841	5.914
6.448×10^{-10}	98.926	96.343	.819	2.491	5.892
1.015×10^{-9}	151.336	148.787	.887	2.425	5.861

Run 5

Time (sec)	$N_{RS}^T(t)$	$N_P^T(t)$	$2N_{R_2}^T(t)$	$N_R(t)$	Σ_R
1.561×10^{-11}	.586	.003	.317	5.264	6.163
3.525×10^{-11}	1.130	.016	.524	4.477	6.115
5.764×10^{-11}	1.647	.039	.662	3.806	6.077
8.316×10^{-11}	2.141	.074	.756	3.221	6.044
1.122×10^{-10}	2.614	.122	.819	2.706	6.017
2.262×10^{-10}	3.891	.355	.906	1.510	5.952
4.676×10^{-10}	5.240	.939	.931	.668	5.900
6.448×10^{-10}	5.831	1.385	.934	.506	5.886
1.015×10^{-9}	6.828	2.317	.936	.427	5.875
2.067×10^{-9}	9.453	4.935	.939	.408	5.865
4.090×10^{-9}	14.432	9.918	.940	.402	5.857
6.988×10^{-9}	21.511	17.000	.941	.398	5.850
1.040×10^{-8}	29.806	25.298	.942	.396	5.845

Time (sec)	<u>Run 6</u>				
	$N_{RS}^T(t)$	$N_P^T(t)$	$2N_{R_2}^T(t)$	$N_R(t)$	\sum_R
1.561×10^{-11}	.061	.003	.343	5.725	6.126
3.525×10^{-11}	.123	.013	.611	5.369	6.090
5.764×10^{-11}	.188	.032	.828	5.075	6.059
8.316×10^{-11}	.258	.061	1.009	4.826	6.031
1.122×10^{-10}	.332	.100	1.161	4.613	6.006
2.262×10^{-10}	.600	.296	1.505	4.131	5.940
4.676×10^{-10}	1.114	.779	1.804	3.727	5.866
6.448×10^{-10}	1.473	1.139	1.913	3.586	5.834
1.015×10^{-9}	2.201	1.872	2.042	3.417	5.788
2.067×10^{-9}	4.189	3.868	2.195	3.201	5.717
4.090×10^{-9}	7.869	7.553	2.295	3.039	5.650
6.988×10^{-9}	12.988	12.676	2.351	2.936	5.600
1.040×10^{-8}	18.905	18.594	2.383	2.869	5.562

Time (sec)	<u>Run 7</u>				
	$N_{RS}^T(t)$	$N_P^T(t)$	$2N_{R_2}^T(t)$	$N_R(t)$	\sum_R
1.561×10^{-11}	.089	---	.743	8.372	9.203
3.525×10^{-11}	.177	.003	1.285	7.684	9.143
5.764×10^{-11}	.266	.008	1.704	7.132	9.093
8.316×10^{-11}	.358	.015	2.038	6.670	9.051
1.122×10^{-10}	.456	.026	2.310	6.273	9.014
2.262×10^{-10}	.796	.082	2.887	5.319	8.921
4.676×10^{-10}	1.406	.251	3.327	4.341	8.823
6.448×10^{-10}	1.802	.406	3.463	3.921	8.781
1.015×10^{-9}	2.541	.785	3.603	3.364	8.724
2.067×10^{-9}	4.314	2.092	3.731	2.690	8.644
4.090×10^{-9}	7.271	4.878	3.798	2.389	8.581
6.988×10^{-9}	11.296	8.890	3.833	2.300	8.539
1.040×10^{-8}	15.959	13.558	3.853	2.256	8.510
2.013×10^{-8}	28.987	26.594	3.877	2.194	8.463
4.427×10^{-8}	60.579	58.195	3.897	2.128	8.409

Run 8

Time (sec)	$N_{RS}^T(t)$	$N_P^T(t)$	$2N_{R_2}^T(t)$	$N_R(t)$	\sum_R
1.561×10^{-11}	.116	---	1.274	10.897	12.286
3.525×10^{-11}	.226	.005	2.149	9.825	12.196
5.764×10^{-11}	.335	.012	2.799	9.003	12.126
8.316×10^{-11}	.448	.023	3.305	8.339	12.068
1.122×10^{-10}	.565	.039	3.711	7.782	12.019
2.262×10^{-10}	.970	.117	4.550	6.497	11.900
4.676×10^{-10}	1.691	.334	5.176	5.246	11.779
6.448×10^{-10}	2.158	.525	5.370	4.726	11.728
1.015×10^{-9}	3.032	.983	5.568	4.043	11.660
2.067×10^{-9}	5.128	2.532	5.751	3.216	11.564
4.090×10^{-9}	9.592	6.772	5.858	2.796	11.475
6.988×10^{-9}	13.353	10.524	5.893	2.717	11.439
1.040×10^{-8}	21.171	18.350	5.928	2.644	11.393
2.013×10^{-8}	34.133	31.321	5.954	2.583	11.349
4.427×10^{-8}	71.231	68.430	5.981	2.503	11.285
6.560×10^{-8}	103.438	100.642	5.991	2.466	11.254

Time (sec)	<u>Run 9</u>				
	$N_{RS}^T(t)$	$N_P^T(t)$	$2N_R^T(t)$	$N_R(t)$	$\sum R$
1.561×10^{-11}	.063	---	.004	6.036	6.102
3.525×10^{-11}	.129	.001	.007	5.941	6.076
5.764×10^{-11}	.202	.004	.010	5.841	6.050
8.316×10^{-11}	.282	.007	.013	5.738	6.025
1.122×10^{-10}	.369	.013	.016	5.629	6.001
2.262×10^{-10}	.693	.048	.022	5.262	5.929
4.676×10^{-10}	1.323	.180	.027	4.668	5.838
6.448×10^{-10}	1.750	.317	.029	4.333	5.795
1.015×10^{-9}	2.570	.785	.031	3.817	5.734
2.067×10^{-9}	4.585	2.078	.033	3.102	5.643
4.090×10^{-9}	7.982	5.218	.034	2.771	5.569
6.988×10^{-9}	12.644	9.843	.035	2.685	5.520
1.040×10^{-8}	18.079	15.272	.035	2.644	5.486
2.013×10^{-8}	33.354	30.543	.035	2.585	5.431
4.427×10^{-8}	70.613	67.801	.036	2.519	5.367
6.560×10^{-8}	103.066	100.254	.036	2.487	5.335

Run 10

Time (sec)	$N_{RS}^T(t)$	$N_P^T(t)$	$2N_{R2}^T(t)$	$N_R(t)$	\sum_R
1.561×10^{-11}	---	---	.035	5.776	6.122
3.525×10^{-11}	.001	---	.621	5.465	6.088
5.764×10^{-11}	.002	---	.848	5.208	6.058
8.316×10^{-11}	.003	---	1.038	4.990	6.031
1.122×10^{-10}	.004	---	1.201	4.801	6.006
2.262×10^{-10}	.007	---	1.575	4.358	5.939
4.676×10^{-10}	.013	.002	1.906	3.948	5.864
6.448×10^{-10}	.017	.004	2.025	3.791	5.829
1.015×10^{-9}	.026	.007	2.167	3.596	5.781
2.067×10^{-9}	.048	.022	2.332	3.348	5.706
4.090×10^{-9}	.088	.057	2.440	3.166	5.637
6.988×10^{-9}	.143	.111	2.500	3.052	5.584
1.040×10^{-8}	.206	.175	2.534	2.980	5.546
2.013×10^{-8}	.381	.350	2.576	2.877	5.483
$4.4 \times 7 \times 10^{-8}$.798	.767	2.609	2.773	5.412
6.560×10^{-8}	1.158	1.127	2.602	2.726	5.377
1.108×10^{-7}	1.906	1.875	2.632	2.669	5.332
2.131×10^{-7}	3.561	3.530	2.643	2.603	5.277

Run 11

Time (sec)	$N_{RS}^T(t)$	$N_P^T(t)$	$2N_{R_2}^T(t)$	$N_R(t)$	Σ_R
1.561×10^{-11}	.061	.025	.343	5.743	6.122
3.525×10^{-11}	.124	.083	.616	5.430	6.087
5.764×10^{-11}	.190	.150	.840	5.177	6.057
8.316×10^{-11}	.261	.222	1.029	4.962	6.030
1.122×10^{-10}	.338	.300	1.191	4.777	6.005
2.262×10^{-10}	.617	.580	1.563	4.430	5.940
4.676×10^{-10}	1.158	1.121	1.892	3.936	5.864
6.448×10^{-10}	1.536	1.500	2.011	3.783	5.830
1.015×10^{-9}	2.300	2.263	2.153	3.593	5.782
2.067×10^{-9}	4.380	4.345	2.319	3.354	5.707

Time (sec)	<u>Run 12</u>				
	$N_{RS}^T(t)$	$N_P^T(t)$	$2N_{R_2}^T(t)$	$N_R(t)$	\sum_R
8.377x10	.284	---	.020	5.728	6.032
1.775x10	.489	---	.039	5.497	6.024
2.719x10	.647	---	.056	5.317	6.020
4.629x10	.882	.002	.089	5.044	6.014
7.548x10	1.127	.003	.134	4.750	6.008
1.053x10	1.306	.006	.177	4.527	6.004
2.097x10	1.700	.016	.302	4.009	5.995
4.060x10	2.117	.040	.474	3.433	5.984
6.997x10	2.537	.084	.640	2.878	5.972
1.046x10	2.942	.144	.761	2.402	5.961
2.028x10	3.882	.344	.914	1.490	5.942

AN ANALYTICAL STUDY OF THE
DIFFUSION KINETICS OF A RADIATION-INDUCED
CHEMICAL REACTION SYSTEM

by

MORRIS JACKSON COOLBAUGH

B. S., Kansas State University, 1964

AN ABSTRACT OF
A MASTER'S THESIS

submitted in partial fulfillment of the

requirements for the degree

MASTER OF SCIENCE

Department of Nuclear Engineering

KANSAS STATE UNIVERSITY
Manhattan, Kansas

1968

ABSTRACT

The objectives of this work were two-fold. The first was to develop a general computational scheme applicable to the solution of the equations representing the diffusional and kinetic behavior of reacting species in a single cluster along the track of a particle of ionizing radiation. The second was to apply this method to the investigation of the spatial and time behavior of the concentrations of reactants in a typical radiation-induced chemical chain reaction. This investigation was done for a variety of initial concentrations and chemical reaction rate constant parameters.

The extent of reaction as a function of time for each reacting species was determined for each set of parameters. This enabled general conclusions to be drawn for the effects of the parameters on the possibility of cluster overlapping in a chain reaction. These data were also used to qualitatively determine the effects of variation of dose rate and to give an indication of the dose rates at which spur overlap may become important.

The spatial and time dependencies of concentration were determined for one set of parameters in order to indicate the feasibility of utilizing a modified form of the prescribed-diffusion hypothesis.